

**The Effect of Aging on Timing and Decision Making in Mice:
Combination of Behavioral, Computational and
Neurobiological Approaches**

by

Ezgi Gür

A Dissertation Submitted to the
Graduate School of Social Sciences and Humanities
in Partial Fulfillment of the Requirements for
the Degree of

Doctor of Philosophy

in

Psychology



KOÇ ÜNİVERSİTESİ

January, 2020

**The Effect of Aging on Timing and Decision Making in Mice:
Combination of Behavioral, Computational and Neurobiological Approaches**

Koç University

Graduate School of Social Sciences and Humanities

This is to certify that I have examined this copy of a doctoral dissertation by

Ezgi Gür

and have found that it is complete and satisfactory in all respects,
and that any and all revisions required by the final
examining committee have been made.

Committee Members:

Prof. Fuat Balcı

Asst. Prof. Çağlar Akçay

Asst. Prof. Terry T. Eskenazi

Asst. Prof. Mehmet Kocatürk

Asst. Prof. David M. Freestone

Date: _____

Statement of Authorship

This dissertation contains no material which has been accepted for any award or any other degree or diploma in any university or other institution. It is affirmed by the candidate that, to the best of his knowledge, the dissertation contains no material previously published or written by another person, except where due reference is made in the text of the thesis.

The author acknowledges that copyright of published works contained within this thesis resides with the copyright holder(s) of those works.

Signature

Ezgi Gür



[dedication here]

ABSTRACT

The Effect of Aging on Timing and Decision Making in Mice: Combination of Behavioral, Computational and Neurobiological Approaches

Ezgi Gür

Doctor of Philosophy in Psychology

January 13, 2020

The aim of this thesis was to investigate age-related alterations in interval timing and decision-making at the levels of behavioral output and latent variables along with their neurobiological correlates in mice. In the first experiment (Chapter 2), age-related alterations in interval timing behavior and its neurobiological correlates were investigated in young, adult, and old mice using dual peak interval procedure. Behavioral outputs were evaluated to make inferences regarding the source of variability in timing behavior within the framework of Scalar Expectancy Theory. In the second experiment (Chapter 3), in addition to age-related changes in interval timing ability, how probabilistic information is integrated into temporal decisions was investigated in young and old mice using the switch paradigm. In the third experiment (Chapter 4), we expanded the scope of our study to include perceptual decisions and investigated how latent variables of simple perceptual decision process changes with aging and the neurobiological correlates of these age-related changes in young, adult and old mice using a bright discrimination task we adapted for mice.

In both first and second experiments, we found that the core timing ability of old mice was intact; however, they exhibited a pronounced deficit in termination of an ongoing timed response. In the first experiment, we also found that the acquisition of response termination took a longer time and the contribution of threshold variance relative to clock/memory variance was higher in old mice. In the second experiment, the observed deficit disappeared when mice were supposed to adopt a switch strategy from a low probability short option to a high probability long option as opposed to switching from a high probability short option to a high probability long option. Consequently, we suggested that such a deficit might be due to age-dependent changes in the decisional component of interval timing. Decrements in both dopaminergic (VTA & SNc) and cholinergic (MS/DB complex) neuron counts and dopaminergic axon terminal densities (DLS & DMS) were evident in old mice (Experiment 1). From all these neurobiological measures the number of dopaminergic neurons in VTA and the number of cholinergic neurons in MS/DB complex were negatively correlated with the time of response termination and the acquisition of response termination, respectively, which pointed at the role of dopaminergic and cholinergic functions in the observed age-dependent alterations in timing behavior. In the third experiment, we found that brightness discrimination accuracy was lower in old mice with no difference in response times. Modeling of the decision outputs within the framework of the Hierarchical Drift Diffusion

Model revealed that observed accuracy difference was due to a decrease in the quality of evidence integration (i.e., drift rate) during the decision-making process suggesting slowing down of information processing in aging in the domain of perceptual decision making. The quality of evidence integration was positively correlated with mesocortical (number of dopaminergic neurons in VTA) and nigrostriatal (density of dopaminergic axon terminals in DMS) dopaminergic function.

Overall, the results of these three experiments suggest that a healthy aging process is characterized by different deficits (i.e. decision component vs. information processing) in different cognitive domains (i.e. interval timing vs. decision making) despite their overlapping neurobiological correlates. Taken together, these results constitute a comprehensive characterization of a healthy cognitive aging process in a mouse model of cognitive aging based on behavior, cognition, and neurobiology and highlight the translational value of animal models of cognitive aging.



ÖZETÇE

**Yaslanmanın Farelerde Zamanlama ve Karar Verme Üzerine Etkisi:
Davranışsal, Hesaplamalı ve Nörobiyolojik Yaklaşımlar**

Ezgi Gür

Psikoloji, Doktora

13 Ocak 2020

[Turkish abstract here]

ACKNOWLEDGMENTS



Author's note: Chapter 3 has been published in *Frontiers in Behavioral Neuroscience*. Chapter 2 revised and resubmitted to *Neurobiology of Aging*. Chapter 4 is submitted to *Brain Structure and Function*.

Gür, E., Duyan, Y. A., & Balçı, F. (2019). Probabilistic Information Modulates the Timed Response Inhibition Deficit in Aging Mice. *Frontiers in Behavioral Neuroscience*, *13*, 196.

Gür, E., Duyan, Y. A., Arkan, S., Karson, A. & Balçı, F. (revised & resubmitted). Interval Timing Deficits and Its Neurobiological Correlates in Aging Mice. *Neurobiology of Aging*.

Gür, E., Duyan, Y. A., Türkakın, E., Arkan, S., Karson, A. & Balçı, F. (submitted). Aging Impairs Perceptual Decision Making in Mice: Integrating Computational and Neurobiological Approaches. *Brain Structure & Function*.

TABLE OF CONTENTS

ABSTRACT.....	v
ÖZETÇE	vii
ACKNOWLEDGMENTS	viii
LIST OF FIGURES	xiii
ABBREVIATIONS	xvi
Chapter 1 INTRODUCTION	1
1.1 Interval Timing.....	2
1.2 Decision Making	3
Chapter 2 INTERVAL TIMING DEFICITS AND ITS NEUROBIOLOGICAL CORRELATES IN AGING MICE.....	5
2.1 Abstract	5
2.2 Introduction.....	5
2.3 Method	8
2.3.1 Subjects.....	8
2.3.2 Apparatus	8
2.3.3 Procedure	9
2.3.4 Data Analysis.....	10
2.4 Results	12
2.4.1 Behavioral Results	12
2.4.2 Age Differences in IHC Outputs	16
2.4.3 IHC Output in Relation to Behavioral/Neurobiological Correlates.....	19
2.5 Discussion	19
Chapter 3 PROBABILISTIC INFORMATION MODULATES THE TIMED INHIBITION DEFICIT IN AGING MICE.....	26
3.1 Abstract	26
3.2 Introduction.....	27
3.3 Material and Methods	28

3.3.1	Subjects.....	28
3.3.2	Apparatus.....	28
3.3.3	Procedure.....	29
3.3.4	Data Analysis.....	30
3.4	Results.....	32
3.4.1	Acquisition During Training and Test Phase.....	32
3.4.2	Switch Rates in Training vs. Test Sessions.....	33
3.4.3	Switch Times in Test Session.....	36
3.4.4	Timed Anticipatory Responses During Test Session.....	37
3.5	Discussion.....	39
Chapter 4 AGING IMPAIRS PERCEPTUAL DECISION-MAKING IN MICE: INTEGRATING COMPUTATIONAL AND NEUROBIOLOGICAL APPROACHES		
	43	
4.1	Abstract.....	43
4.2	Introduction.....	43
4.3	Method.....	49
4.3.1	Subjects.....	49
4.3.2	Apparatus.....	50
4.3.3	Procedure.....	50
4.3.4	Data Analysis.....	52
4.4	Results.....	55
4.4.1	Behavioral Analysis.....	55
4.4.2	HDDM Fits.....	56
4.4.3	IHC Outputs and Their Relation to Latent Variables.....	60
4.5	Discussion.....	63
Chapter 5 CONCLUSION.....		
	68	
REFERENCES.....		
	72	
Appendix A.....		
	88	
A.1	Operant Chambers.....	88
A.2	IHC Protocol & Histological Confirmation.....	88
A.3	Estimation of peak time & spread from the average response curves.....	89

A.4	Estimation of start & stop times via single-trial analysis.....	90
A.5	Variability of Start and Stop Times	90
A.6	Examination of Acquisition of Stop Times.....	91
A.7	Start Times Throughout Session Blocks	91
A.8	Stop Times Throughout Session Blocks	92
A.9	Dual Peak Task Illustration.....	94
A.10	Mean Neuron Counts.....	95
A.11	Mean Optic Density of Axon Terminals	95
A.12	Scatterplots	96
Appendix B	97
B.1	Switch Rate and Switch Latencies (Times) in the First Hour of the Initial Test Session.....	97
B.2	Results of Tosun et al. (2016) for Comparison to the Results of Current Study	97
B.3	Analysis of Complementary Measures	99
Appendix C	101
C.1	Model Fits	101
C.2	Brightness Discrimination Task.....	102
C.3	Posterior Distributions	103

LIST OF FIGURES

Figure 2.1: Normalized average response curves of young (straight green line), adult (dashed red line), and old (dashed and dotted blue line) mice for the PI trials of short (upper panel) and long (lower panel) intervals in every 10 sessions from the beginning to the end of the experiment.....	13
Figure 2.2: Mean normalized start and stop times separately for short and long intervals for young, adult, and old mice. Error bars show 95% confidence intervals. ***: $p \leq 0.001$	14
Figure 2.3: Mean correlation coefficients for start-stop, start-spread and middle-spread pairs. Error bars show 95% confidence intervals. **: $p \leq 0.01$; ***: $p \leq 0.001$	14
Figure 2.4: Average normalized start and stop times across session blocks for short and long target intervals by age. Error bars show 95% confidence intervals.....	15
Figure 2.5: Representative images of dark brown immunoreactive TH+ neurons in VTA and SNc on 40 μm sections (5x) for young (G), adult (H) and old mice (I). Images at A, C, E and B, D, F shows smaller windows within targeted regions for VTA and SNc, respectively (20x).	17
Figure 2.6: Representative images of dark brown immunoreactive ChAT+ neurons in MS/DB complex (D-F) are shown for each age group on 40 μm sections (5x). A-C and G-I, respectively, show enlarged images of selected upper and lower windows on MS/DB complex (20x). Dark brown immunoreactive TH+ axon terminals in DMS (J-L) and DLS (M-O) are shown for each age group on 40 μm sections (5x).....	18
Figure 3.1: Graphical depiction of the procedures applied during training and testing along with the depiction of the typical behavior observed in the corresponding trials. Top right table depicts the four different experimental groups (2 age groups X 2 probability conditions).	30
Figure 3.2: Raster plots of short (grey) and long (cyan) location responses in the long trials of training (columns 1 & 3) and test (columns 2 & 4) sessions. Upper and lower panels show the data collected from young and old mice, respectively. Horizontal tick black lines separate the data collected from each mouse. Vertical dotted black lines show the time of reward delivery in the long trials (9 seconds). Mice rarely switched from the short location to the long location during the long trials of the training session; however, timed switches were apparent from the outset during the long trials of testing in both age	

groups. Green, red, and blue dots correspond to the start time of short location responses, stop time of short location response, and start time of long location responses estimated from the single trial analysis, respectively..... 34

Figure 3.3: Mean switch rates for the last training session and two test sessions combined (A). Mean switch times of young and old mice by short probability conditions (B). Error bars show 95% confidence intervals (Mean \pm 1.96*SE)..... 36

Figure 3.4: Normalized averaged response curves for short and long location responses during long trials of test sessions for young (red) and old (black) mice in different probability conditions. Dotted vertical lines represent the time of reward delivery in short and long locations; however, note that there was no reward delivery in the short location during long trials. Early in the trial, the normalized response rate was higher for the short location (dotted black and red curves) and it peaked around 3 seconds. For the long location, the normalized response rate increased (solid black and red curves) later in the trial. Error bars show the standard error of the actual mean values..... 38

Figure 3.5: Mean start time of short location responses (A) and mean stop time of short location responses (B) depending on age and probability conditions. Error bars show 95% confidence intervals (Mean \pm 1.96*SE)..... 39

Figure 4.1: Graphical illustration of the diffusion process in a single trial along with the DDM parameters..... 45

Figure 4.2: a) Mean choice accuracy along with individual data points in test trials during the steady-state performance for young, adult, and old mice; a statistically significant difference was found between young and old mice only. b) Mean correct and incorrect RTs along with individual data points during the steady-state performance for different age groups. Error bars show the 95% confidence intervals..... 56

Figure 4.3: Drift rates (a), decision thresholds (b), and non-decision times (c) estimated for each session block. Parameter estimates for individual animals are shown with thin lines whereas the average estimates are shown as thick lines. Shades denote the 95% confidence interval around the mean estimates. While the figures display only the mean parameter estimates for the subjects and label them by age, note that hypothesis testing was done based on the entire posterior distributions of each session block, and differences between the age groups were not factored in at this stage (models that included age as a factor had higher DIC scores compared to the model without age). The labels and line types for different age groups are therefore for demonstration purposes and not part of the

underlying model. Green-straight, red-dashed, blue-dotted lines are for young, adult, and old mice, respectively. 58

Figure 4.4: The posterior distributions for drift rate (a), decision threshold (b), and non-decision time (c) in the last five sessions for the age groups. Green-straight, red-dashed, blue-dotted lines are for young, adult, and old mice, respectively. 59

Figure 4.5: Representative images of VTA and SNc after IHC staining for young, adult, and old mice (from top to bottom panel). The middle panel shows dark brown immunoreactive TH⁺ neurons of VTA and SNc on 40 μm sections (5x). Images to the left (VTA) and right (SNc) of the middle panel provide a closer look to smaller windows within these target regions (20x). 61

Figure 4.6: Representative images of MS/DB complex and STR stainings for young, adult, and old mice. The left upper panel shows dark brown immunoreactive ChAT⁺ neurons in MS/DB complex (5x) and the left-lower panel shows enlarged images of selected windows from the target region (20x). At the right panel, immunoreactive TH⁺ axon terminals are seen in dark brown on DMS (right-upper panel) and DLS (right-lower panel); images are magnified 5x. 62

Figure 4.7: Scatterplots showing the significant relationship found between drift rate and number of dopaminergic neurons in the VTA and optic density of dopaminergic axon terminals in DMS. 62

ABBREVIATIONS

2AFC	Two Alternative Forced Choice
a	Boundary Separation/Threshold
A β	Amyloid-Beta
ChAT	Choline Acetyltransferase
CUSUM	Cumulative Sum
CV	Coefficient of Variation
dc	Drift Criterion
DDM	Drift-Diffusion Model
DIC	Deviation Information Criterion
DLS	Dorsolateral Striatum
DMS	Dorsomedial Striatum
FC	Frontal Cortex
FEF	Frontal Eye Field
FI	Fixed Interval
FOF	Frontal Orienting Fields
FR	Fixed Ratio
FT	Fixed Time
HDDM	Hierarchical Drift-Diffusion Model
IACUC	Institutional Animal Care and Use Committee
IHC	Immunohistochemistry
ITI	Inter-trial Interval
KUARF	Koç University Animal Research Facility
LIP	Lateral Intraparietal Cortex
LT	Long Target
M	Mean
MCMC	Markov Chain Monte Carlo

MD	Mean Difference
MFC	Medial Frontal Cortex
MS/DB	Medial Septal/Diagonal Band
PI	Peak Interval
PPC	Posterior Parietal Cortex
pre-SMA	Pre-supplementary Motor Area
RAGE	A β influx transporter
RSI	Response to Stimulus Interval
RT	Reaction/Response Time
SAT	Speed-Accuracy Tradeoff
SBF	Striatal-Beat-Frequency
SE	Standard Error
SET	Scalar Expectancy Theory
SNc	Substantia Nigra Pars Compacta
SNR	Signal-to-Noise Ratio
ST	Short Target
STR	Striatum
T ₀	Non-decision Time
TH	Tyrosine Hydroxylase
v	Drift Rate
VTA	Ventral Tegmental Area
z	Starting Point

Chapter 1

INTRODUCTION

The decline in cognitive health accompanies aging has profound effects on one's well-being and quality of life. The cognitive decline might interfere with everyday activities, social life, and one's profession depending on the domain and extent of the deficit. Understanding the nature of the cognitive decline in aging, firstly, would allow for interventions that could delay, slow down or prevent this decline and thereby increase the quality of life for the elderly. Secondly, the cognitive and neurobiological changes that arise long before the recognition of symptoms of some neurodegenerative disorders could be distinguished by isolating cognitive alterations observed in healthy aging, both in qualitative and quantitative terms (Deary et al., 2009; Harada et al., 2013). Therefore, investigation of cognitive decline in aging along with associated neurobiological mechanisms is of crucial importance.

Given the value of animal models in facilitating translational research and methodological constraints in human studies, the study of cognitive aging in animal models is necessary to fully understand the effect of aging on behavioral, cognitive and neurobiological levels. In a relatively recent special issue, the studies of cognitive aging across species were evaluated and several cognitive domains that are extensively studied across species were highlighted. These domains include associative memory, recognition memory, spatial and contextual memory, working memory and executive functioning (Roberson et al., 2012). From these, memory research domain dominated the studies of animal models of cognitive aging. On the other hand, domains such as interval timing and decision making which also have widespread relevance for daily functioning were overlooked in the comparative investigation of cognitive aging.

In fact, previous work reported age-dependent alterations both in interval timing and decision making in humans (e.g. Balçı et al., 2009a; Ratcliff et al., 2006a). Moreover, neurotransmitter systems (e.g. dopaminergic and cholinergic) and neural pathways (e.g., cortico-striatal circuitry) that are subject to change in aging are also implicated in both of these cognitive domains (Coull et al., 2011; Forstmann et al., 2010; Marschner et al., 2005). Importantly, rodents, primates, and humans have homologous neural mechanisms supporting interval timing and decision-making processes and both processes can be characterized by generative models that enable making inferences about the latent variables underlying these processes. Altogether, these factors make interval timing and decision-making ideal candidate systems to study cognitive aging in animal models.

In this thesis, age-dependent alterations in interval timing and decision-making processes are investigated from a behavioral, psycho-mechanistically meaningful computational (i.e., Hierarchical Drift Diffusion Model and Information Processing variant of Scalar Expectancy Theory) and neurobiological (i.e., immunohistochemistry) perspectives. Given that animal models provide useful insight regarding the cognitive architecture of humans, the mouse model of cognitive aging is used in three different experiments.

1.1 Interval Timing

Interval timing ability requires perception, encoding, storage, retrieval, estimation, and discrimination of durations in seconds-to-minutes range. Consequently, execution of an interval timing task relies on the engagement of different components of the timing system such as attention, memory, and decision in addition to a core timing component (i.e. hypothetical clock). Aging studies conducted with human participants reported changes in the interval timing performance and suggested that these changes are due to attention, memory, or clock components depending on the nature and the complexity of the timing task (e.g. Lustig, 2003; Perbal et al., 2002; Vanneste et al., 2001). Although rodents are often the subjects of interval timing studies, only a limited number of aging studies have been conducted with a comparative approach and these studies rarely addressed the possible sources of interval timing deficits observed in aging. Neurobiological changes leading to interval timing deficits in aging are even less understood. In the first experiment (Chapter 2), age-dependent alterations in interval timing performance and sources of variability that contributed to behavioral outputs were

examined through testing young, adult, and old mice in the peak interval procedure. Relationships between behavioral and immunohistochemistry outputs were examined to elucidate the neurobiological correlates of age-dependent alterations in interval timing behavior. In the second experiment (Chapter 3), we examined how young and old mice spontaneously integrate probabilistic information to the temporal decisions for adaptive behavioral outputs, in addition to the investigation of age-dependent alterations in timing behavior, using a switch task with a pretraining phase (developed earlier in Tosun, Gür & Balci, 2016).

1.2 Decision Making

Decision making is the process of choosing one option among others by gathering the available information. Perceptual decision making which relies on sensory information is usually investigated in the laboratory settings by two-alternative forced-choice paradigms and two measures are used to characterize the choice behavior: accuracy and response times. In such tasks, decision making in older population is usually characterized by slower response times, while the accuracy differences are mostly observed under the speed instructions (e.g. Ratcliff et al., 2007; Ratcliff and McKoon, 2008). Although these observations were initially attributed to a general slowing down in cognitive processes in aging, separate evaluation of the measures collected during a simple choice task does not provide any information about the latent variables of the decision process that gives rise to both of these decision outputs. On the other hand, computational modeling of decision outputs in a unified fashion reveals the differences at the level of latent decision variables. For instance, the application of the drift-diffusion model to decision outputs showed that slower reaction times of the elderly could be explained by the longer time spent on stimulus encoding, response execution, and a cautious response criterion (i.e., decision threshold) in a majority of cases (Ratcliff et al, 2006a). At the neural level, our primary knowledge about decision-making comes from the studies conducted with human and non-human primates. Only with recent methodological developments, several studies started to utilize various two alternative forced choice protocols to study decision making in rodent models and use modeling to understand the latent decision variables along with their neural correlates. To our knowledge, age-dependent alterations in these latent variables and their neurobiological correlates have not been studied in a mouse model of cognitive aging yet. In the third experiment (Chapter 4), young, adult, and old mice were

tested with a two alternative forced choice (i.e. bright discrimination) task that was adapted for mice and the examination of the latent variables are done by fitting the decision outputs with the Hierarchical Drift-Diffusion model. The outputs of immunohistochemistry were utilized for investigating the neurobiological correlates of age-dependent alterations in the latent decision variables.



Chapter 2

INTERVAL TIMING DEFICITS AND ITS NEUROBIOLOGICAL CORRELATES IN AGING MICE

2.1 *Abstract*

Age-related neurobiological and cognitive alterations suggest that interval timing (as a related function) is also altered in aging, which can, in turn, disrupt timing-dependent functions. We investigated alterations in interval timing with aging and accompanying neurobiological changes. We tested 4-6, 10-12, and 18-20 months-old mice on the dual-peak-interval procedure. Results revealed a specific deficit in the termination of timed responses (stop-times). The decision processes contributed more to timing variability (vs. clock/memory process) in the aged mice. We observed age-dependent reductions in the number of dopaminergic neurons in the VTA and SNc, cholinergic neurons in the medial septum/diagonal band (MS/DB) complex, and density of dopaminergic axon terminals in the DLS/DMS. Negative correlations were found between the number of dopaminergic neurons in the VTA and stop times, and the number of cholinergic neurons in MS/DB complex and the acquisition of stop times. Our results point at age-dependent changes in the decisional components of interval timing and the role of dopaminergic and cholinergic functions in these behavioral alterations.

2.2 *Introduction*

Interval timing, a function that relies on neurobiological and cognitive constituents subject to change with aging, is also altered in aging (Balci et al., 2009a). For instance, the cholinergic and dopaminergic inputs gradually decline with aging (Marschener et al., 2005; Schliebs & Arendt, 2011) and both neuromodulatory functions are known to have

central roles in interval timing. Specifically, dopamine levels have been associated with the internal clock speed (e.g., faster clock speed with higher dopaminergic tone; Meck, 1983) whereas the cholinergic activity has been associated with the temporal memory process (e.g., longer recalled time with lower cholinergic activity; Meck & Church, 1987). In support of this assertion, anecdotal reports indeed suggest that subjective time elapses faster with age -at least when evaluated retrospectively (Wittmann & Lehnhoff, 2005). In line with the slower information-processing account of cognitive aging (Salthouse, 1996), this observation can be accounted for by assuming lower clock speed. However, experimental human prospective timing studies have led to equivocal findings regarding age-related alterations in interval timing (Balci et al., 2009a; Turgeon et al., 2016; Paraskevoudi et al., 2018). The importance of interval timing for many other functions from motor planning to decision making to learning makes the study of age-dependent alterations in this function particularly relevant for cognitive aging.

The question of how interval timing is altered with aging has also been investigated in animal models particularly using the Peak Interval (PI) Procedure (Roberts, 1981). In this procedure, animals are trained to anticipate reward delivery after a fixed delay (Fixed Interval, FI, trials) and tested in the longer probe trials without reward (PI trials). Anticipatory response data averaged across trials yield a bell curve; its peak time reflects the timing accuracy and its width reflects the timing precision. The examination of PI data on a trial-by-trial basis reveals a different behavioral pattern (Balci et al., 2009a; Gibbon & Church, 1990). In a single PI trial, subjects transition from low to high rate of responding in an abrupt fashion (i.e. start time) and then abruptly transition back to the low rate (i.e. stop time) after the omission of anticipated reward. Mean of start and stop times is referred to as the middle time and the difference between the start and stop times (i.e. spread) indexes timing precision.

Data gathered from the PI procedure is typically conceptualized within the Scalar Expectancy (Timing) Theory framework (SET; Gibbon, 1977; Gibbon et al., 1984). SET assumes that the pulses generated by a pacemaker are integrated in the accumulator during the timed event. When a reward is delivered, the content of the accumulator is transferred to the reference memory during which the clock readings are perturbed by Gaussian distributed noise (with mean of 1) resulting in a reference memory density function with a veridical mean. At the decision stage, the current clock reading in the accumulator is

compared with a random sample from the reference memory according to a ratio rule (i.e., $|\text{Accumulated Time-Random Memory Sample}|/\text{Random Memory Sample}$). When this decision variable first crosses the threshold, the animal starts its anticipatory responding and when the reward is omitted, the second crossing of the threshold terminates the anticipatory responding.

Consequently, SET predicts certain correlational patterns between the measures of single-trial analysis (Gibbon & Church, 1990; 1992). Clock/memory variance would result in positive start-stop, start-spread, and middle-spread correlations since a common bias would affect these variables in the same direction. Threshold variance would result in negative start-stop and start-spread correlations and no middle-spread correlation given that an increase in the threshold would separate the start and stop times away from each other and thereby increasing the spread without changing the time estimate. Consequently, different correlation patterns and their relative strengths would reflect the relative contributions of these sources to the timing variability. Empirical studies typically reported positive correlations between the start and stop times, middle and spread, and a negative correlation between the start and spread in pigeons, rats, and humans (Balci et al., 2013; Cheng & Westwood, 1993; Church et al., 1994).

In relation to aging, animal PI studies have indeed revealed age-related deficits in timing behavior. For instance, Lejeune et al. (1998) found delayed anticipatory timed responses of old rats. Meck and his colleagues reported age-related deficits in both temporal accuracy (e.g. underestimation of time; Meck et al., 1986; Meck, 2006) and precision (Meck et al., 1986). Another study found that the accuracy of temporal responses of rats decreased with age while precision showed an increasing trend (Church et al., 2014). In a more recent study, different analysis approaches provided inconclusive results regarding temporal precision in rats (Garces et al., 2018). From these studies, Garces et al. (2018) and Lejeune et al. (1998) also looked at the correlation patterns and reported partially different patterns than what is usually observed (e.g. weak start-stop correlations or negative middle-spread correlations) without age-related differences. Other studies utilizing alternative timing tasks in aging did not provide consistent results either (Cheng et al., 2011; LeBlanc et al., 1996; LeBlanc & Soffie, 1999). Briefly, similar to human literature, the results of animal studies have also led to inconsistent findings regarding how timing is altered in aging.

The neurobiological correlates of the age-dependent changes in interval timing are even less understood than the behavioral alterations. Earlier studies have found the role cholinergic function in age-dependent changes in temporal accuracy (Meck et al., 1986; Meck, 2002; Meck, 2006), which has been typically attributed to altered temporal memory with aging. In a more recent study, Church et al. (2014) reported that the decreased accuracy of temporal responses observed in aged rats was negatively related to the levels of amyloid-beta ($A\beta$), $A\beta$ 42, RAGE ($A\beta$ influx transporter) while increased precision had a positive relationship with these $A\beta$ -related biomarkers.

In light of the literature, we aimed to investigate how timing behavior is altered with aging in mice and elucidate how age-related alterations in dopaminergic and cholinergic functions mediate these behavioral alterations. Specifically, we tested young, middle age, and old mice in the dual PI procedure and investigated the relationship between the behavioral observations and dopaminergic and cholinergic biomarkers. Overall, our findings showed that altered timing behavior is likely due to the decision rather than clock/memory processes and suggest the role of dopaminergic neurons in the ventral tegmental area (VTA) in mediating stop times and the role of cholinergic neurons in MS/DB complex in the acquisition of stop times.

2.3 Method

2.3.1 Subjects

Subjects were 38 naive male C57BL/6J mice (KUARF). Young ($n = 12$), adult ($n = 13$) and old mice ($n = 13$) were 4, 10 and 18 months old at the beginning of the experiment (+2 months at steady state), respectively. One adult mouse died of natural causes. Mice were group-housed in polycarbonate cages in a room on a 12:12-h light:dark cycle. Subjects were tested daily in one-hour long sessions during the light cycle. Food intake was restricted to maintain the weight of mice at 85% of their free-feeding weight with ad libitum access to water. Additional pellets were provided after each session. All procedures were approved by Koç University IACUC (2014-13).

2.3.2 Apparatus

Operant chambers (ENV-307W; Med Associates) that housed two retractable levers, a house light, and feeding hoppers were used for behavioral testing. Details of the apparatus

are provided in the Appendix A.1 Operant Chambers. A peristaltic pump (Ismatec-Reglo) was used for transcardial perfusion. Brain sections were cut using a cryostat (Leica CM1520). The examination of the brain sections after staining was done under an optical microscope (Zeiss Primostar). The images of the sections were photographed with a digital camera system (Axiovision, Version 4.8.2 SP2, Zeiss).

2.3.3 Procedure

Magazine/Lever Press Training

In the first four sessions of magazine/lever press training, sessions started with inserting one of the two levers into the box and food was provided every 60 seconds (FT60) or earlier if there was a lever press (FR1). When pressed, the lever was retracted, FT60 schedule was reset, and one of the levers was inserted into the box in random order for the next trial. After four sessions of FR1-FT60 training, all mice had only FR1 sessions, until they collected 40 rewards in a session for two consecutive days. Mice meeting the FR1 requirement (on average after 4 sessions) proceeded to the experiment with dual PI procedure consisting of intermixed FI and PI trials.

Intermixed FI Training and PI Testing

In this phase (50 sessions), mice were trained and tested for two target intervals (Appendix A.9 Dual Peak Task Illustration: Figure A.1). Each session consisted of FI and their corresponding PI trials separately for two target intervals (25 s and 50 s). Each lever was associated with one of the intervals (counterbalanced across subjects). All trials started with the insertion of one lever into the box along with illumination of house light to signal time interval. In the FI trials, after the first response emitted following the FI, the lever was retracted, house light was turned off, and liquid reinforcement was delivered for 3 s in the illuminated food hopper. The PI trials lasted three times longer than their corresponding FI trials and terminated by retraction of the lever and turning the house light off without any reinforcement. Inter-trial intervals were on average 60 s (variable with minimum 30 s). Trials for the two target intervals were presented with equal probability (3 FI:1 PI trial). There were at most 6 consecutive FI trials and at most 2 consecutive PI trials.

Immunohistochemistry (IHC) & Histological Confirmation

IHC stainings were done for 9 mice from each age group in this experiment to see the relation of these measures with the behavioral data. Target regions were substantia nigra pars compacta (SNc), VTA, MS/DB complex, and striatum (STR; dorsolateral: DLS and dorsomedial: DMS). All coordinates were obtained from the stereotaxic atlas of Paxinos and Franklin (2012). Additionally, we combined our neurobiological data gathered from 27 mice with the same measures gathered from the sex and age-matched mice involved in another behavioral experiment (Gür et al., under review) to compare these neurobiological parameters (overall N = 54).

One-to-four days after the completion of the behavioral phase of the experiment (2 days on average), mice were transcardially perfused and decapitated. After keeping the brains in a fixative and sucrose solution, snap-frozen brains were stored at -80°C until further use. The IHC staining protocol for free-floating sections was followed after all mice completed the behavioral phase of the experiment. Tyrosine Hydroxylase (1:500) and Choline acetyltransferase (1:100) were used as the primary antibodies (Santa Cruz) to identify tyrosine hydroxylase-positive (TH+, dopaminergic) neurons and choline acetyltransferase-positive (ChAT+, cholinergic) neurons, respectively. To confirm the localization and morphology of the targeted regions, sections were stained with thionin acetate (Sigma Aldrich). The examination of the sections was done under an optical microscope. Details of the IHC staining are presented in Appendix A.2 IHC Protocol & Histological Confirmation.

2.3.4 Data Analysis

Behavioral Data Analysis

The steady-state PI data from the last 10 sessions of the FI-PI phase were compared between target intervals and age groups. The peak times and spread were estimated from the response curves (Appendix A.3 Estimation of peak time & spread from the average response curves). Start and stop times were extracted from steady-state individual trials (normalized by the target intervals) from which middle and spread values were also calculated (see Appendix A.4 Estimation of start & stop times via single-trial analysis for details). All these measures (except middle and spread of single-trial analysis) were compared between target intervals and age groups using 2x3 mixed-design ANOVA.

Analysis of the variability of start and stop times are described in Appendix A.5

Variability of Start and Stop Times. Normalized single-trial measures pooled for the short and long target intervals were used to calculate the correlation coefficients to infer the possible sources of variability in timing behavior and they were compared between the age groups using one-way ANOVA.

In addition to the analysis of steady-state timing performance, the change point algorithm (Balci et al., 2009c) was also run on the entire PI-trial data collected over 50 sessions to extract the start and stop times (normalized by target intervals) in each trial for the examination of the evolution of the timing behavior throughout the experiment. These measures were averaged for every 10 sessions and compared between target intervals, age groups and session blocks using 2 x 3 x 5 mixed-design ANOVA. Furthermore, since the stop times emerge later in training, we found the point (n^{th} trial) during the FI-PI phase at which the temporally-controlled stop times emerged (i.e. acquisition of the stop time threshold) for each subject using the change point algorithm for binomial data (details are provided in Appendix A.6 Examination of Acquisition of Stop Times). The number of trials it took for the mouse to acquire the stop time threshold was compared between target intervals and age groups using 2 x 3 mixed-design ANOVA.

Quantification in IHC

The visualization of targeted regions (SNc, VTA, MS/DB complex, and STR) was performed under an optic microscope. The images of the sections were photographed at x5 and x20 magnification. After the determination of the location and boundaries of the regions in brain sections, dark-brown reaction products were interpreted as immunoreactive. Images were converted into grayscale using ImageJ software (version 1.49; NIH) and the mean immunoreactivity density was measured within the designated regions. Gray levels ranged from 0 (light gray) to 255 (dark gray). The number of TH+ neurons in SNc and VTA ($n = 16$), number of ChAT+ neurons in MS/DB complex ($n = 27$), and optic density of TH+ axon terminals in DLS and DMS ($n = 18$) were analyzed. Although the same number of samples were stained for each target region, the quantification was performed only for the sections with clear images. For each mouse, the mean value of the series of stained sections for the target area was used. The number

of neurons was calculated per μm^2 . Optic density measure was weighted for each subject by the mean value of the group formed for the staining protocol (see Gulcebi et al., 2017).

After neurobiological measures were taken, correlations between these measures and steady state behavioral measures (normalized and pooled across durations) were examined. Additionally, measures collected from each target region (from twice as large sample size, see section 2.3.3) were compared between age groups using one-way ANOVA. All the analysis and statistical tests described above were run on MATLAB or SPSS. Follow-up tests were conducted for the significant effects.

2.4 Results

2.4.1 Behavioral Results

Figure 2.1 shows the normalized average response curves of each age group for the short and long PI trials in 10 session bins. Normalized steady-state peak time and spread measures estimated from the response curve (rightmost column of Figure 2.1) were compared between the age groups and target intervals. The normalized peak time for short target (ST) [Mean (M) = 0.95, Standard Error (SE) = 0.04] was significantly later than the normalized peak time for long target (LT) [M = 0.85, SE = 0.03; $F(1,34) = 4.51$, $p = 0.04$, $\eta_p^2 = 0.12$]. Neither the effect of age [$F(2,34) = 0.72$, $p = 0.50$] nor the interaction effect of age and target interval [$F(2,34) = 0.69$, $p = 0.51$] were significant. The average normalized spread for ST (M = 0.99, SE = 0.04) was wider than the average normalized spread for LT [M = 0.66, SE = 0.04; $F(1,34) = 55.98$, $p < 0.001$, $\eta_p^2 = 0.62$]. The effect of age [$F(2,34) = 0.53$, $p = 0.59$] and the interaction effect of age and target interval [$F(2,34) = 0.59$, $p = 0.56$] were not significant.

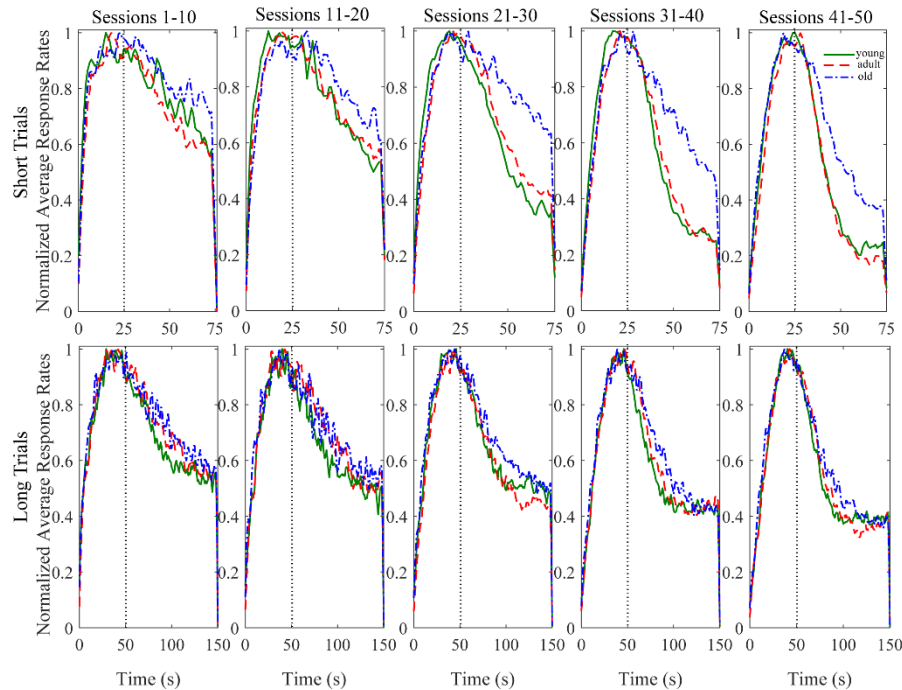


Figure 2.1: Normalized average response curves of young (straight green line), adult (dashed red line), and old (dashed and dotted blue line) mice for the PI trials of short (upper panel) and long (lower panel) intervals in every 10 sessions from the beginning to the end of the experiment.

The normalized steady-state start and stop times were also compared between age groups and target intervals (Figure 2.2). For the normalized start times, neither the main effects of the target interval [$F(1,34) = 2.95$, $p = 0.10$] and age [$F(2,34) = 0.06$, $p = 0.94$] nor their interaction effect [$F(2,34) = 1.03$, $p = 0.37$] were significant. The normalized stop times was later for ST ($M = 2.02$, $SE = 0.05$) than LT ($M = 1.58$, $SE = 0.05$) [$F(1,34) = 134.08$, $p < 0.001$, $\eta_p^2 = 0.80$]. The main effect of age on the normalized stop times was significant, $F(2,34) = 17.97$, $p < 0.001$, $\eta_p^2 = 0.51$. The post hoc comparisons showed that the average normalized stop time in old mice was significantly later than in young ($MD = 0.31$, $SE = 0.08$, $p = 0.001$) and adult ($MD = 0.45$, $SE = 0.08$, $p < 0.001$) mice. The interaction between target interval and age was not significant [$F(2,34) = 1.75$, $p = 0.19$].

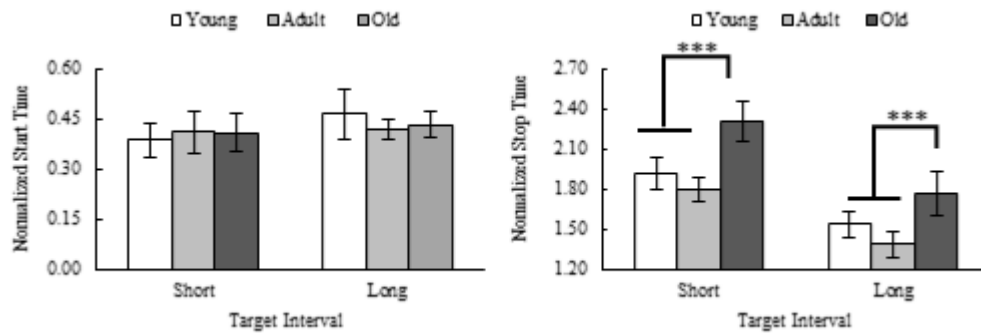


Figure 2.2: Mean normalized start and stop times separately for short and long intervals for young, adult, and old mice. Error bars show 95% confidence intervals. ***: $p \leq 0.001$.

We compared the correlation coefficients between single-trial variables between young, adult and old mice to see the age differences regarding the sources of variability/noise in timing behavior (Figure 2.3). The effect of age was significant on start-stop [$F(2,34) = 11.47$, $p < 0.001$, $\eta_p^2 = 0.40$] and start-spread [$F(2,34) = 6.05$, $p = 0.01$, $\eta_p^2 = 0.26$] correlations, but not on the middle-spread correlation [$F(2,34) = 1.71$, $p = 0.20$]. Specifically, the start-stop correlation of old mice was significantly weaker compared to the start-stop correlations of young (MD = -0.26, SE = 0.06, $p < 0.001$) and adult (MD = -0.24, SE = 0.06, $p = 0.001$) mice. The start-spread correlation of old mice was significantly stronger than the start-spread correlations of adult mice (MD = -0.18, SE = 0.05, $p = 0.004$).

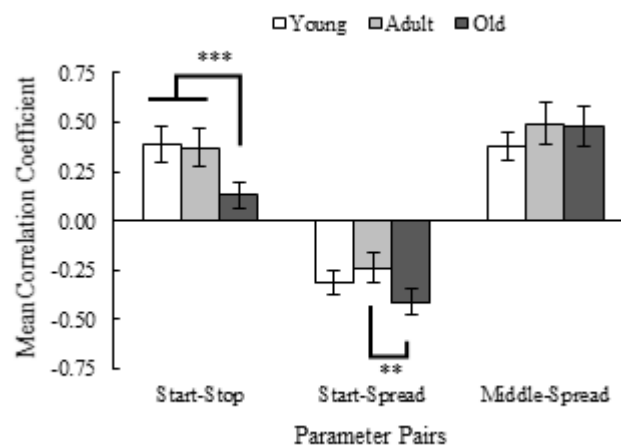


Figure 2.3: Mean correlation coefficients for start-stop, start-spread and middle-spread pairs. Error bars show 95% confidence intervals. **: $p \leq 0.01$; ***: $p \leq 0.001$.

Figure 2.4 shows the progression of the timing behavior throughout the experiment for different age groups and target intervals. For the normalized start times, main effects of block [$F(3.02,102.65) = 38.35, p < 0.001, \eta_p^2 = 0.53$] and age [$F(2,34) = 3.29, p = 0.049, \eta_p^2 = 0.16$] were significant while the main effect of target interval was not significant [$F(1,34) = 2.75, p = 0.11$]. There were significant interactions between the age and target interval [$F(2,34) = 6.87, p = 0.003, \eta_p^2 = 0.29$] and between the target interval and block [$F(4,136) = 4.07, p = 0.004, \eta_p^2 = 0.11$] but not between the age and block [$F(6.04,102.65) = 1.33, p = 0.25$]. There was a significant three-way interaction between block, age and target interval [$F(8,136) = 2.53, p = 0.01, \eta_p^2 = 0.13$]. Therefore, we do not report further statistics for the lower order significant effects.

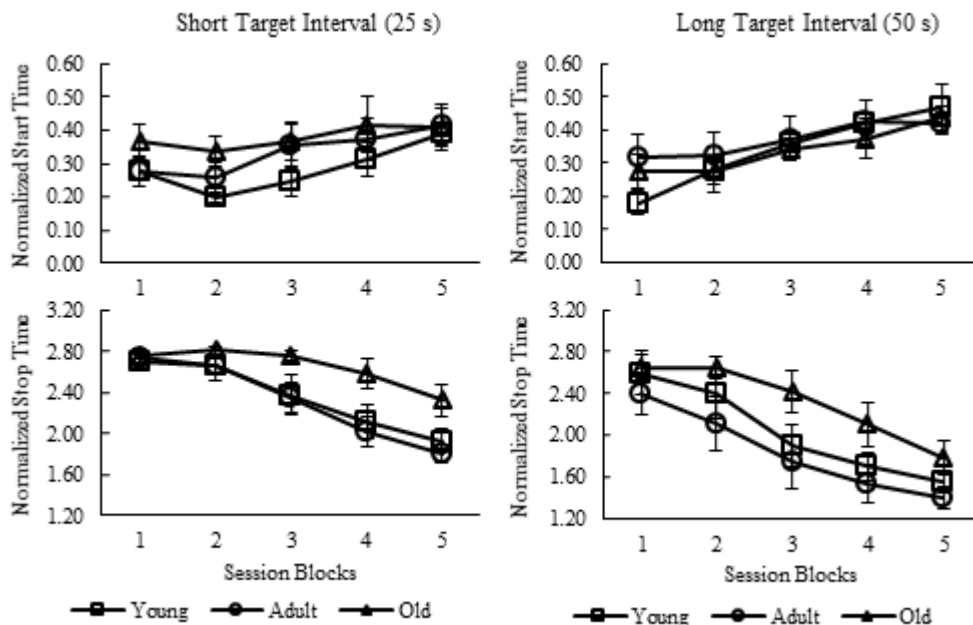


Figure 2.4: Average normalized start and stop times across session blocks for short and long target intervals by age. Error bars show 95% confidence intervals.

We compared the age groups at each level of blocks for two target intervals, revealing that the interaction between age and block was different for the two target intervals. For ST, age differences in normalized start times were evident only in the first three session blocks (in the first 3 blocks $ps \leq 0.01$) showing that the average normalized start time of old mice was significantly later than the average normalized start time of young mice (first 3 sessions) and adult mice (first 2 sessions) but these differences disappeared between all pairs with further training (4th and 5th blocks $ps > 0.05$). For LT, significant

age effect was observed only in the first block ($p \leq 0.01$ - see Appendix A.7 Start Times Throughout Session Blocks for details).

For the normalized stop times, main effects of block [$F(2.67,90.90) = 149.86, p < 0.001, \eta_p^2 = 0.82$], age [$F(2,34) = 17.63, p < 0.001, \eta_p^2 = 0.51$], and target interval [$F(1,34) = 111.86, p < 0.001, \eta_p^2 = 0.77$] were significant. Two-way interactions between age and block [$F(5.35,90.90) = 4.07, p = 0.002, \eta_p^2 = 0.19$] and between target interval and block [$F(4,136) = 9.86, p < 0.001, \eta_p^2 = 0.23$] were also significant but the interaction between the age and target interval was not significant [$F(2,34) = 1.97, p = 0.16$]. Finally, the three-way interaction between block, age and target interval was statistically significant [$F(8,136) = 2.73, p = 0.01, \eta_p^2 = 0.14$]. Therefore, we do not report further statistics for the lower order significant effects. Both for ST and LT, the normalized stop times of older mice were later than the younger two age groups for most of the blocks (for ST first 2 blocks' $ps > 0.05$, remaining blocks' $ps < 0.001$; for LT first block's $p > 0.05$, remaining blocks' $ps \leq 0.01$; see Appendix A.8 Stop Times Throughout Session Blocks for details).

In light of these findings and to address whether the stop times were acquired differently by different age groups, the number of trials to the acquisition of the stop thresholds for the short and long target intervals was compared between the age groups. The main effect of age was significant [$F(2,34) = 21.77, p < 0.001, \eta_p^2 = 0.56$]. It took longer for the old mice to acquire the stop thresholds than the young (MD = 55.51, SE = 10.39, $p < 0.001$) and adult (MD = 61.93, SE = 10.39, $p < 0.001$) mice. The main effect of target interval was also significant [$F(1,34) = 38.56, p < 0.001, \eta_p^2 = 0.53$], showing that it took more number of trials on average for the mice to acquire the stop threshold for the ST interval (M = 113.54, SE = 6.83) than the LT interval (M = 80.05, SE = 6.79). There was no significant interaction between age group and the target interval [$F(2,34) = 0.90, p = 0.42$].

2.4.2 Age Differences in IHC Outputs

The neurobiological parameters were compared between the age groups separately for each region. For SNc and VTA (Figure 2.5 & Appendix A.10 Mean Neuron Counts Figure A.2), TH+ neurons were counted for 38 mice in total (young: 10, adult: 13, old: 15). The number of TH+ neurons in SNc [$F(2,35) = 6.52, p = 0.004, \eta_p^2 = 0.27$] and VTA [$F(2,35) = 7.44, p = 0.002, \eta_p^2 = 0.30$] differed significantly between the age groups. The mean number of TH+ neurons in SNc was lower for the old mice compared to the

young (MD = -60.54, SE = 19.86, $p = 0.012$) and adult (MD = -56.40, SE = 18.44, $p = 0.012$) mice. Similarly, the mean number of TH+ neurons in VTA was lower for the old mice compared to the young (MD = -51.65, SE = 13.99, $p = 0.002$) and adult (MD = -33.70, SE = 12.98, $p = 0.04$) mice.

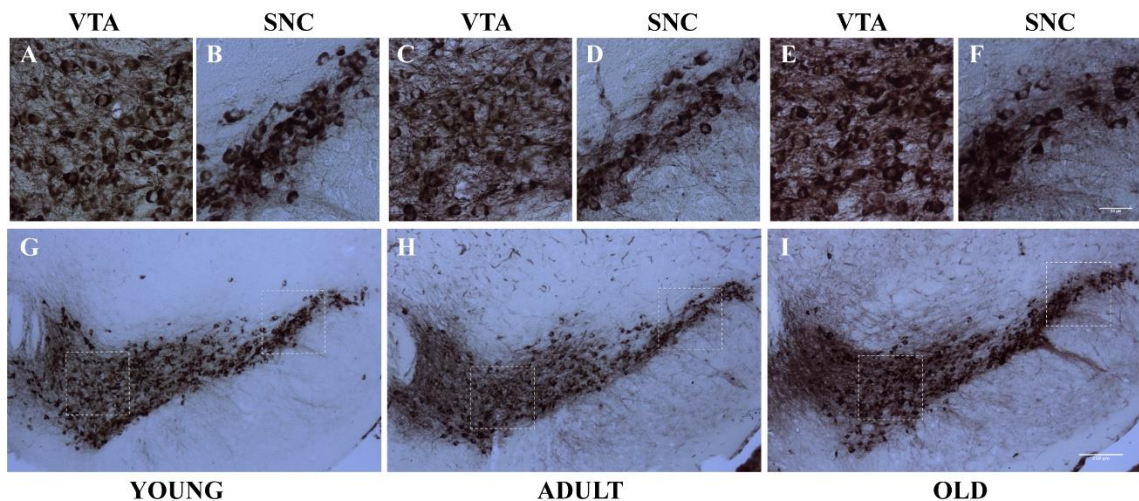


Figure 2.5: Representative images of dark brown immunoreactive TH+ neurons in VTA and SNc on 40 μm sections (5x) for young (G), adult (H) and old mice (I). Images at A, C, E and B, D, F shows smaller windows within targeted regions for VTA and SNc, respectively (20x).

For the MS/DB complex (Figure 2.6 & Appendix A.10 Mean Neuron Counts Figure A.2), ChAT+ neuron counts were done for 54 mice in total (young: 18, adult: 18, old: 18). The number of ChAT+ neurons differed significantly between the three age groups [$F(2,51) = 8.69$, $p = 0.001$, $\eta_p^2 = 0.25$]. The mean number of ChAT+ neurons was significantly lower in the old mice compared to the young (MD = -31.08, SE = 7.87, $p = 0.001$) and adult (MD = -24.67, SE = 7.87, $p = 0.01$) mice.

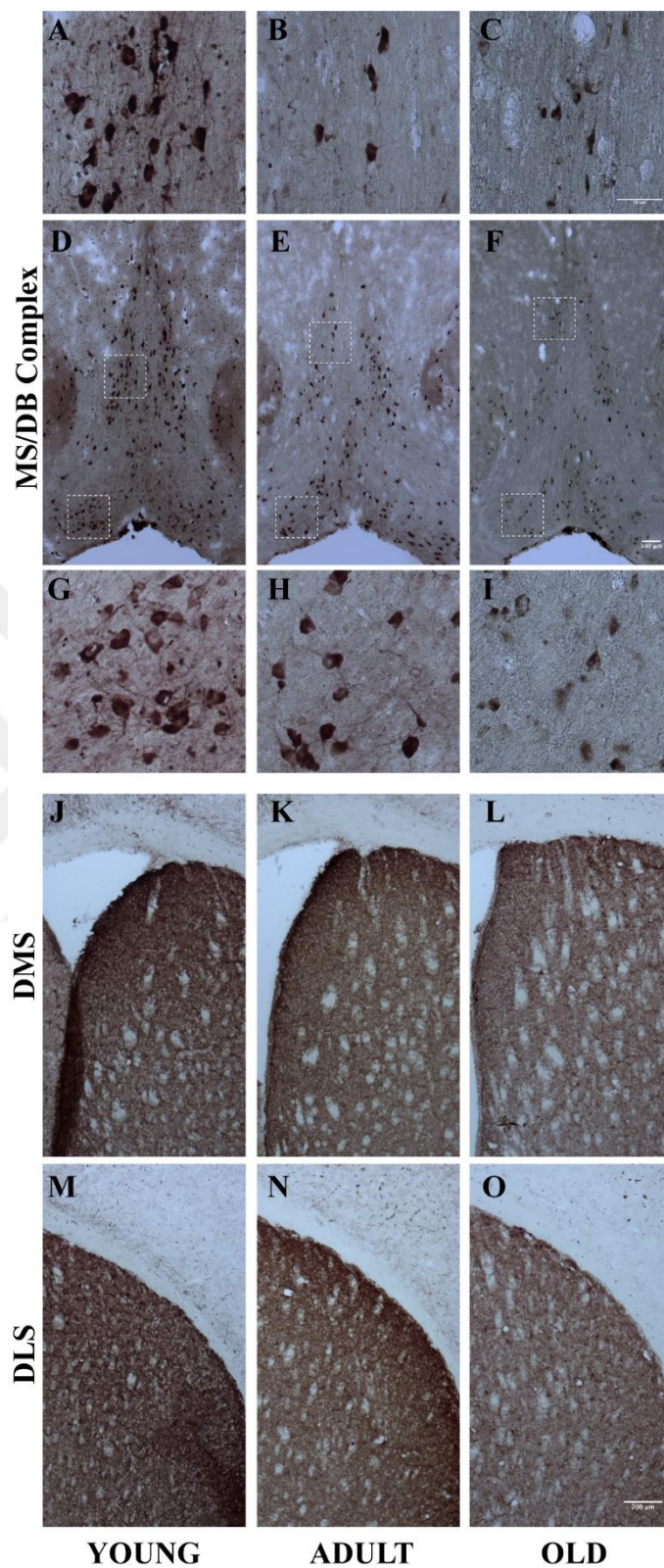


Figure 2.6: Representative images of dark brown immunoreactive ChAT+ neurons in MS/DB complex (D-F) are shown for each age group on 40 μm sections (5x). A-C and G-I, respectively, show enlarged images of selected upper and lower windows on MS/DB

complex (20x). Dark brown immunoreactive TH+ axon terminals in DMS (J-L) and DLS (M-O) are shown for each age group on 40 μ m sections (5x).

For DLS and DMS regions (Figure 2.6 & Appendix A.11 Mean Optic Density of Axon Terminals Figure A.3), the density of the TH+ axon terminals was measured from 42 mice in total (young: 14, adult: 14, old: 14). There was a significant effect of age on the density of the axon terminals of TH+ neurons both in DLS [$F(2,39) = 4.86$, $p = 0.01$, $\eta_p^2 = 0.20$] and DMS [$F(2,39) = 7.48$, $p = 0.002$, $\eta_p^2 = 0.28$]. The mean density in DLS was significantly lower for the old mice compared to young mice (MD = -19.93, SE = 6.44, $p = 0.01$). Similarly, the mean density in DMS was significantly lower for the old mice compared to young mice (MD = 19.91, SE = 5.15, $p = 0.001$).

2.4.3 IHC Output in Relation to Behavioral/Neurobiological Correlates

There was a significant negative correlation between the normalized stop times and the number of TH+ neurons in VTA ($r = -0.55$, $n = 16$, $p = 0.03$). There was also a significant negative correlation between the average number of trials for the acquisition of stop threshold and the number of ChAT+ neurons in MS/DB complex ($r = -0.38$, $n = 27$, $p = 0.049$ - see Appendix A.12 Scatterplots Figure A.4 for scatterplots and correlation coefficients of all measures).

2.5 Discussion

How interval timing is altered with aging is largely unanswered. This is a relevant research question since neurobiological and cognitive functions that are known to change with aging are also implicated for interval timing. Furthermore, interval timing has important roles in many fundamental functions ranging from motor planning to associative learning and thus the elucidation of this question would also be informative in understanding cognitive aging in general. The related-human work has largely led to inconsistent results, which is primarily attributed to the engagement of the compensatory cognitive mechanisms (Turgeon et al., 2016). Thus, although animal research is a better fit to address this question along with its neurobiological aspects, there is only a limited number of related animal studies, which also revealed equivocal findings.

The current work aimed to fill this empirical gap investigating the alterations in the interval timing behavior as well as the relevant neurobiological correlates that accompany it by testing young, adult, and aged mice in the dual PI procedure. Our results revealed

that compared to the young and adult mice, old mice terminated their timed anticipatory responses later in the trial without any apparent differences in start times or the timing accuracy or precision, and overall old mice acquired timed response termination later in training compared to the young and adult mice. Interestingly, the relative contribution of the decision threshold variability was higher (compared to clock speed/memory variability) in the aged mice compared to young and adult mice. These behavioral differences were coupled with prominent age-dependent differences in the number of dopaminergic neurons in the VTA and SNc, cholinergic neurons in the MS/DB complex, and density of dopaminergic axon terminals in the DLS and DMS. From these measures, the number of TH+ neurons in the VTA and ChAT+ neurons in the MS/DB complex were negatively correlated with the stop times and the acquisition of the stop time thresholds, respectively.

The observed behavioral signature of cognitive aging regarding the stop times closely resembled the signature observed with two different transgenic mouse models (i.e., Balci et al., 2009b) and a rat model (i.e., Garces et al., 2018) of Huntington's Disease, behavioral observations with the rodent models of aging (Church et al., 2014, Figure 4), and the effect of scopolamine on peak responding in mice (Abner et al., 2001; Balci et al., 2008). These findings can be interpreted in terms of the loss of temporal control over anticipatory responding in aging; aged animals have difficulty in inhibiting the already initiated goal-directed anticipatory responding following the omission of the reinforcement at the expected delay. This interpretation is in line with the disrupted inhibitory control account of cognitive aging (e.g., Hasher & Zacks, 1988), which can be observed in the form of disrupted behavioral inhibition, cognitive perseveration, or impulsivity (e.g. Head et al., 2009; Morales-Vives & Vigil-Colet, 2012; Potter & Greal, 2008). A recent analysis of the inhibition deficit due to aging indeed suggested that inhibition in terms of ignoring the distraction is intact in elderly; however, it is the suppression of ongoing response in which elderly fails compared to the young subjects (Rey-Mermet & Gade, 2018), very similar to the one we observed in our experiment.

Although mice were trained in a double PI procedure, only one lever was available on any given trial. This makes the interpretation of the differences in stop times complicated since this measure can also be affected by other factors. For instance, Sanabria et al. (2009) showed that the presence of other reinforcers could improve temporal acuity by

constraining the dispersion of timed responding. Under this rationale, the stop time differences could be due to the fact that old mice valued pressing the lever more than engaging in alternative activities such as grooming. Matell & Portugal (2007) also found that providing an alternative response option in the PI procedure might increase the temporal control over behavior through the modulation of thresholds for response initiation/termination. This has been said, findings from one of our recent studies (Gür et al., 2019) support our original interpretation. In that study, mice had two concurrent options associated with reward after a short or long interval and we still observed an age-dependent deficit in terminating timed responding for the short interval (except when probabilistic information favored responding on the shorter option).

In addition to the delayed stop times at steady-state, we also observed that the controlled response terminations occurred later in training in the old mice. Relatedly, while there were no age differences at the beginning of the training in terms of stop times, they started to appear as training proceeded and persisted until the end of the testing. Several previous studies also reported differential acquisition of timed responses (Garces et al., 2018; LeBlanc et al., 1996; LeBlanc & Soffie, 1999) between young and old subjects. Such differences can be attributed to the decision processes provided that clock speed or memory alterations would also affect other indices of timing.

Recently, De Corte et al. (2019) showed that while blocking of D1 receptor in the DMS delayed the stop times as observed in our experiment, blocking of D2 receptors in DMS delayed both the start and stop times. They argued that such a difference might occur due to the differential tuning of start and stop thresholds by striatal dopamine. This argument is compatible with a model of SET (Gibbon & Church, 1990) in which start and stop thresholds can be independent of each other while memory sample varies between trials. The fact that we found age differences between stop times but not start times is consistent with this argument. Moreover, from the analysis of start and stop times over the session blocks, we can conclude that there is differential acquisition of thresholds for the start and stop times, which is consistent with the previous findings demonstrating that controlled stops in the PI procedure emerge later during the training (Balci et al., 2009c).

We found positive start-stop, negative start-spread, and positive middle-spread correlations similar to those reported previously in different species (Balci et al., 2013;

Cheng & Westwood, 1993; Church et al., 1994). While the contribution of clock/memory variability was higher in young and adult mice compared to old, the contribution of threshold variability was higher in aged mice. Previous aging studies that reported uncommon correlation patterns did not find any age differences between the correlations (e.g. Garces et al., 2018; Lejeune et al., 1998). Mattel and Portugal (2007) provided very similar correlational patterns to the ones we observed in aged mice when impulsive responding was not controlled in extensive PI training. In their data, they observed impulsivity in the form of premature responding when mice extensively trained in the PI procedure without an alternative response option. Perseveration or response inhibition, which are different facets of impulsivity, can also lead to the same correlational patterns, as we propose to be the case for the performance of the aged mice in the PI procedure.

Dopaminergic and cholinergic functions are known to be impaired in aging. In support of this view, the number of cholinergic and dopaminergic neurons was also found to differ significantly between the age groups; the aged mice had less number of ChAT+ neurons in MS/DB complex (see also Onozuka et al., 2002) and less number of TH+ neurons in VTA and SNc compared to the young and adult mice (see also Brandt et al., 2017). Importantly, earlier work has shown specifically the mediation of age-related timing deficits by the cholinergic function. In one of these studies, Meck et al. (1986) tested rats intermittently between 10-30 months of age in the PI procedure and arginine vasopressin injection at a young age reversed the disruption in temporal accuracy and precision observed in old rats. The same treatment partially recovered the choline uptake in the frontal cortex. Therefore, Meck et al. (1986) argued that the age-dependent alteration of timing behavior was due to a change in the content of temporal memory which was related to the change in cholinergic activity in the frontal cortex. In another study Meck (2002) did not find any age differences in timing behavior; however, the activity of cholinergic neurons during the behavioral activation was positively correlated with the absolute deviation of subjective time from the target time (i.e., content of the temporal memory). Complementing these earlier studies, Meck (2006) found peak times of old rats were later than the adult rats and single administration of ChAT inhibitor increased the peak time for both age groups gradually with a more prominent effect in the aged rats that were presumed to have a compromised cholinergic function.

Although we did not observe a memory-mediated effect of aging on timing performance, some of the neurobiological (including dopaminergic and cholinergic) factors were associated with several behavioral signatures. For instance, we found that as the number of TH+ neurons in the VTA decreased, stop times of mice increased; this relation did not hold for cell counts in SNc. These findings are in line with the differential behavioral effects of VTA and SNc lesions in rats (Pioli et al., 2008). Pioli et al. (2008) found that bilateral SNc partial lesions disrupted fine motor functions whereas the bilateral VTA partial lesions induced perseveration. The relationship between the cell count in VTA and stop times might be mediated by the prefrontal dysfunction due to lowered dopaminergic input. Relatedly, by use of pharmacological manipulation and optogenetics Narayanan et al. (2012) found that temporal control relies on the mesocortical dopaminergic modulation of the prefrontal cortex via D1 receptor both in rats and mice. But since Narayanan et al. (2012) only looked at FI responding, these results are based only on the “pre-peak” leg of the response curve, which did not differ between the age groups in our study.

Although previous studies reported the role of corticostriatal projections in timing behavior (Emmons et al, 2017;2019; De Corte et al., 2019), we did not find any significant correlations between the timing indices and the dopaminergic axon density in DMS or DLS. For instance, Emmons et al. (2017) showed that inactivation of corticostriatal projections deteriorated interval timing behavior and time-related neural ramping activity. Importantly, optogenetic stimulation of axonal projections of medial frontal cortex (MFC) in DMS recovered interval timing performance and time-related activity in the STR only when MFC was inactivated (Emmons et al., 2019) and the blockade of both D1 and D2 receptors in DMS and DLS disrupted different indices of timing behavior (De Corte et al., 2019). Despite the lower density of dopaminergic axon terminals in DMS/DLS of old mice, the fact that we did not find significant relationships between timing behavior and STR might suggest that top-down control of striatal activity was still intact in old mice. Future studies can elucidate the adaptive/protective mechanism(s) in old mice that compensates for such neurobiological changes given that neuron density in a specific region alone might not be a direct indicator of the overall functioning of this region.

Another significant finding is that the number of ChAT+ neurons in MS/DB complex was negatively correlated with the rate of the stop threshold acquisition. In relation to the

acquisition of an operant response, previous work showed that cholinergic input to the rodent primary visual cortex from the basal forebrain region has a role in the acquisition of reward timing but not in its expression (Chubykin et al., 2013). This observation is in line with the relation of ChAT+ cell count in MS/DB complex with the acquisition of stop times but not their parametric expression. Pointing at the non-temporal effects of cholinergic function, Zhang et al. (2019) showed that although scopolamine administration impairs timing behavior in FI schedule, this effect was due to altered stimulus-related processing rather than temporal processing in the MFC. Different from these studies, Meck and Church (1987) however showed that lesioning medial septal area resulted in a gradual reduction in the remembered time of the reinforcement in the PI procedure, which was attributed to its effect on temporal memory. The opposite pattern was observed with lesions of nucleus basalis magnocellularis and frontal cortex.

Oprisan & Buhusi (2011) have offered a clearer theoretical link between cholinergic function, mesocortical dopamine projections to the frontal cortex and interval timing within the framework of Striatal-Beat-Frequency (SBF) Model. They attributed dopaminergic activity in the mesocortical projections to clock-speed (via changing the firing frequency of cortical oscillators) whereas cholinergic activity was attributed to long-term memory. They demonstrated that their model accounts for the behavioral effects of pharmacological manipulations. Our findings constitute at least a partial challenge for this model; we did not observe any relationship between ChAT+ neurons and behavioral outputs that would reflect temporal memory alterations. Furthermore, although our study was not designed to test for clock speed effects since these effects would be observable in acute treatment regimes, changes in the clock speed would also be expected to be reflected in temporal precision, which was not observed in our study. The lack of a relationship between start times and the number of TH+ neurons in VTA form a challenge also for approaches that attribute dopaminergic effects on timing behavior to incentive motivation (Balci, 2014). Further studies are needed to elucidate the role of these different neurobiological mechanisms in age-dependent alterations in timing behavior (e.g., by integrating optogenetics with aging experiments). Although we have observed only two statistically significant direct relations between the neurobiological measures and behavioral measures, one can also observe that the absence of behavioral differences is accompanied by the absence of differences in neurobiological measures

between young and adult mice. Note that the outputs of the pre-planned correlation analyses between neurobiological and behavioral variables were not corrected for multiple-comparisons and thus they should be interpreted with caution.

Based on our findings, it is unclear whether the observed deficits are due to a learning deficit or a performance deficit because subjects were both trained and tested within their particular age range. One way to address this issue would be to train all subjects at a young age but to test their timing performance at different ages (although this would result in differential retention intervals for different age groups). Another important issue is that visual inspection of Figure 2.1 suggested that the age-dependent differences were more prominent for short compared to the long target interval. Thus, caution should be exercised in concluding that the aging deficit applies to all interval ranges.

Our results show that aging in mice leads to a prominent deficit in terminating timed anticipatory responses and that age-related differences in VTA-localized dopaminergic function underlies this impairment whereas age-related changes in cholinergic function is associated with the acquisition of the termination of timed responding. Overall, our results point at the age-dependent changes in the decisional components of interval timing. These findings could have implications regarding the nature of aging-related cognitive and behavioral deficits, particularly in relation to perseveration in the context of timing.

Chapter 3

PROBABILISTIC INFORMATION MODULATES THE TIMED INHIBITION DEFICIT IN AGING MICE

3.1 *Abstract*

How interval timing is affected by aging constitutes one of the contemporary research questions. There is however a limited number of studies that investigate this research question in animal models of aging. The current study investigated how temporal decision-making is affected by aging. Initially, we trained young (2-3 month-old) and old C57BL/6J male mice (18-19 month-old) independently with short (3s) and long (9s) intervals by signaling, in each trial, the hopper associated with the interval that is in effect in that trial. The probability of short and long trials was manipulated for different animals in each age group (25% or 75%). During testing, both hoppers were illuminated, and thus active trial type was not differentiated. We expected mice to spontaneously combine the independently acquired interval-location-probability information to adaptively guide their timing behavior in test trials. This adaptive ability and the resultant timing behavior were analyzed and compared between the age groups. Both young and old mice indeed adjusted their timing behavior in an abrupt fashion based on the independently acquired temporal-spatial-probabilistic information. The core timing ability of old mice was also intact. However, old mice had difficulty in terminating an ongoing timed response when the probability for the short trial was higher and this difference disappeared in the group that was exposed to a lower probability of short trials. These results suggest an inhibition problem in old mice as reflected through the threshold modulation process in timed decisions, which is cognitively penetrable to the probabilistic information.

3.2 Introduction

How temporal information processing is altered in aging is a fundamental research question (Xu & Church, 2017). Results gathered from human and animal studies targeting this very question have vastly led to equivocal conclusions regarding the health of temporal information processing in aging (e.g., Balcı et al., 2009a; Turgeon et al., 2016). Most of these studies have assessed timing performance with no-to-minimal focus on how other relevant parameters such as probabilities and spatial locations are integrated into temporal information processing. In order to fill this empirical gap, the current study investigated how the core features of interval timing performance, the integration of probabilistic information into timing behavior, and the spontaneous behavioral adjustments based on previously acquired information regarding these parameters are altered in the mouse model of aging.

Anecdotal evidence based on the personal reports suggests that subjective time flows faster with aging (Friedman, 2013). Theoretic treatment of this observation coupled with convergent evidence suggesting slower information processing in old age (Salthouse, 1996; but see Starns & Ratcliff, 2010) suggests that the internal clock slows down with aging. This conclusion is supported by slower and more variable tapping in very simple tasks (i.e., unpaced finger-tapping - Turgeon & Wing, 2012; Vanneste et al., 2002). Other studies using dual-task paradigms have also demonstrated disrupted timing performance, which is attributed to the disrupted allocation of attentional resources between temporal and non-temporal aspects of the tasks (for review see Balcı et al., 2009a). These earlier studies do not address the ability of older organisms to integrate other task-relevant parameters with temporal information for guiding adaptive actions.

Our earlier work has shown that humans and mice can integrate probability information into their temporal decisions in an adaptive fashion (e.g., maximizing reward-rate; Akdoğan & Balcı, 2016; Balcı et al., 2009b; Çoşkun et al., 2015; Kheifets & Gallistel, 2012) and they can do this abruptly and spontaneously (Tosun et al., 2016; for a review see Gür et al., 2018). Regarding these functional endpoints, earlier studies show that sensitivity to probabilistic information is higher in young compared to elderly (Howard et al., 2008), which becomes more pronounced with extended practice (Simon et al., 2010). Despite these differences in the utilization of probabilistic information, the ability

to detect probabilities were reported to be intact in elderly when young and old participants were equated on memory encoding capacity (Spaniol & Bayen, 2005).

The current study investigated how the nature and degree of integration of probabilistic information into temporal decisions as well as the resultant timing behavior change with aging. To this end, we first trained young and old mice independently on two temporal options with different probabilities in an autoshaping setting. In order to probe and assess the timing performance of mice and their ability to modulate their timing behavior based on previously and independently experienced probabilistic and spatiotemporal relations, we introduced an experimental setting that required the spontaneous integration of these variables for adaptive anticipatory responding.

3.3 *Material and Methods*

3.3.1 *Subjects*

Subjects were 34 experimentally naive male C57BL/6J mice purchased from Koç University Animal Research Facility. Sixteen of the mice were approximately two months old and 18 mice were 18 months old at the start of the experiment. Two old mice died of natural causes and could not complete the experiment. Another old mouse was excluded from the data analysis due to the lack of data points required to make the model fits. Consequently, data from 31 subjects were analyzed. Animals were housed in groups of three to five in polycarbonate cages (Allentown type I long individually ventilated cages) in rooms that were illuminated on a 12:12-h light:dark cycle (lights on at 6:00 AM). Subjects were tested during the light cycle on consecutive days. Three days prior to the start of the experiment, mice were subjected to a food deprivation protocol with ad libitum access to water. After each experimental session, they were given additional food pellets to maintain them at 85% of their free-feeding weight. All procedures reported here were approved by Koç University Animal Research Local Ethics Committee (Protocol Numbers: 2013-2 and 2014-13).

3.3.2 *Apparatus*

Mice were tested in operant chambers with metal end walls, and transparent plexiglass side walls and ceiling. In one of the end walls, there were three illuminable food hoppers. Hoppers at the extreme sides were active to deliver 0.01 mL of diluted liquid feed (Nestlé

Nutrition Isosource, vanilla flavor) as the reward and to signal time intervals. On the opposite wall, levers were retracted at all times. The nose poke hole in between the levers was used for mice to initiate the trials. Head entries to the food magazines and the nose poke hole were detected via IR beam break detectors. MED-PC IV software was used to run the experiment and record the data. All events were logged and time-stamped with a resolution of 10 ms. The boxes were ventilated throughout all sessions.

3.3.3 Procedure

Training Phase

Mice were trained on two types of trials, 3 s (short) trials and 9 s (long) trials, which were presented in a randomly intermixed fashion. Each feeding hopper was associated with one of the two trial types (counterbalanced between subjects). The nose poke hole was illuminated to signal that a trial could be initiated upon responding there. When the subject initiated the trial, the feeding hopper associated with the current trial type was illuminated. The light stayed on for the duration of the trial type and the reward was delivered irrespective of the subject's response at the light offset for 6 s (autoshaping). The inter-trial interval (ITI) was fixed 30 s delay plus an exponentially distributed random variable with a mean of 60 s. Each session lasted for an hour. Regardless of the subjects' performance to collect rewards, each subject took the first test session after 20 training sessions. Importantly, mice in each age group were divided into two groups and trained separately with the following probability conditions for trial type: $p(\text{short}) = .25$ and $p(\text{short}) = .75$. Upper panel of Figure 3.1 depicts the training protocol and typical behavioral pattern observed during short and long trials.

Test Phase

The test phase was identical to the training phase, except that instead of a single (active) hopper illumination, both feeding hoppers were illuminated for the entire duration of the trial type. Same short trial probabilities used in the training were used during testing. The test session was two-hours long. The lower panel of Figure 3.1 shows the long test trials and typical switch behavior observed during these trials. After the test session, subjects went through the training protocol for one daily session and testing protocol for one daily session, each lasted for two hours, in two consecutive days.

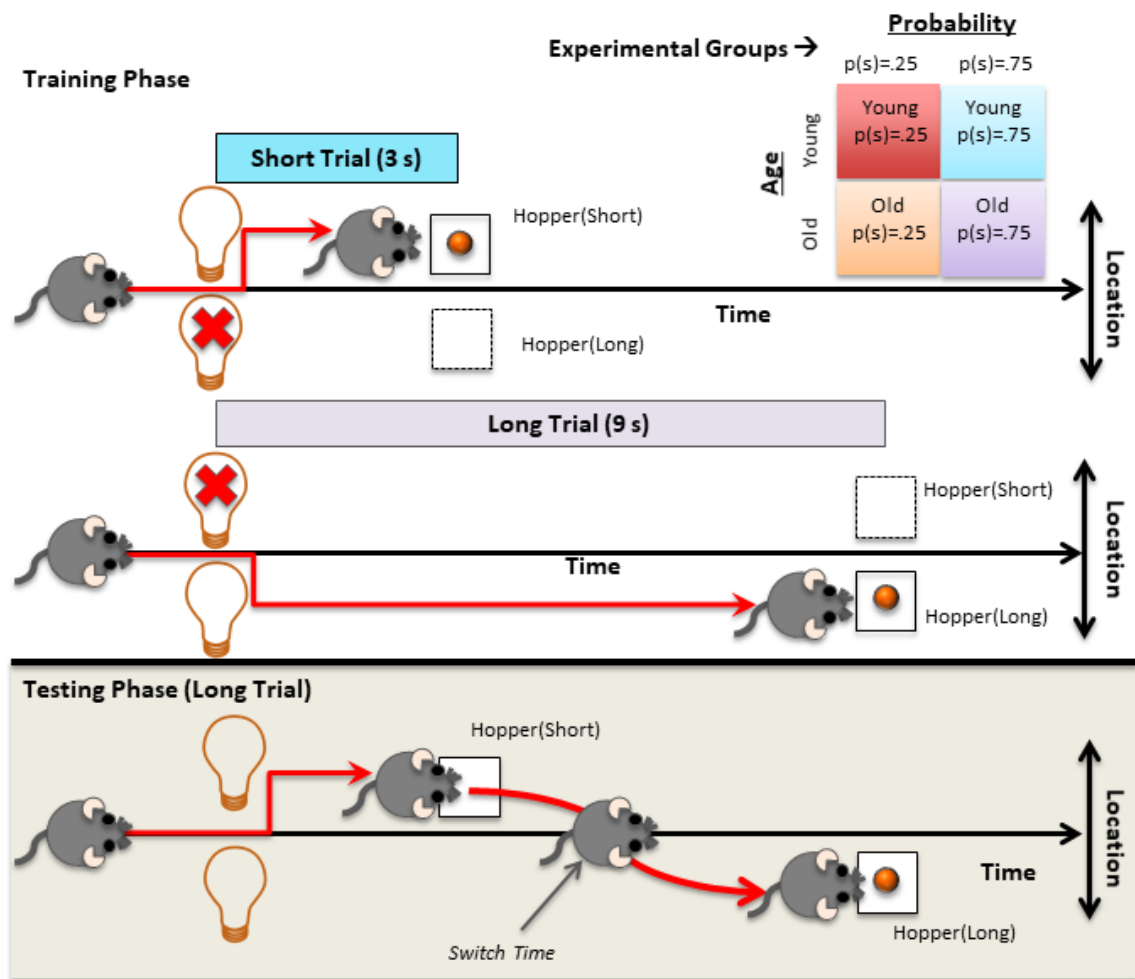


Figure 3.1: Graphical depiction of the procedures applied during training and testing along with the depiction of the typical behavior observed in the corresponding trials. Top right table depicts the four different experimental groups (2 age groups X 2 probability conditions).

3.3.4 Data Analysis

Switch latencies (or switch times) were defined as the time mice left the short duration hopper for the long duration hopper in the long trials since the illumination of the hopper(s). These latencies were used to calculate the mean switch time and coefficient of variation ($CV = \text{Standard Deviation}/\text{Mean}$) for each subject based on the Weibull function fits to the data collected during two test sessions. Model fits were done using maximum likelihood estimation method. Note that in the calculation of switch rates we limited our definition of switches in the long trials to the ones which were earlier than 9 s given that switches after that point were “contaminated” by the presentation of reward in the hopper associated with the long duration. This resulted in only a few exclusions in the training

phase as switch behavior was rare during this phase (2 young and 3 old mice had relatively higher switch rates – see Figure 3.2). We also computed switch rates (the number of switches divided by the number of long trials) for the last training session and two test sessions combined. Two test sessions were evaluated by combining the data since the results were similar when we applied the analysis for individual test sessions. The same analysis (on switch rate and time) was conducted also for the first hour of the initial test session to be able to compare the results to those of Tosun et al. (2016) study. The results of this additional analysis that replicated our earlier findings are presented in Appendix B along with the comparable analyses of the data from Tosun et al. (2016).

Acquisition of the task during training in relation to the timing of first responses in both locations was examined in order to see whether there was a difference between the age and probability groups throughout the training. First, the time of first visits to the short location in the short trials and the time of first visits to the long location in the long trials were extracted, which were then averaged for each session and mouse. Then, the time of first visits was regressed on the session order for each mouse separately for the first short and first long location responses in the short and long trials, respectively. The acquired slopes were compared between the age and probability groups as well as between the short and long trials. Additionally, to see if there is any learning/adjustment in switch times throughout the first test phase, we first regressed the switch times on their order of occurrence and compared them between the experimental groups.

We were also interested in the beginning and termination of reward anticipation in short location and the beginning of reward anticipation in the long location in the long trials of the test sessions. Since long trials terminated with reward delivery, we could not compute the termination of reward anticipation for the long location. The anticipation of reward is captured by the high state of responding at the location of reward delivery in a given trial. Time points that mark the beginning and end of the high state are referred to as start (s_1) and stop (s_2) times. Here, we used cumulative sum test (CUSUM) with absolute residuals to detect the trial times at which subjects transitioned from low-to-high (s_1) or high-to-low (s_2) state of responding at the short and long locations in each long trial (Church et al., 1994). Times that maximized the difference between high and low rates were calculated by $t_1(r-r_1)+t_2(r_2-r)+t_3(r-r_3)$ separately for the short and long location responses, respectively; t_1 is the time from the beginning of trial until s_1 , t_2 is the time

between s_1 and s_2 , t_3 is the time between s_2 and the end of trial, r is the overall mean response rate, r_1 , r_2 , and r_3 are the mean response rates during t_1 , t_2 , and t_3 , respectively (Church et al., 1994). During the detection of start/stop times for a given trial, the algorithm detected the start and stop times of short location responses first. The search for the start time of long location responses was started from the stop time of short location responses. If there was no short response in that trial, the start time of long location responses was searched from the beginning of the trial. Any start or stop time later than 9 seconds (time of reward delivery) were excluded from the analysis (8% of all trials).

After the detection of start/stop times of short location responses and start times of long location responses, CV of each measure was also calculated for individual subjects. The point of maximum expectancy for the reward in the short location (i.e. middle time) was defined as the mean of start and stop times of short location responses. Difference between start and stop times of short location responses (spread) was also calculated as an index of timing uncertainty for a given trial.

The analysis of variance was used to make comparisons between age and probability groups for the slope of the first response times for training, slopes of switch times during the test, switch rates during training/testing, switch times, CV of switch times, start and stop times of short location responses. In the case of assumption violation, we used t-test by splitting subjects by one of the variables. We refer the readers to the Appendix B.3

Analysis of Complementary Measures for the statistical comparisons of age and probability conditions for CVs of start and stop times of short location responses, middle times and spread of the short location responses, start time of the long location responses and its CV. Raw data were processed using Matlab to acquire parameters for each individual subject. Statistical comparisons were conducted using SPSS 24 and/or JASP (Jasp Team, 2019).

3.4 Results

3.4.1 Acquisition During Training and Test Phase

Comparison of the individual slopes acquired from the timing of first responses at short and long locations on the short and long trials, respectively, revealed that the (absolute value of) slopes of the first response time of short location responses was significantly

higher than the slopes of the first response time of long location responses, $[F(1, 26) = 14.78, p < .001 (M_{\text{short}} = -.67 (.06) \text{ vs. } M_{\text{long}} = -.41 (.06)]$. Neither the main effect of age $[F(1, 26) = 1.08, p = .31]$ nor the probability $[F(1, 26) = 3.15, p = .09]$ were significant. The interaction effects of trial type*age $[F(1, 26) = .94, p = .34]$, trial type*probability manipulation $[F(1, 26) = 2.70, p = .11]$, age*probability manipulation $[F(1, 26) = .05, p = .83]$, and trial type*age*probability manipulation $[F(1, 26) = 3.20, p = .09]$ on these slopes throughout the training phase were also not statistically significant.

The analysis of slopes of switch times as a function of their order of occurrence within the first test session based on conventional tests revealed that there was a significant slope in only 4 out of 31 cases. Consistently, the corresponding Bayesian analysis supported the alternative hypothesis only in 6 cases, and only two of these six cases were based on strong evidence while the rest had only anecdotal evidence. Comparison of these values between age and probability groups revealed that there was no main effect of age $[F(1, 27) = .04, p = .85]$, main effect of probability $[F(1, 27) = 1.19, p = .29]$, or age*probability interaction $[F(1, 27) = 2.73, p = .11]$. Briefly, our results did not point at any age-dependent differences in the acquisition of timed responses.

3.4.2 Switch Rates in Training vs. Test Sessions

Difference between the switch rates during the long trials of training and test sessions reflects whether mice can utilize information acquired during the training phase to adaptively respond in the ambiguous situation created in the test session. Raster plots show the response patterns observed in every trial both for training and testing sessions of each subject (Figure 3.2). During training, switch behavior was rare when only the location of reward delivery was signaled (first and third columns of Figure 3.2). However, in the test sessions in which both options were signaled, in the long trials mice often switched to the long location after first visiting the short location (second and fourth columns of Figure 3.2). We compared the difference between switch rates of training and testing as well as the age differences in the switch rates.

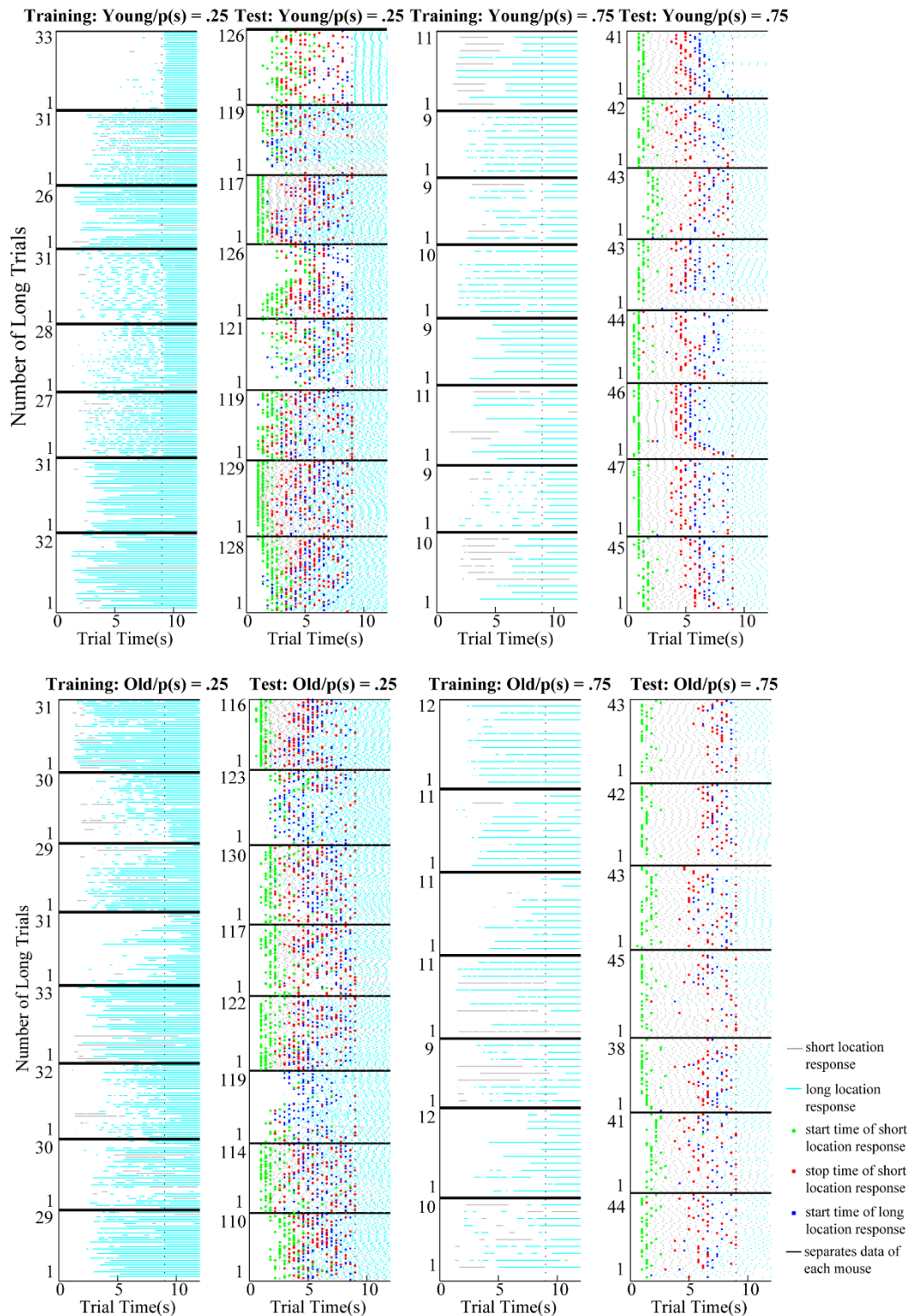


Figure 3.2: Raster plots of short (grey) and long (cyan) location responses in the long trials of training (columns 1 & 3) and test (columns 2 & 4) sessions. Upper and lower panels show the data collected from young and old mice, respectively. Horizontal tick black lines separate the data collected from each mouse. Vertical dotted black lines show the time of reward delivery in the long trials (9 seconds). Mice rarely switched from the

short location to the long location during the long trials of the training session; however, timed switches were apparent from the outset during the long trials of testing in both age groups. Green, red, and blue dots correspond to the start time of short location responses, stop time of short location response, and start time of long location responses estimated from the single trial analysis, respectively.

A mixed design ANOVA with age as the between-subjects factor and time of measurement (last training session vs. test sessions) as the within-subjects factor revealed a significant main effect of phase on switch rates both for $p(\text{short}) = .25$ [$F(1, 14) = 93.66$, $p < .001$, partial $\eta^2 = .87$; $M_{\text{training}} = .11 (.02)$ vs. $M_{\text{test}} = .69 (.06)$] and $p(\text{short}) = .75$ [$F(1, 13) = 82.33$, $p < .001$, partial $\eta^2 = .86$; $M_{\text{training}} = .25 (.07)$ vs. $M_{\text{test}} = .83 (.03)$] conditions. In other words, mean switch rates increased substantially from the training phase to the test phase in both probability conditions (Figure 3.3A). The main effect of age on switch rates was not significant in $p(\text{short}) = .25$ [$F(1, 14) = .23$, $p = .64$; $M_{\text{young}} = .39 (.05)$ vs. $M_{\text{old}} = .42 (.05)$] or $p(\text{short}) = .75$ [$F(1, 13) = .62$, $p = .44$; $M_{\text{young}} = .57 (.06)$ vs. $M_{\text{old}} = .50 (.07)$] groups. Interaction of age and time of measurement was not significant [$p(\text{short}) = .25$: $F(1,14) = .15$, $p = .71$ & $p(\text{short}) = .75$: $F(1,13) = .87$, $p = .37$], either. These results suggested that timed-switching was an emergent behavior due to new (ambiguous) task demands both in young and old mice regardless of probability condition [Note: Probability was not included in the analysis as a factor but when it was included, nonparametric tests (Mann-Whitney U Test) were run due to the violation of homogeneity of variance assumption. The effect of probability on switch rate was not significant ($p_{\text{training}} = .47$, $p_{\text{test}} = .09$)]. The same results held even when the data from the first hour of the initial test session was analyzed between the phases and age groups (for details see Appendix B.1 Switch Rate and Switch Latencies (Times) in the First Hour of the Initial Test Session).

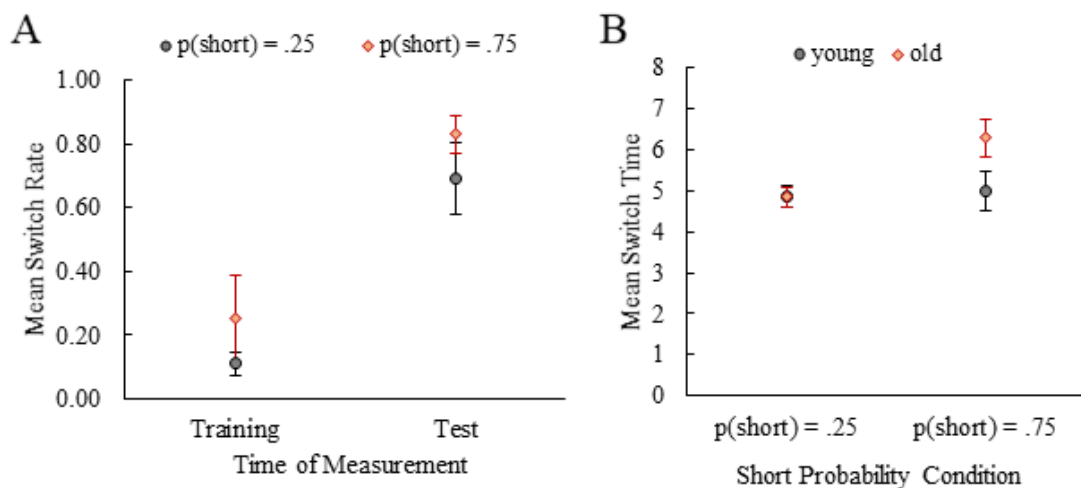


Figure 3.3: Mean switch rates for the last training session and two test sessions combined (A). Mean switch times of young and old mice by short probability conditions (B). Error bars show 95% confidence intervals (Mean \pm 1.96*SE).

3.4.3 Switch Times in Test Session

We also analyzed the effect of age and probability manipulation on switch time as well as their interaction given that timed behavior might have deteriorated with age and previous work showed that probability manipulation exerts an effect on switch times. A 2x2 ANOVA with age (young vs. old) and probability condition (.25 vs. .75) as between-subject factors revealed main effects of age ($F(1, 27) = 12.09$, $p = .002$, partial $\eta^2 = .31$) and probability manipulation ($F(1, 27) = 18.31$, $p < .001$, partial $\eta^2 = .40$). Old mice ($M = 5.52$, $SE = .23$) had later switch times compared to young mice ($M = 4.93$, $SE = .13$). Switch times were later for the mice in $p(\text{short}) = .75$ condition ($M = 5.60$, $SE = .23$) compared to $p(\text{short}) = .25$ condition ($M = 4.85$, $SE = .09$). Importantly, these main effects were coupled with a significant interaction of age and probability, $F(1, 27) = 12.52$, $p = .001$, partial $\eta^2 = .32$. In $p(\text{short}) = .25$ condition, mean switch times of young and old mice did not differ, $MD = .01$, $SE = .26$, $p = .97$. In $p(\text{short}) = .75$ condition, on the other hand, the mean switch time of old mice was significantly later than mean switch time of young mice, $MD = -1.29$, $SE = .27$, $p < .001$. Figure 3.3B shows the mean switch times for both probability conditions by age. These results revealed an age difference in timed switching behavior moderated by training with different trial probabilities. When we analyzed the switch times from the first hour of the initial test session, the effect of probability manipulation was evident, but we did not observe an age and probability

interaction (see Appendix B.1 Switch Rate and Switch Latencies (Times) in the First Hour of the Initial Test Session).

As an indicator of temporal precision, we analyzed the CV values. A two-way ANOVA was conducted to see the effects of age and probability on CV of the switch times. Results showed that there was a significant main effect of probability condition; mice in $p(\text{short}) = .25$ condition ($M = .39$, $SE = .02$) had higher CV on average compared to $p(\text{short}) = .75$ condition ($M = .20$, $SE = .01$) regardless of the age ($F(1, 27) = 63.02$, $p < .001$, $\text{partial } \eta^2 = .70$). There was no main effect of age, $F(1, 27) = .08$, $p = .79$ or interaction effect between age and probability manipulation, $F(1, 27) = .12$, $p = .74$. These results suggested that the temporal precision of young and old mice was comparable.

3.4.4 Timed Anticipatory Responses During Test Session

Not only the timed-switching pattern of a subject in the timed switch task but also the timing of short and long location responses separately might allow us to characterize anticipatory behavior in more detail to investigate age differences in interval timing. To do so, we compared several measures of timing behavior that reflect distinct processes within interval timing between age and probability groups. The analysis was limited to long trials during testing, allowing us to characterize timing behavior during reward omissions for short location responses, and prior to reward presentation for long location responses. Figure 3.2 provides each subject's data on a trial-by-trial basis showing short location responses and long location responses during training and test sessions as well as start and stop times extracted for the test phase. Figure 3.4 presents the normalized averaged response curves for the short and long location responses in order to provide an overall idea about the timing performance of young and old mice.

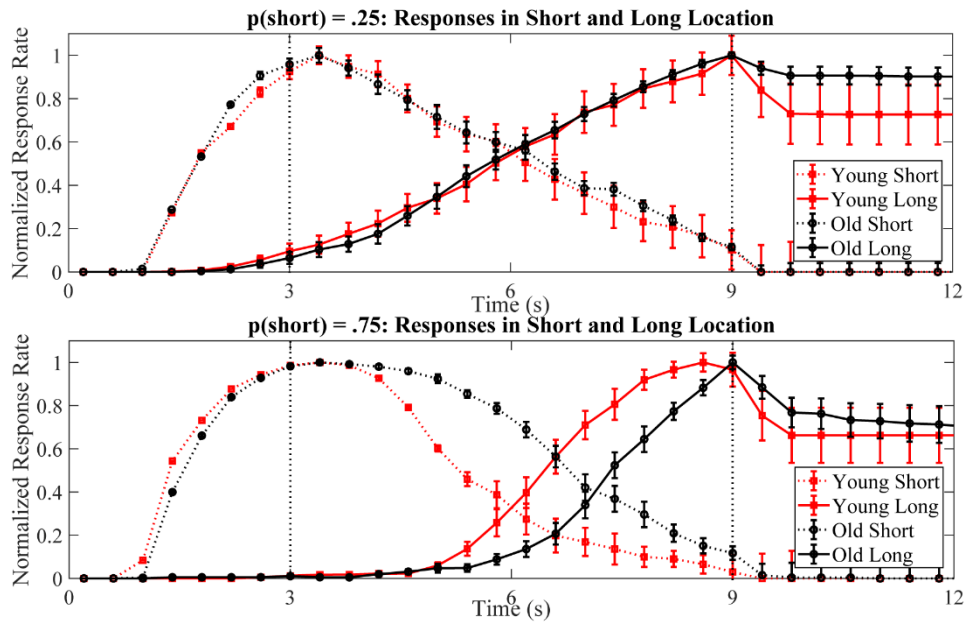


Figure 3.4: Normalized averaged response curves for short and long location responses during long trials of test sessions for young (red) and old (black) mice in different probability conditions. Dotted vertical lines represent the time of reward delivery in short and long locations; however, note that there was no reward delivery in the short location during long trials. Early in the trial, the normalized response rate was higher for the short location (dotted black and red curves) and it peaked around 3 seconds. For the long location, the normalized response rate increased (solid black and red curves) later in the trial. Error bars show the standard error of the actual mean values.

Comparisons of start times of the short location responses were done between young and old mice and probability conditions (Figure 3.5A) by splitting data for one of the variables due to the violation of homogeneity of variance assumption. When the data were split by age, we found that start times of the short location responses were later in $p(\text{short}) = .25$ condition compared to $p(\text{short}) = .75$ condition both in young ($t(8.90) = 3.15, p = .01$) and old mice ($t(8.81) = 3.22, p = .01$) on average. After splitting the data by probability condition, there were no differences between young and old mice in $p(\text{short}) = .25$ ($t(14) = .20, p = .85$) and $p(\text{short}) = .75$ ($t(13) = -.89, p = .39$) conditions. Mean start time of the short location responses were 2.68 (SE = .40) and 1.35 (SE = .15) for young mice and 2.58 (SE = .31) and 1.52 (SE = .11) for old mice in $p(\text{short}) = .25$ and $p(\text{short}) = .75$ conditions, respectively.

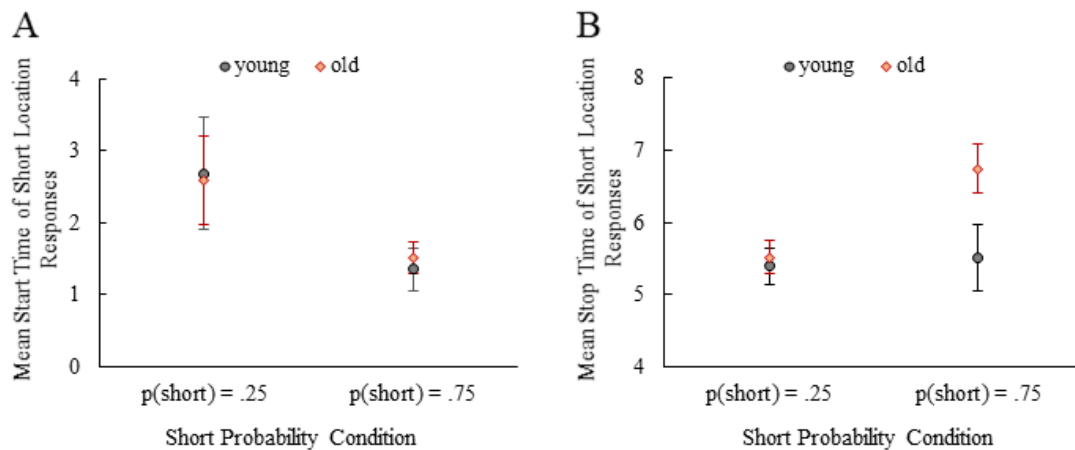


Figure 3.5: Mean start time of short location responses (A) and mean stop time of short location responses (B) depending on age and probability conditions. Error bars show 95% confidence intervals (Mean \pm 1.96*SE).

The effect of age and probability was also examined for the stop times of short location responses (Figure 3.5B). Mean stop time of short location responses was significantly earlier for young mice compared to old mice, $F(1,27) = 16.52$, $p < .001$, partial $\eta^2 = .38$. There was also a significant main effect of probability manipulation showing that mean stop time of short location responses were earlier in $p(\text{short}) = .25$ condition compared to $p(\text{short}) = .75$ condition, $F(1,27) = 16.28$, $p < .001$, partial $\eta^2 = .38$. Importantly, we found a significant interaction of age and probability on the mean stop time of short location responses, $F(1,27) = 11.11$, $p = .003$, partial $\eta^2 = .29$. Simple effect analysis showed that the mean stop time of short location responses were comparable between young and old mice in $p(\text{short}) = .25$ condition, $MD = -.12$, $SE = .23$, $p = .60$. However, aged mice stopped responding in the short location significantly later than the young mice in $p(\text{short}) = .75$ condition, $MD = -1.24$, $SE = .24$, $p < .001$. These findings can also be observed at normalized averaged response curves in Figure 3.4 (compare two panels).

3.5 Discussion

This study investigated age differences in temporal decision-making, anticipatory timing behavior, and spontaneous integration of task parameters into temporally controlled goal-directed responses. Our results revealed that both young and old mice were able to adopt a novel action plan during testing (i.e. timed switching) that required them to take into account the previously and independently learned temporal characteristics and probabilities of reinforcement at two different choice locations. This observation was

evident in significantly higher timed switching rate found in test sessions compared to training regardless of the age group (irrespective of the duration of testing). Age differences were observed in switch times and stop times for short location timed responses that were moderated by the probabilities of options. Specifically, when the probability of reward delivery after the short interval was high; old mice persevered more at the short-latency option. As expected, this difference between the age groups was reflected in both switch time and stop times for the short location responses; two highly correlated measures [$r = .95$, $N = 31$, $p < .001$].

Observed response perseveration shows parallelism to other findings reported in the literature in relation to neurodegenerative conditions (e.g., Huntington's Disease, Balci et al., 2009b), disruptive effect of scopolamine (typically used as a model of dementia; Ebert & Kirch, 1998) on the peak interval responding (Abner et al., 2001; Balci et al., 2008) and it is consistent with the effect of aging on single peak procedure (see Figure 4 bottom panel at Church et al., 2014). On the other hand, interestingly the observed disruption of timing behavior in terms of the termination of timed responses was present only when the probability was an independent source of bias favoring the reward delivery at the short-latency option. Combined with our previous findings outlined above, this empirical observation suggests that the inhibition deficit can be rescued when the likelihood of the corresponding option does not favor the option associated with the to-be inhibited action (i.e., $p(\text{short})=.25$) possibly as an independent source of cognitive control.

In line with this rationale, previous studies on behavioral inhibition have also suggested that the manipulation of stimulus probabilities that signal to act or not to act alters the behavioral inhibition performance by modulating the strength of response preparation process (e.g., Bruin & Wijers, 2002). Therefore, we suggest that the inhibitory control integrates multiple sources of information including different quantities/dimensions such as time and probability.

Our empirical observations are also consistent with the weakened inhibitory control theory of cognitive aging (Coxon et al., 2012; Kramer et al., 1994; Potter & Grealy, 2008). For instance, older individuals have also been shown to persevere with a previous rule on the Wisconsin Card Sorting task (Ashendorf & McCaffrey, 2007). Possibly reflecting similar perseverative tendencies, older rats and mice were found to exhibit lower

spontaneous alternation performance compared to young rats (Willig et al., 1987) and mice (Stone et al., 1992). These results point to cognitive perseveration as the possible common factor. Inhibitory (action) control in aging is typically evaluated in relation to the signaled termination of an initiated response (e.g., stop signal reaction time task). These studies reported a slower reaction to stop signals for the elderly (Bruin & Wijers, 2002; van de Laar et al., 2011). A recent meta-analytic study also concluded that inhibition deficits due to aging are specifically seen in the form of suppressing dominant response rather than ignoring distractor information or response interference (Rey-Mermet & Gade, 2018). In our case, such inhibition problem in old mice was evident in the delayed switch and stop times (and thus an ongoing response) specifically when the trial probability favored the short option, which presumably turns the ongoing responses in the short location into a dominant response that could not be inhibited by older mice.

Several different neural mechanisms have been implicated for such inhibitory control deficits. However, the current study cannot differentiate if the observed deficit in inhibitory control is due to altered functional connectivity in cortico (right inferior frontal gyrus and presupplementary motor area)-subthalamic nucleus (Coxon et al., 2012), fronto-basal ganglia (Suchy et al., 2013; for instance in relation to hyperkinetic perseveration; Goldberg, 1986) or another circuit that has been implicated with inhibitory control deficit in aging. Future studies needed to elucidate the role of these candidate neural circuitries for the observed effects and their relationship to timing behavior.

Our results also show that the processes of spontaneous integration of information that were gathered independently during the prior experience were not affected by cognitive aging. All the indices of timing performance (except for the stop times for short location) were comparable between the two age groups. There was an interaction effect of age and probability on the stop times of the short location responses. A disruption in the core timing component (i.e. clock) or memory would predict shifts in both the start and stop times by the same amount and in the same direction, which was not the case in our study.

Observed differences in our study are most likely related to the factors that relate to the decision component of interval timing. Specifically, old mice set a higher threshold (criterion) for response terminations when the probability of the short trial was higher, which in turn resulted in later response terminations and delayed switch times. Given that

there was no difference between the age groups in terms of the start times, we propose that in our case, the modulation of timed responses by probabilistic information was (partially) via altering the threshold setting of specifically when to terminate an ongoing response. This claim is supported by the independence of decision processes that guide the initiation and termination of timed responding (Balci et al., 2009c; Church et al., 1994; MacDonald et al., 2012). Finally, we observed higher CV of the start times of the short location responses in older mice, which might be due to the higher trial-to-trial variation in the motivational states of the old mice (e.g., Balci, 2014); however, this possibility requires further investigation.

The current study also constituted the direct replication of our previous work (Tosun et al., 2016 - see Appendix B.2 Results of Tosun et al. (2016) for Comparison to the Results of Current Study for the results of the comparable statistical analysis) when the first hour of the initial testing was analyzed to match the one-hour long testing in the previous work. Consistent with Tosun et al. (2016), we found that during the test sessions mice can immediately and rapidly integrate previously learned task parameters to plan and guide their choice behavior. The resultant timing behavior was sensitive to probabilistic manipulations and did not change over the course of testing for the majority of the cases (both for the entire two hour long first test session and during its first one hour). These results challenge the theoretical approaches that solely rely on gradual learning based on trial-by-trial response-outcome experiences (for review see Gür et al., 2018; Malet-Karas et al., 2018).

One of the limitations of the current work is that animals received feedback (in the form of reinforcement) for correct responses during testing, which introduces a possible means for animals to learn based on differential reinforcement (albeit this learning would still have to be very abrupt to account for our observations). Future research can omit reinforcement from all test trials for a cleaner characterization of the emergent behavior. The use of a single set of intervals also limits the generalizability of our conclusions to other intervals. Finally, given our experimental design, we do not know how much pre-training would be necessary to observe the abrupt emergence of timed-switching behavior. These are issues that can be addressed by future research.

Chapter 4

AGING IMPAIRS PERCEPTUAL DECISION-MAKING IN MICE: INTEGRATING COMPUTATIONAL AND NEUROBIOLOGICAL APPROACHES

4.1 Abstract

Decision-making is one of the cognitive domains which has been under-investigated in animal models of cognitive aging along with its neurobiological correlates. This study investigated the latent variables of the decision process using hierarchical drift-diffusion model (HDDM). Neurobiological correlates of these processes were examined via immunohistochemistry. Young (n = 11, 4 months old), adult (n = 10, 10 months old), and old (n = 10, 18 months old) mice were tested in a perceptual decision-making task (i.e. two alternative forced choice; 2AFC). Observed data showed that there was an age-dependent decrease in the accuracy rate of old mice while response times were comparable between age groups. HDDM results revealed that age-dependent accuracy difference was a result of a decrease in the quality of evidence integration during decision-making. Significant positive correlations observed between evidence integration rate and the number of tyrosine hydroxylase positive (TH+) neurons in ventral tegmental area (VTA) and axon terminals in dorsomedial striatum (DMS) suggest that decrease in the quality of evidence integration in aging is related to decreased function of mesocortical and nigrostriatal dopamine.

4.2 Introduction

Cognitive aging is associated with the impairment of various cognitive functions such as learning, memory, and attention. Age-related alterations in these functions have been reported convergently based on vast human and animal research while some other

cognitive domains have been under-investigated in relation to cognitive aging. Maybe one of the least studied domains in animal models of (and arguably human) cognitive aging is the health of simple perceptual decision-making. This appears as a prominent translational gap particularly given that perceptual decisions determine the adaptiveness of individuals in many aspects of life including motor, traffic, and consumer behaviors. Consequently, we have only limited information regarding how basic decision processes are altered in aging and the neurobiological correlates of these age-related changes. The current study convergently fills this gap by investigating how decision-processes are altered in the mouse model of aging based on the analytical treatment of behavioral data in the light of a computational decision-theoretic approach and the investigation of the neurobiological correlates of the age-related alterations in the corresponding components of the decision process.

Decision-making is a cognitive function that leads to the choice of an option or action from multiple alternatives based on the processing and assessment of the information available to the decision-maker. Choosing one lane over another one in the traffic, studying radiological scans, picking the ripest blueberries from a bunch all involve some sort of a decision process in which the individual processes information regarding the flow of traffic, image contrasts or color. Although such decisions are relatively simple, research shows that the decision processes that successfully applied to account for such simple perceptual decisions (Ratcliff and McKoon, 2008) can also account for more complex decisions such as value-based judgments (Mormann et al., 2010). One of the core features of these decisions that determines their adaptiveness (e.g., reward rate) is the emergent tradeoff between the accuracy and speed of the decisions (i.e., speed-accuracy tradeoff; SAT); namely, the fact that deliberating decisions lead to more accurate but slower decisions while rushing decisions speed up choices at the expense of their accuracy (Bogacz et al., 2006).

This integral property of choice behavior emerges as a natural by-product of the diffusion decision model (DDM) that offers a computational framework to explain the decision-making based on psychologically meaningful and analytically trackable parameters. The drift-diffusion model assumes that a) sensory evidence is a noisy input (due to the task/environment, limits of the sensory organs and/or the neural activity [Scott et al., 2015]), b) the difference between the sensory evidence supporting different options is

integrated over time, c) when the integrated evidence hits one of the two thresholds (each of which represents one of the two alternatives being considered in 2AFC) the corresponding choice is made and d) the delay to the threshold first crossing time denotes the decision time. The diffusion process in a single trial is illustrated in Figure 4.1 along with the basic DDM parameters.

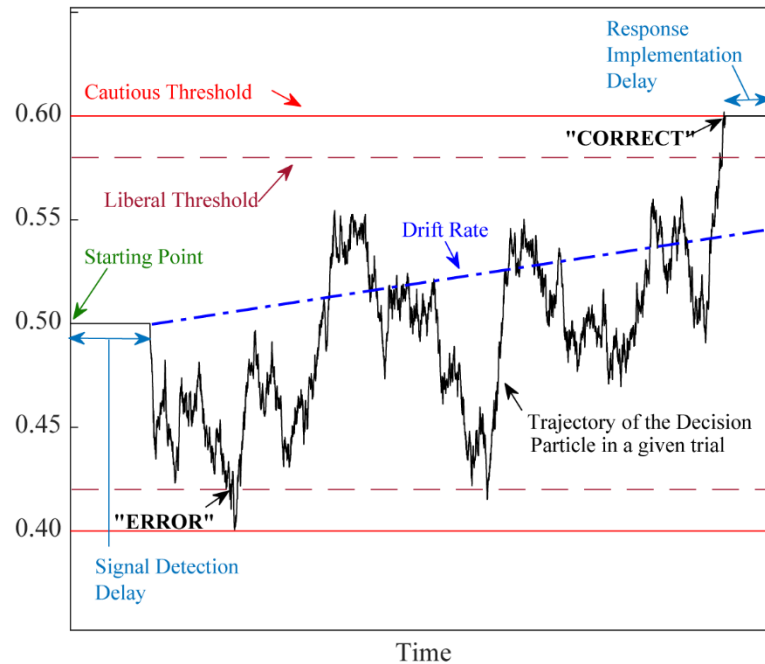


Figure 4.1: Graphical illustration of the diffusion process in a single trial along with the DDM parameters.

Formally speaking, DDM captures response times and decision accuracy in a unified fashion based on four core parameters: drift rate (v), boundary separation (a), starting point of the evidence accumulation (z), and non-decision time (T_0) (Ratcliff and Rouder, 1998): a) Drift rate reflects the signal-to-noise ratio (quality of evidence; SNR) in the decision process as well as the individual's ability to integrate the evidence, b) boundary separation reflects the degree of cautiousness, c) starting point reflects the prior belief state of the decision-maker regarding the likelihood of different alternatives, d) non-decision time accounts for the time spent on stimulus encoding and response execution, and together with the decision time, it corresponds to response time (RT). Besides starting point, drift criterion (dc) is an additional parameter for quantifying decision bias, as it moves the zero-point of drift rate away from zero in either direction, with drift rates above

the criterion moving towards one boundary and those below moving towards the other (Ratcliff and McKoon, 2008).

Although the accumulated evidence on average (drift rate) favors the correct threshold over the incorrect threshold when the SNR is positive, accumulated evidence might still first hit the incorrect threshold due to the random noise that the evidence accumulation is subject to (diffusion). This results in the speed-accuracy tradeoff in choice behavior; for instance, lowering decision thresholds speeds up the decisions at the expense of an increased likelihood of hitting the incorrect threshold due to randomness in the decision process (Ratcliff and Rouder, 1998; Ratcliff and Tuerlinckx, 2002). The treatment of decision outputs (i.e., accuracy and RTs) in a unitary fashion in light of this computational decision-theoretic approach has revealed differences at the level of latent decision process between many groups of interest in humans (e.g., White et al., 2010).

Previous studies compared the choice behavior and the underlying decision performance of older participants compared to younger participants in simple choice tasks (Ratcliff et al., 2001; 2003a; 2004a; 2004b; 2006a; Thapar et al., 2003). RTs were longer for older participants in all settings while age difference in accuracy was dependent on the task and instructions favoring accuracy or speed. Older participants had lower accuracy when instructions favored the speed. The treatment of the behavioral outputs in the light of the drift-diffusion model pointed at three possible sources of age difference in humans: higher decision thresholds, longer non-decision times, and lower drift rates in older compared to young adults (Ratcliff et al., 2001, 2003a, 2004b; Ratcliff et al., 2004a; Starns and Ratcliff, 2010; Thapar et al., 2003). However, the difference in drift rates was more prominent in perceptual tasks with advanced age (75-90 years old; Ratcliff et al., 2007). A significant benefit of practice through a decrease in the boundaries and an increase in the drift rates was also observed in the elderly (Ratcliff et al., 2006b). Moreover, individual differences in basic DDM parameters were consistent across tasks, suggesting a common decision process that applies to different decision domains (Ratcliff et al., 2006a).

Animal studies offer a culture-free means of studying cognitive aging along with its neurobiological correlates; however, to our knowledge, how the decision processes outlined above are affected in the animal models of cognitive aging and the neurobiological changes that accompany these alterations are not yet known.

Foundational work regarding the neural basis of perceptual decision-making was carried out primarily with non-human primates. These studies revealed a resemblance between diffusion decision processes and neural firing rates over time in different brain structures such as frontal eye field (FEF; Ding and Gold, 2012), lateral intraparietal cortex (LIP; de Lafuente et al., 2015), superior colliculus (Ratcliff, et al., 2003b) that translate sensory input to motor output (Gold and Shadlen, 2001, 2007; Smith and Ratcliff, 2004).

Such findings suggested that evidence accumulation has a distributed neural network. However, silencing of frontal orienting fields (FOF) and posterior parietal cortex (PPC) (homologous to FEF and LIP) neurons in rats revealed that neither FOF nor PPC was central to the evidence accumulation process (Erlich et al., 2015). Another study suggested the involvement of dorsal striatum in evidence accumulation and choice bias (Ding and Gold, 2010). Results of recent work, conducted with rats utilizing behavioral, pharmacological, optogenetics, electrophysiological and computational approaches also revealed that anterior dorsal striatum is causally responsible for the computation of evidence accumulation (Yartsev et al., 2018).

Several other studies pointed at the role of neurochemical systems in the decision process. For instance, dopaminergic input from the VTA to the frontal cortex (FC) was found to be crucial for healthy executive functions and modulating SNR in neural processing (Kroener et al., 2009). Lo and Wang (2006) proposed a model in which dopamine-dependent plasticity in the cortico-striatal pathway modulates the decision criterion. In line with this proposal, lower decision boundaries were associated with higher activation of pre-supplementary motor area (pre-SMA) and striatum (Forstmann et al., 2008), and flexible modulation of decision boundaries was associated with stronger cortico-striatal connections (Forstmann et al., 2010). Providing causal evidence for this claim, Berkay et al. (2018) and Tosun et al (2017) showed that increasing and decreasing the activity of preSMA via theta-burst stimulation protocols lead to lower and higher decision thresholds, respectively.

Animal studies have also shown the roles of dopamine and acetylcholine function and their interaction effect on the decision-making performance (Hoebel et al., 2007; Mendez et al., 2013; Stocco et al., 2012; Xie et al., 2012). Importantly, neurochemical changes that are implicated in age-dependent alterations in decision-making are attributed

primarily to dopaminergic (Berry et al., 2018; Samanez-Larkin and Knutson, 2015) and cholinergic functions (e.g., Bossaerts and Murawski, 2016). The cholinergic system is implicated in aging, age-dependent cognitive dysfunction, and Alzheimer's Disease (Muir, 1997). The medial septal area, a part of the cholinergic basal brain, is found to modulate the activity of dopaminergic neurons in the substantia nigra pars compacta (SNc) and VTA (Bortz and Grace, 2018a).

In light of the previous studies, dopaminergic input from SNc to dorsal striatum can be thought to modulate thresholds (Bogacz et al., 2010; Lo and Wang, 2006) whereas mesocortical dopaminergic function can be thought to modulate the efficacy of evidence integration over time (drift rate - but also see Yartsev et al., 2018 for the potential role of dorsal striatal involvement). Supporting the latter rationale, for instance, recent work showed that methylphenidate administration only increases the drift rate in humans (Beste et al., 2018; see also Kroener et al., 2009). Although both dopaminergic and cholinergic neurotransmitter systems are known to alter with age (Bossaerts and Murawski, 2016), how they relate to age-related changes in decision process largely remains unknown.

Recent methodological developments offer alternatives to elucidate the information processing basis of age-dependent alterations in decision-making and their neurobiological correlates. For instance, several studies utilized various 2AFC protocols in freely moving or head-fixed mice/rats in recent years (e.g. Burgess et al., 2017; Scott et al., 2013). Behavioral data provided consistent results with human studies (e.g. Brunton et al., 2013; Odoemene et al., 2018; Scott et al., 2015). With new behavioral protocols and technologies, rodent models have already facilitated the research progress in animal-based decision science.

Capitalizing on these procedural developments and to bridge the corresponding gap in the literature, we tested young, adult and old mice in a 2AFC brightness discrimination task (as a task underlain by perceptual decision making; Liston & Stone, 2013; Ratcliff, 2002; Ratcliff et al., 2003a) and characterized the behavioral outputs based on the drift-diffusion model. We also compared the number of TH+ (dopaminergic) neurons in SNc and VTA, and the number of choline acetyltransferase positive (ChAT+; cholinergic) neurons in medial septum /diagonal band (MS/DB) complex as well as the density of TH+ axon terminals in the dorsomedial and dorsolateral striatum (DMS and DLS, respectively).

Finally, we investigated the relationship between the latent variables of the decision process and the neurochemical variables. We hypothesized that aged mice would perform worse in the decision making task and observed performance difference could be explained by the latent processes, provided by the drift-diffusion framework, which in turn would be related to neurobiological changes observed in healthy aging. Specifically, we expected lower drift rates in aged mice, which (for a given SNR in the sensory input) would point at lower efficacy in the integration of sensory evidence over time. We also expected higher decision thresholds in aged mice, which would point at a more cautious decision strategy (i.e., accuracy bias). We expected the differences in drift rate to be associated with TH+ neurons in VTA given the role of the mesocortical dopamine pathway in executive functions (Kroener et al., 2009) and the threshold changes to be associated with the number of TH+ neurons in SNc and TH+ axon terminals in DLS in light of the cortico-striatal theory of speed-accuracy tradeoff (for review see Bogacz et al., 2010). Our results showed higher error rates and lower drift rates in old mice and a significant relationship between the drift rate and TH+ axon terminal density in DMS as well as the number of TH+ neurons in VTA.

4.3 Method

4.3.1 Subjects

Subjects were 34 naive male C57BL/6J mice bred in the Koç University Animal Research Facility. Young (n = 12), adult (n = 11), and old (n = 11) mice were 4-, 10-, and 18-months old at the beginning of the experiment, respectively. One mouse from each group was excluded from the data collection process due to health issues and consequently, a total of 31 mice completed the experiment. Mice were housed in groups of three to five in polycarbonate individually ventilated cages (Allentown type I long) in a room on a 12:12-h light:dark cycle (lights on at 6:00 AM). One hour-long experimental sessions were run during the light cycle on consecutive days. Food restriction started 3 days before the data collection and mice were maintained at 85% of their free-feeding weight with ad libitum access to water in their home cages. Additional food pellets were provided after experimental sessions. Neurobiological measures were collected from 27 mice out of these 31 mice (randomly chosen) with 9 mice from each age group at the end of the experiment. All procedures were approved by the Koç University Animal Research Local Ethics Committee (Protocol Number: 2014-13).

4.3.2 Apparatus

Experiments were conducted in five-choice serial reaction time task boxes (SO-MED-NP5M-B1; Med Associates) contained in ventilated sound-attenuating cubicles (ENV-022MD; Med Associates). One of the walls had five illuminable nose-poke holes in which light density could be manipulated (ENV-115C; Med Associates). The middle one (H3) was used to initiate trials and the other two at the left (H2) and the right (H4) of the H3 were the choice options. At the opposite wall, there was an illuminable pellet receptacle (ENV-303W and ENV-303RL, Med Associates) in which sucrose pellets (TestDiet Sucrose Tablet 20mg) were delivered via a pellet dispenser (ENV-203-20, Med Associates). Nose entries were detected via IR beam break detectors in nose-poke holes and pellet receptacle. MED-PC IV software was used to control the boxes and record data. All events were logged and time-stamped with a resolution of 10 ms.

4.3.3 Procedure

Magazine and Nose Poke Training

Initially, mice went through two sessions in which sucrose pellets were delivered in every 60 seconds (FT60) by illuminating the food hopper for 3 seconds. In the following three sessions, in addition to the FT60 schedule, the middle nose poke hole was illuminated and each nose poke (FR1) resulted in food delivery as well (FR1-FT60 concurrent schedule training). Finally, mice were trained on the FR1 schedule until the collection of 40 pellets in two consecutive sessions. Mice met the criterion on 6-7 days on average without a difference between the age groups. Daily sessions were one-hour long.

2AFC Training and Testing

Two nose-poke holes (H2 and H4) were associated with dim and bright light intensities. When the signal light was dim, mice were required to poke H2 (correct response) and when the signal light was bright, mice were required to poke H4 (correct response) to receive the reward (counterbalanced across subjects). Dim and bright light signals were presented in random order with equal probability. In the first 50 sessions, 75% of the trials were training trials and the rest was test trials. For the remaining 40 sessions, test trials constituted 50% of the trials in each session. The presentation order for training and test trials were random.

Mice initiated each trial by nose poking in the H3 which was illuminated in middle light intensity. After a nose poke into H3, the light was turned off. In training trials, only one of the nose poke holes (H2 or H4) associated with a dim or bright light was illuminated to signal the correct location for the associated/presented light intensity there. The correct nose poke in the correct (illuminated) hole terminated the stimulus and was reinforced. The trial was terminated if there was no response within 15 seconds (<1% at the steady-state performance). In the test trials, after a nose poke into H3, both nose-poke holes (H2 and H4) were illuminated with the same intensity (dim or bright light) forcing the animal to make a choice based on previously learned association between the light intensity and corresponding nose poke hole. To receive the reward, mice were required to poke the hole associated with the presented light intensity during the training trials. Appendix C.2

Brightness Discrimination Task: Figure C.1 provides an illustration of the task.

Immunohistochemistry (IHC) and Histological Confirmation

On average 2 days after the completion of behavioral testing (range: 1-4 days), transcardial perfusion with physiological saline and 10% formaldehyde (Tekkim, Turkey) was performed under ketamine (90 mg/kg, i.p.) + xylazine (10 mg/kg) anesthesia using a peristaltic perfusion pump (5 mL/min). Following the perfusion, mice were decapitated, brains were collected and kept in the fixative solution overnight. On the next day, brains transferred to 30% sucrose solution were stored in +4°C until they sank to the bottom of the tubes. Finally, brains were fast frozen at -20°C for 3 minutes in dry ice (2-isomethylbutane, Sigma-Aldrich, USA) and stored at -80°C until further processing. The staining protocol outlined below was followed when the testing was complete for all mice.

The SNc, VTA, MS/DB complex, and striatum (STR separated anatomically as DLS and DMS) were the target regions for IHC staining. The stereotaxic atlas of Paxinos and Franklin (2012) was used to determine the coordinates of all target regions. Bregma was the reference point on the anteroposterior axis. For the examination of SNc and VTA, sections were taken from the region between -2.7 mm and -3.8 mm. For the examination of MS/DB complex and STR, sections were taken from the region between 1.4 mm and .4 mm.

Thawed brains were embedded in Tissue-Tek (Sakura-Finetek, USA) to cut 40 µm coronal sections at -20°C using a cryostat. The sections were first immersed in phosphate-

buffered saline (PBS) in well plates and then incubated with 3% hydrogen peroxide (H₂O₂) solution using an orbital shaker, which lasted 10 min. After sections were rinsed with TBS-Tween 20 (3x5 min), they were incubated with Ultra V Block solution (Thermo Scientific, USA) for 30 min and then incubated with primary antibodies [Tyrosine Hydroxylase (1:500) and Choactase (1:100), Santa Cruz, USA] in 0.5% TBS-Triton X-100 solution at +4°C overnight. On the next day, secondary antibody (UltraVision Quanto Detection System, Thermo Scientific, USA) was used for 20 min incubation. After being rinsed with TBS-Tween 20 (3x5 min), sections were incubated with horseradish peroxidase (HRP) solution (Thermo Scientific, USA) for 30 min and rinsed again with TBS-Tween 20 (3x5 min). Finally, the sections stained with AEC Substrate System (Lab Vision Mount, Thermo Scientific, USA) were rinsed with TBS-Tween 20, mounted on positively charged slides and then coverslipped. An equal number of brains from each age group was used every time staining protocol was performed to avoid any systematic biases in the data; groups formed during this process consisting one mouse from each age were the basis for the quantification of IHC data (for the optic density measure) and the selection of the mice for the staining groups was random (with the constraint that each age group had the same number of subjects). Thionin acetate (Sigma Aldrich, USA) staining was also performed on the sections containing SNc, VTA, MS/DB complex, and STR to confirm the localization and morphology of the target regions. For the thionin staining following protocol was used: xylene (2 min), 100% alcohol (2 min), 98% alcohol (2 min), 70% alcohol (2 min), 50% alcohol (2 min), thionin acetate (1 min), 50% alcohol (1-2 sec), 70% alcohol (1-2 sec), 98% alcohol (1-2 sec), 100% alcohol (1-2 sec), xylene (1-2 sec). The examination of sections was done under an optical microscope.

4.3.4 Data Analysis

Behavioral Analysis

First of all, the accuracy rates in test trials for every 10 sessions were calculated to characterize the acquisition of task performance in terms of error rates. Mixed-design ANOVA was used to compare accuracies across session blocks (9 levels), and the age group was the between-group factor. Data from the test trials in the last 5 sessions of the experiment was used to compare the steady-state performance of age groups with one-way ANOVA. Mixed-design ANOVA was also performed by separating the accuracies for bright and dim trial types to evaluate accuracy rates in two options which might reflect

a bias towards one of the choice options. Response times collapsed across correct and incorrect responses were compared between bright and dim trial types along with age groups using mixed-design ANOVA. Response times were also compared using mixed-design ANOVA with age group as the between-subject factor and the choice accuracy as the within-subject factor. One-way ANOVA was used to compare the arrival time to the food hopper (after a correct response) between age groups. The time it took for a mouse to collect food was calculated as the absolute difference between the time of response and the time of first head-in in the food hopper following this response. We excluded the extreme scores (3 SD above the mean), before getting the subject means of the arrival time to the food hopper for the comparisons. Note that not excluding these data does not change the results. The significant overall differences were followed-up by post hoc comparisons when necessary.

Modeling

Comparisons within-session blocks and between age groups were applied using the posterior distributions of parameters estimated by HDDM. HDDM takes a hierarchical Bayesian approach to the drift-diffusion model (Wiecki et al., 2013) and is shown to provide reliable parameter estimates even with a relatively low number of trials from human participants (Ratcliff and Childers, 2015). We chose to use uninformative priors for our analyses since the informative priors of the parameters in HDDM are informed by human data. The change in parameters over session blocks was modeled using the HDDMRegression module as a within-subject model with the drift rate, threshold, and non-decision time as free parameters allowed to change with the progression of 9 session blocks. The final parameters of the three age groups in the last five sessions, determined as the steady-state, were compared in a between-subjects model using the StimCoding module, allowing the investigation of any potential decision bias in addition to the other parameters. For both sets of models, we decided on the inclusion of parameters in the models using model comparisons via changes in the Deviation Information Criterion (DIC). The models that reduced the DIC by more than 10 over the simpler models were considered to be worth the increased complexity due to the added parameters (Spiegelhalter et al., 2002). For all models, we used Markov Chain Monte Carlo (MCMC) estimation with 5000 samples with the first 20 draws discarded as burn-in. We visually inspected the traces, autocorrelations, and distributions of the Markov chains to assess

model convergence. Hypothesis testing was conducted on the posterior distributions of the parameters for each condition. The P values reported in the HDDM results are calculated as the proportion of the MCMC samples in which the difference between the two relevant estimates is above zero, and we consider any such probability above 0.95 to be significant by convention.

Quantification in IHC

The images of the sections containing target regions (SNc, VTA, MS/DB complex, and STR) were taken at x5 and x20 magnification. Location and boundaries of the regions were determined on these images and reaction products in dark brown color were interpreted as immunoreactive. Image J software (version 1.49; National Institutes of Health) was used to convert images into grayscale in which levels ranged between 0 (light gray) and 255 (dark gray) and to measure the mean immunoreactivity density within the designated regions. Light intensity and threshold settings were the same for all the evaluated sections. The threshold was set to 75%; therefore, a cell was considered as immunoreactive when the density exceeded the background density of the section by 75% (Moers-Hornikx et al., 2009). The number of TH+ neurons in SNc and VTA ($n = 22$), number of ChAT+ neurons in MS/DB complex ($n = 27$) were counted, and (optic) density of TH+ axon terminals in DLS and DMS ($n = 24$) was measured. Although samples from 9 mice in each age group were stained for each target region, quantification could not be performed for all due to the unclarity of some images. The number of neurons was calculated per μm^2 for each section and the mean value of the series of stained sections for the target area was used for each mouse. On average, evaluations were based on 4 sections. The optic density measure values extracted for each subject were divided by the mean value of the group that staining protocol performed together (see Gulcebi et al., 2017 for the details). All these measures were compared between age groups using one-way ANOVA and correlations between these measures and model parameters were examined. Analysis and the statistical tests were run on MATLAB, SPSS for the behavioral data analysis and IHC outputs, and on Python for modeling.

4.4 Results

4.4.1 Behavioral Analysis

Evaluation of choice accuracy as a function of training separately for three different age groups and test vs. guided (training) trials revealed that the performance of mice was nearly at the ceiling in the guided trials and their performance rose above the chance level with training in the test trials. The overall accuracy rate was 95.68% in guided trials at the steady-state performance with no significant difference between the age groups ($F(2,28) = 3.01, p = .07, \eta_p^2 = .18$). The statistical comparison of accuracy in test trials over session blocks to see whether or not there is a linear increase in the choice accuracy showed that it increased in a monotonic fashion as a function of training $F(1,28) = 210.43, p \leq .001, \eta_p^2 = .88$. The accuracy increased from chance level performance ($M = .48, SE = .01$) to above-chance level performance ($M = .65, SE = .01$) irrespective of the age group. There was no significant difference between the age groups in terms of choice accuracy (over the entire session blocks; $F(2,28) = 2.70, p = .08, \eta_p^2 = .16$) and there was no interaction between age and session blocks, $F(2,28) = 1.67, p = .21, \eta_p^2 = .11$. Consequently, the monotonic increase in choice accuracy was independent of the age group.

Figure 4.2a shows the choice accuracy separately for three different age groups during steady-state performance (i.e., last five sessions). One-way ANOVA revealed a significant age effect on choice accuracy, $F(2,28) = 5.30, p = .01, \eta_p^2 = .28$. The post-hoc comparison of the accuracies revealed a significant difference between young ($M = .70, SE = .02$) and old ($M = .61, SE = .02$) mice ($p = .01$). There were no other significant differences ($M_{\text{adult}} = .67, SE = .02$). When we introduce the accuracy in those trials with brighter and dimmer stimulus separately into the ANOVA, we did not observe any significant effect of stimulus type, $F(1,28) = .13, p = .73, \eta_p^2 = .0004$. There was not a significant interaction between stimulus type and age groups $F(2,28) = .41, p = .67, \eta_p^2 = .03$. Main effect of age, independent of the stimulus type, was still evident $F(2,28) = 4.97, p = .01, \eta_p^2 = .26$; young mice performed significantly better than old mice and there were no differences between young and adult, and adult and old mice ($ps > .05$). Comparison of RTs for stimulus type and age groups did not reveal any significant differences [stimulus type: $F(1,28) = .19, p = .67, \eta_p^2 = .01$; age: $F(2,28) = .21, p = .81, \eta_p^2 = .02$; stimulus type*age: $F(2,28) = .14, p = .87, \eta_p^2 = .01$].

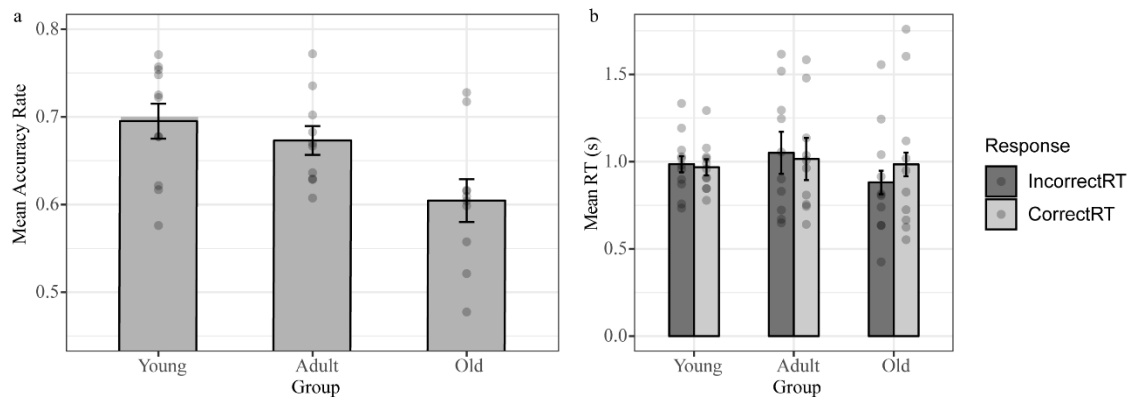


Figure 4.2: a) Mean choice accuracy along with individual data points in test trials during the steady-state performance for young, adult, and old mice; a statistically significant difference was found between young and old mice only. b) Mean correct and incorrect RTs along with individual data points during the steady-state performance for different age groups. Error bars show the 95% confidence intervals.

Figure 4.2b shows the correct and error RTs separately during the steady-state performance for three different age groups. The correct and error RTs were not significantly different from each other, $F(1,28) = .33$, $p = .57$, $\eta_p^2 = .01$. We did not find a significant effect of age ($F(2,28) = .31$, $p = .74$, $\eta_p^2 = .02$) or an interaction between age and RT for correct and error responses ($F(2,28) = 2.09$, $p = .14$, $\eta_p^2 = .13$). Comparison of arrival time to the food hopper after a correct response was comparable between all age groups ($F(2,28) = 1.25$, $p = .30$, $\eta_p^2 = .08$).

4.4.2 HDDM Fits

Initially, four models were evaluated against the null model for the entire dataset categorized in 9 session blocks to evaluate if possible changes in the latent processes took place throughout the experimental sessions. The model with the lowest DIC score included the three core parameters of the drift-diffusion model (i.e., drift rate, decision threshold, non-decision time), with all parameters allowed to vary with age group. Appendix C.1 Model Fits: Table C.1 presents the models fit to the entire dataset in 9 session blocks along with the DIC scores associated with them.

Data simulated based on the best fit model parameter values were consistent with the empirical data, namely that empirical data were within the 95% credible interval of the distribution of simulated data. The fit quality for the first two session blocks was below the desirable level, which is an expected observation with very low drift rates reducing

the credibility of the parameter estimation. The fit quality criteria displayed the desirable profile for the remaining session blocks.

Figure 4.3a shows that the drift rate increased in a monotonic fashion as a function of session blocks pointing at perceptual learning. Following the 2nd session block (after 20th session), the drift rate was significantly higher than 0 for all bins ($P_{v_3>0} = .998$). In order to analyze if this increase in drift rates was significant, we compared the posterior distribution of drift rates between each consecutive posterior distribution. This comparison revealed that the increase in drift rate from the previous session was significant from the 3rd through the 6th session blocks ($P_{v_n>v_{n-1}} > .95$ for all comparisons within this range). This increase in the drift rate saturated in the final blocks as the mice learned the task.

We also analyzed the change in decision thresholds (Figure 4.3b) and non-decision times (Figure 4.3c) and did not find any significant change in these parameters except for between the first two blocks. Of note, the parameter estimates from the first few blocks are not reliable due to low fit quality. There was no difference between the consecutive posterior distributions of either parameter from the 3rd through the 9th session blocks ($P_{a_n>a_{n-1}} < 0.80$, $P_{t_n<t_{n-1}} < 0.75$ for all comparisons).

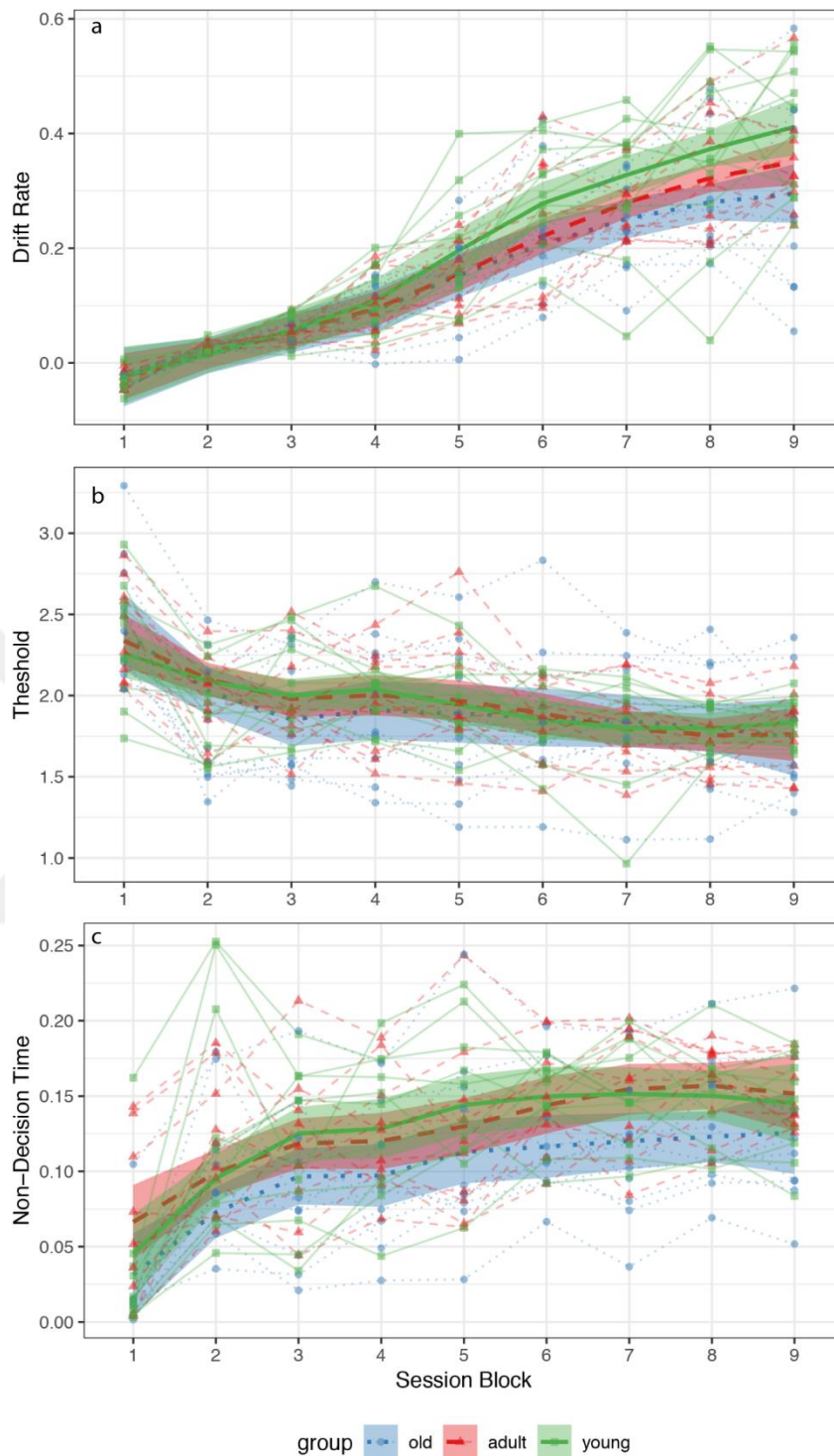


Figure 4.3: Drift rates (a), decision thresholds (b), and non-decision times (c) estimated for each session block. Parameter estimates for individual animals are shown with thin lines whereas the average estimates are shown as thick lines. Shades denote the 95% confidence interval around the mean estimates. While the figures display only the mean parameter estimates for the subjects and label them by age, note that hypothesis testing was done based on the entire posterior distributions of each session block, and differences between the age groups were not factored in at this stage (models that included age as a

factor had higher DIC scores compared to the model without age). The labels and line types for different age groups are therefore for demonstration purposes and not part of the underlying model. Green-straight, red-dashed, blue-dotted lines are for young, adult, and old mice, respectively.

For the evaluation of steady-state data, bias parameters—the starting point and drift criterion—were also included in the evaluation of alternative models to be able to examine possible sources of bias in choice behavior between age groups. In order to measure bias in these models with bias parameters, first, the data were coded according to the stimulus properties (lower boundary/0: bright light, upper boundary/1: dim light). We took the simplest model to be the best model from the previous analysis of session progress (SP4 in the previous set, SS0 in the current set; see Appendix C.1 Model Fits: Table C.1 and Table C.2), and tested models with added bias parameters against it. Comparison of DIC values between alternative models revealed that models that include bias parameters performed better in comparison to the models that did not include these parameters; however, DIC values were not sufficient to differentiate between the models where bias parameters were constant for all age groups and those where they were free to vary between the groups (Appendix C.1 Model Fits: Table C.2). Therefore, the model that had the fewest free parameters (i.e. lower complexity) was selected as the best-fitting model (Model SS2 in Appendix C.1 Model Fits: Table C.2) and used for the evaluation of age differences in the latent decision processes.

We found that the drift rate decreased with advanced age and the difference between young and old mice was significant ($P_{v_young > v_old} > .95$) (Figure 4.4a). Decision threshold (Figure 4.4b) and non-decision time (Figure 4.4c) parameters did not differ significantly between the age groups ($P < .80$ for all comparisons).

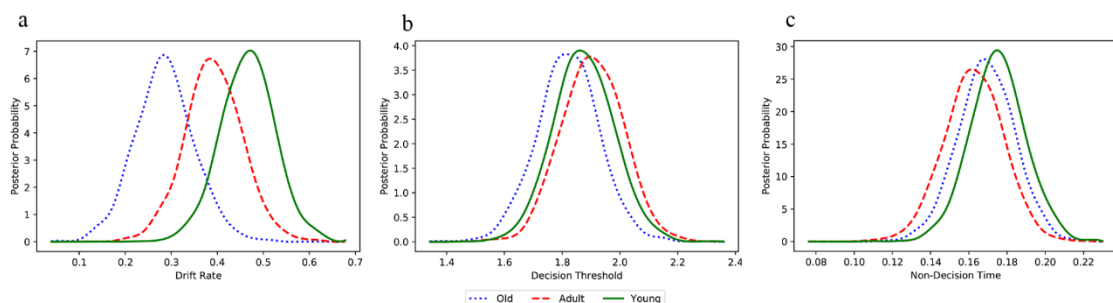


Figure 4.4: The posterior distributions for drift rate (a), decision threshold (b), and non-decision time (c) in the last five sessions for the age groups. Green-straight, red-dashed, blue-dotted lines are for young, adult, and old mice, respectively.

The best model included two bias parameters (starting point and drift criterion) as common parameters for all age groups (see Appendix C.3 Posterior Distributions: Figure C.2 for the posterior distributions of these parameters). The unbiased value for the starting point that is equidistant to the two thresholds is taken to be 0.5. A starting point that is estimated above this value indicates a response bias for the upper boundary (dim light), and a lower value indicates a bias for the lower boundary (bright light). Drift criterion separates the drift rates that move towards the upper and lower boundaries, and an unbiased drift criterion would have a value of 0. A negative drift criterion indicates a bias towards the upper boundary, whereas a positive value indicates a bias towards the lower boundary. The common posterior distribution for all age groups indicated a bias for the dim light both via the upward-shifted starting point ($P_{z>0.5} > .95$) and the negative drift criterion ($P_{dc<0} > .95$).

4.4.3 IHC Outputs and Their Relation to Latent Variables

Figure 4.5 (VTA and SNc) and Figure 4.6 (MS/DB complex, DLS, and DMS) show representative images of stained target regions for young, adult, and old mice. Comparisons of IHC outputs between age groups revealed significant differences for two target regions, VTA [$F(2,19) = 4.38$, $p = .03$, $\eta_p^2 = .32$] and DMS [$F(2,21) = 4.21$, $p = .03$, $\eta_p^2 = .29$]. Post hoc comparisons showed that the number of TH+ neurons in VTA was significantly lower in old mice compared to young mice (MD = -56.48, SE = 19.09, $p = .02$); there was no difference between young and adult mice and between adult and old mice ($p_s > .05$). The density of TH+ axon terminals in DMS was significantly lower in old mice compared to young mice (MD = -19.80, SE = 6.84, $p = .02$) but there was no such difference for young-adult and adult-old comparisons ($p_s > .05$). We did not observe any other significant age differences between the age groups for the measures gathered from DLS [$F(2,21) = 2.44$, $p = .11$, $\eta_p^2 = .19$], MS/DB complex [$F(2,24) = 2.92$, $p = .07$, $\eta_p^2 = .20$], and SNc [$F(2,19) = 3.02$, $p = .07$, $\eta_p^2 = .24$]. Note that the IHC data presented here were also reported as part of a larger dataset in another study for the between-age comparisons, where the trends observed here were statistically significant differences (Gür et al., submitted).

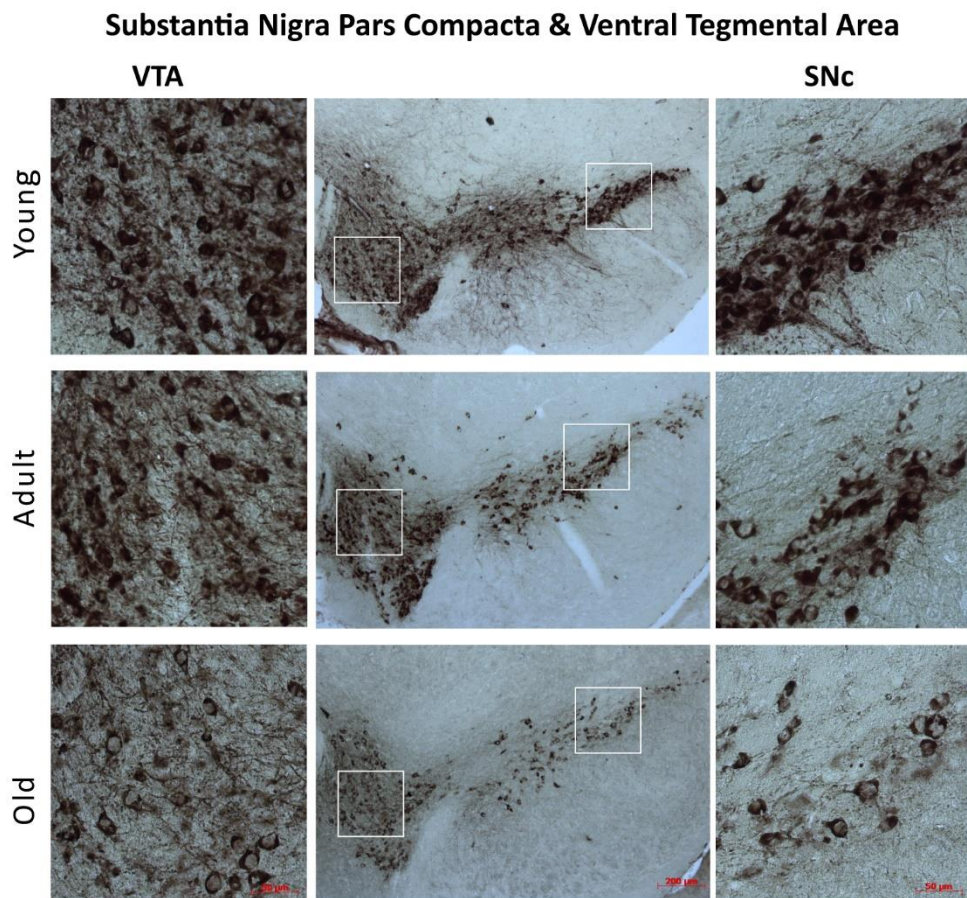


Figure 4.5: Representative images of VTA and SNc after IHC staining for young, adult, and old mice (from top to bottom panel). The middle panel shows dark brown immunoreactive TH⁺ neurons of VTA and SNc on 40 μm sections (5x). Images to the left (VTA) and right (SNc) of the middle panel provide a closer look to smaller windows within these target regions (20x).

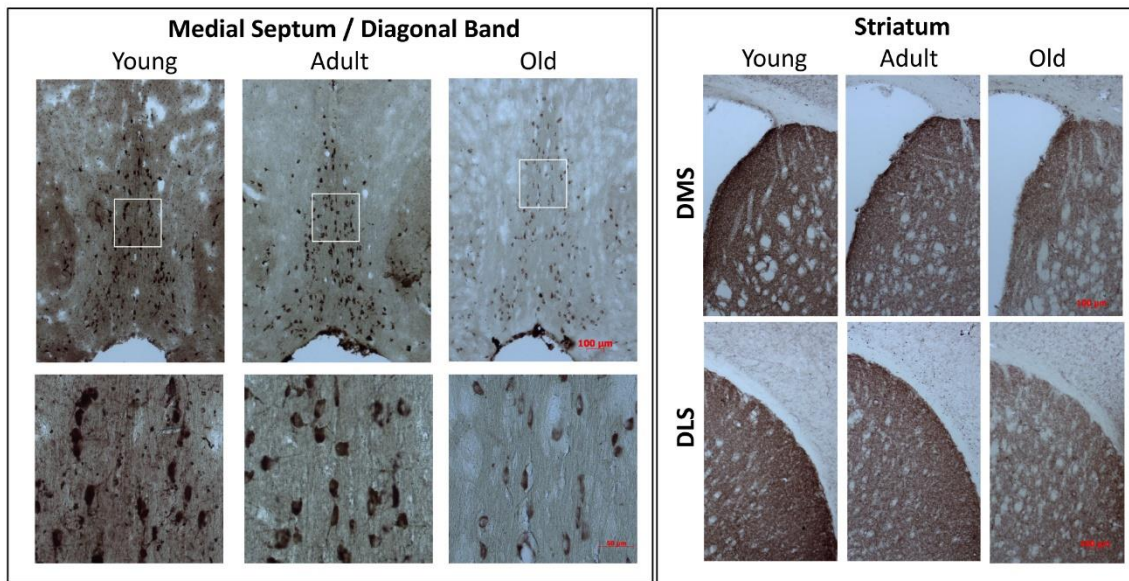


Figure 4.6: Representative images of MS/DB complex and STR stainings for young, adult, and old mice. The left upper panel shows dark brown immunoreactive ChAT+ neurons in MS/DB complex (5x) and the left-lower panel shows enlarged images of selected windows from the target region (20x). At the right panel, immunoreactive TH+ axon terminals are seen in dark brown on DMS (right-upper panel) and DLS (right-lower panel); images are magnified 5x.

We also investigated the correlations between the IHC outputs and the latent decision variables (i.e., drift rate, decision threshold, non-decision time, starting point, drift criterion). Our analysis revealed a significant positive moderate relationship between the drift rate and two dopaminergic outputs [i.e., Number of TH+ neurons in VTA ($r = .43$, $n = 22$, $p = .045$), density of dopaminergic axon terminal density in DMS ($r = .41$, $n = 24$, $p = .048$)]. Figure 4.7 shows the scatterplots for the measures with significant relations.

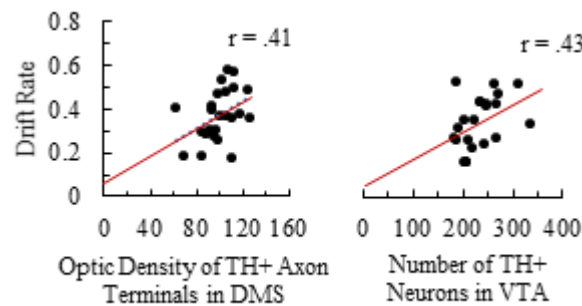


Figure 4.7: Scatterplots showing the significant relationship found between drift rate and number of dopaminergic neurons in the VTA and optic density of dopaminergic axon terminals in DMS.

4.5 Discussion

We investigated how decision-making is altered in the mouse model of aging both at the level of behavioral outputs (i.e., accuracy and RT) and the latent variables of the decision process that explained these behavioral outputs. Our results showed that the accuracy of perceptual decisions of old mice was significantly lower than younger animals and this difference was due to lower drift rate in the older mice. The lack of an age difference in task performance for signaled (training) trials validates our conclusion that the observed age differences were specific to decision-making rather than sensory processing.

Our results regarding the behavioral outputs and latent variables are consistent with those of previous studies that showed lower accuracies (particularly under speed instructions) and lower drift rates of older human participants (particularly those older than 75 years old) compared to younger participants (Ratcliff et al., 2007). Such an overlap between human and animal studies highlight the translational value of 2AFC perceptual decision-making tasks and the treatment of the data in the light of computational decision-theoretic approaches.

Importantly, the characterization of these behavioral and modeling outputs was accompanied by the investigation of their relationship with dopaminergic and cholinergic markers (i.e., TH+ and ChAT+ neuron counts and the density of TH+ axon terminals). We found that the drift rate was associated with the TH+ cell count in the VTA as well as the TH+ axon terminal density in the DMS. To our knowledge, these results constitute the most complete characterization decision-making in an animal model of cognitive aging based on complementary behavioral, decision-theoretic, and neurobiological grounds.

Our results gathered from a mouse model of aging supported the view that cognitive aging is primarily associated with slowing of information processing (Salthouse, 1996) rather than more cautious decision strategies as has been observed in several human studies (Starns and Ratcliff, 2010). Starns and Ratcliff (2010) tested old and young adults in a variety of 2AFC tasks and found that older individuals set their thresholds above the reward rate optimizing decision threshold whereas young adults were closer to the optimal strategy. This result suggested an accuracy bias in older participants, which is consistent with the slower and less error-prone decisions observed in older participants.

The fact that we did not observe such an accuracy bias (in terms of more cautious thresholds) suggest that the observed accuracy bias in humans may be a result of enculturation (e.g., valuing accuracy over reward rate) that is specific to humans and manifested via higher threshold setting (accuracy bias; Balci et al., 2011; Bogacz et al., 2006; Maddox & Bohil, 1998) and slower/lower SNR in information processing might represent a purer marker of cognitive aging. We observed a similar disassociation between the subclinical obsessive-compulsive tendencies in young adults (Erhan & Balci, 2016) and clinical pediatric obsessive-compulsive disorder (Erhan et al., 2017). We found higher thresholds in the subclinical group whereas the drift rate was lower (with a trend for higher thresholds) in the clinical group. This difference might be due to the differential efficacy of cognitively controlled compensatory mechanisms in these two groups of participants either due to age, disease prognosis or their interaction. The fact that we did not observe a difference in the non-decision times (which would have simply shifted the RT distributions without altering their overall shape) also suggests that the age-dependent alteration in decision-making was peculiar to those processes that required neural integration over longer time scales (e.g., ramping like activity, Gold and Shadlen, 2007).

Another interesting and pioneering feature of our dataset is the relation we found between the only decision process that exhibited age-dependent alteration, namely the drift rate and the dopaminergic biomarkers both at the mesocortical and nigrostriatal level. Interestingly, this relation held for the nigrostriatal input to the DMS (with prefrontal associative cortex and visual areas as the afferents; e.g., Devan et al., 2011) but not to DLS (with sensorimotor cortex as the afferent; e.g., Packard and McGough, 1996; Schulz et al., 2009). Provided the fact that DMS but not DLS receives visual input, this finding is consistent with the neuroanatomical connectivities and the visual character of the task used in the current work. This finding is also consistent with the ramping like activity (as predicted by the drift-diffusion model of interval timing; Balci & Simen, 2016; Simen et al., 2011) in the DMS carrying the input from the medial frontal cortex over time (Emmons et al, 2017). Our results suggest that dopamine-mediated gain in the DMS might indeed be disrupted in aging resulting in lower efficiency in integrating evidence. The relationship of dopaminergic input to DMS in drift rate modulation also suggests that the choice behavior is likely still goal-directed in the task used in this study.

The coupling between the ramping activity in the striatum and medial PFC has been shown in the context of interval timing (Emmons et al., 2017). For instance, in that study, the inactivation of medial PFC disrupted the striatal ramping activity supporting the notion that striatal neurons integrated signals from medial PFC. It is of interest whether a similar neuroanatomical functional map also underlies perceptual decision-making, which is also known to involve ramping-like neuronal activity over time (e.g., de Lafuente et al., 2015; Gold and Shadlen, 2007). One cannot treat these pathways separately from the mesocortical dopamine pathway since the input received by DMS would be subject to the downstream effect of altered dopaminergic input to the medial PFC. This rationale is further supported by the fact that mesocortical dopamine input to the prefrontal cortex increases the SNR in neuronal information processing in the PFC (Kroener et al., 2009).

Adding to the translational value of the use of 2AFC perceptual decision-making in animals, the acquisition analyses of behavioral outputs and latent variables revealed a very similar profile to what has been observed in perceptual decision-making (compare to Balci et al., 2011). Specifically, the accuracy and drift rate increased with training (also note the decreasing trend in decision threshold). Note that we did not find any significant differences between the age groups regarding the acquisition profiles, but these differences were apparent at steady-state (i.e., asymptotic performance). A similar acquisition profile in terms of drift rate and decision thresholds have also been observed in the study of old participants (Ratcliff et al., 2006b). These overlaps strengthen the suitability of 2AFC tasks in translational aging research.

To our knowledge, this study constitutes the first investigation of age-dependent alterations in perceptual decision making in mice using both computational approaches and their relation to neurobiological markers. Specifically, we utilized the diffusion decision model as a computational interface to make a mapping between the behavioral and neurochemical processes. This approach constitutes the primary novelty of our study compared to the earlier animal cognitive aging studies (conducted primarily with rats) that focused on decision-making (e.g., Johnson et al., 2017; Yoder et al., 2017). Our work differs, on similar grounds, also from several other earlier works that focus on the study of value-based decision-making in the context of aging (Breton et al., 2015; Simon et al., 2010). It would be of interest to future investigations whether these more complex decisions of animals (including cost-benefit judgments) can be approached with similar

decision-theoretic computational approaches for the mechanistic elucidation of the related decision processes (see Mormann et al., 2010 for a similar approach in humans; Bhatia, 2013).

In order to control for possible differences in visual acuity, we intermixed the test trials with those trials in which the correct hopper was signaled (i.e., guided trials). Although we failed to falsify the null hypothesis that performance in the guided trials differed between the age groups, there was a statistical trend for a possible difference. Thus, it is possible that the differences observed in the test trials were partially due to statistically undetectable age-dependent differences in visual acuity. However, Wong and Brown (2007) showed that the visual detection performance of C57BL/6J was poorest at 6 months of age and increased with age (12, 18, 24 months old). These mice also had better pattern discrimination performance at 24 compared to 6-18 months of age and lower visual acuity threshold at 12-24 compared to 6 months of age. Note that part of these differences could be due to practice effects; however, some other strains of mice showed visual deficits in the same task despite the potential practice effects (Wong and Brown, 2007). Thus, it is not likely that the observed age-related differences are due to differential visual acuity. Finally, given the memory component in the task (i.e., the association between the hopper and light intensity), it is also possible that the observed differences were due to the deficits in remembering the associations that are required to respond correctly (even after the light intensity is judged correctly). An independent test that assesses specifically memory impairments would help elucidate this possibility in future research. Furthermore, in order to address potentially different win-stay and lose-shift strategies between the age groups, we made the corresponding analyses and found that staying following a win was more frequent than shifting following a loss [$F(1,28) = 14.53$, $p < .001$, $\eta_p^2 = .34$] irrespective of the age of the mice tested [$F(2,28) = 1.21$, $p = .31$, $\eta_p^2 = .08$].

Our results revealed clear decision-making deficits in the mouse model of aging and its neurochemical correlates in a fashion that is highly consistent with earlier research. Future studies can focus on the electrophysiological correlates of these age-dependent differences. Another interesting line of future research would constitute the optogenetic stimulation of the systems that were found to be associated with drift rates. For instance, whether the stimulation of VTA or nigro-medial striatal axons would rescue the age-

dependent disruptions in older mouse constitutes a relevant research question for future studies. Finally, the relatively long response to stimulus interval (RSI), time interval between the previous response and the start of the next trial, utilized in this study was not suitable for the characterization of the choice behavior with respect to the optimal policy and thus we did not conduct the optimality analysis of this dataset. Future studies can utilize RSIs that are more suitable for optimality analysis.



Chapter 5

CONCLUSION

While age-dependent cognitive decline is evident in the current literature, further understanding of both preserved and disrupted functions along with their underlying neural mechanisms is of crucial importance. This thesis focused on two cognitive functions: interval timing and decision making. Both of these functions are known to be subject to a change in aging, nonetheless, they are understudied in the animal models of cognitive aging.

The first study provided additional information to the existent body of knowledge in the study of aging on interval timing while complementing the behavioral observations with their neurobiological correlates for a more complete characterization of age-dependent changes in interval timing. Such detailed investigation in the aging domain is relatively scarce in the current interval timing literature despite the extensive use of animal models in this area. We tested the interval timing ability of old mice in comparison to young and adult mice in a dual peak interval procedure and examined the behavioral output in the light of SET to make inferences regarding the relative contribution of different sources of variability in timing behavior across different age groups. Additionally, neurobiological alterations accompanying the age-dependent alterations in the interval timing behavior was studied using immunohistochemistry. Our results revealed that the core timing ability of old mice was intact while the termination of timed anticipatory responses was impaired along with delayed acquisition of thresholds for the response termination. While the response terminations were inversely related to the dopaminergic neuron counts in VTA, delayed acquisition of response terminations was related to lower number of cholinergic neurons in MS/DB complex. These findings together with a higher contribution of

threshold variability (compared to memory variability) to timed responding in old mice suggest an age-dependent alteration in interval timing behavior of old mice due to the decision component of the interval timing. Importantly, we found significant differences between young and old mice in all our neurobiological measures that are implicated in interval timing; however, all these differences were not related to behavior contrary to suggestions by the previous literature (e.g. memory impairment & cholinergic dysfunction). Future studies are needed to elucidate these relations in a fashion that would allow making inferences regarding causal role different neurobiological systems in different components of interval timing in the context of cognitive aging.

The second study extended our question of age-dependent changes in interval timing function to a relatively more complex timing task that requires the integration of previously learned information to the timing behavior for an adaptive response. To do so, we tested the age differences in temporal decision making, timed anticipatory responses, and spontaneous integration of task-related parameters (e.g., probability information) into timed responses using the timed switch task with pretraining. Both young and old mice were able to adopt a novel behavioral strategy (i.e. timed switching behavior) in a spontaneous fashion using previously learned spatiotemporal relations and probabilistic information. Age-dependent differences were observed in the switch times and the stop times for short location only when the probability of reward delivery after the short interval was higher than the probability of reward delivery after the long interval during training. The other indices of timing were comparable between the two age groups and the observed difference in stop times was specific to one probability condition (i.e., higher probability of reward delivery after short interval). Therefore, we suggest that this difference is due to the decision component of the interval timing. In other words, inhibitory control over timed response termination threshold integrates multiple sources of information (e.g., time and probability) such that it can rescue age dependent alterations when probabilistic information favors the termination of timing responding over its continuation. The neural mechanisms underlying such an integration is a research question that remains to be answered in relation to timing behavior. This work was also important given that we replicated our findings from previous work regarding the ability of mice to spontaneously plan decision strategies based on previously learned time intervals, locations, and probabilities (Tosun et al., 2016).

The third study might have important implications given that to our knowledge no study in the domain of perceptual decisions has yet used mice as a model of cognitive aging and more importantly utilized a computational approach to elucidate the relationship between age-dependent alterations in latent decision variables and possible neurobiological markers of aging. Therefore, this study can serve as a reference for further characterization of the neural mechanisms of latent decision variables and their causal relationship to aging. In this study, we tested young, adult and old mice in a bright discrimination task. Age-related differences in the latent variables of the decision process were explored using the Hierarchical Drift-Diffusion model. Relationships between the estimated latent decision variables and neurobiological measures, which are known to be affected in aging, were also examined. Behavioral measures showed that old mice performed worse than young and adult mice in terms of accuracy while response times were comparable between the age groups. Hierarchical Drift-Diffusion modeling of the behavioral outputs revealed that decrease in the quality of evidence integration (i.e., drift rate) underlies the observed accuracy differences between age groups and the rate of evidence integration (drift rate) correlated positively with the number of VTA-localized dopaminergic neurons and the density of DMS-localized dopaminergic axon terminals. Importantly, the perceptual decision-making performance of old mice in terms of observable and latent variables resembled the perceptual decision-making performance described in previous studies of the elderly (Ratcliff et al., 2006b; 2007), highlighting the validity and translational value of mouse models.

This thesis was a comprehensive attempt to characterize the healthy cognitive aging process in a mouse model of cognitive aging based on behavioral, computational, and neurobiological outputs for two overlooked cognitive domains in the aging literature: interval timing and decision making. Delayed stop times observed for old mice in the first two experiments, without any other apparent differences between age groups, pointed at the disruption in inhibitory control of timing behavior in aging, which can be explained with weakened inhibitory control account of aging (Hasher and Zacks, 1988) at least in the case of suppression of an ongoing goal-directed response in the context of timing behavior. The decrease in the quality of evidence integration found in old mice in simple perceptual decision-making, on the other hand, provided support for the slower information-processing account of aging (Salthouse, 1996). Overall, these results

demonstrate how different domains of cognition are subject to change along with their neurobiological correlates in a mouse model of cognitive aging and how overlapping neurobiological systems can differentially relate to the components of different cognitive functions in the context of cognitive aging.



REFERENCES

- Abner, R. T., Edwards, T., Douglas, A., & Brunner, D. (2001). Pharmacology of temporal cognition in two mouse strains. *International Journal of Comparative Psychology, 14*(3).
- Akdoğan, B., & Balci, F. (2016). The effects of payoff manipulations on temporal bisection performance. *Acta Psychologica, 170*, 74-83. doi: 10.1016/j.actpsy.2016.06.007
- Ashendorf, L., & McCaffrey, R. J. (2008). Exploring age-related decline on the Wisconsin Card Sorting Test. *The Clinical Neuropsychologist, 22*(2), 262-272.
- Balci, F. (2014). Interval timing, dopamine, and motivation. *Timing & Time Perception, 2*(3), 379-410.
- Balci, F., Day, M., Rooney, A., & Brunner, D. (2009b). Disrupted temporal control in the R6/2 mouse model of Huntington's disease. *Behavioral Neuroscience, 123*(6), 1353.
- Balci, F., Freestone, D., & Gallistel, C. R. (2009). Risk assessment in man and mouse. *Proceedings of the National Academy of Sciences, 106*(7), 2459-2463. <https://doi.org/10.1073/pnas.0812709106>
- Balci, F., Gallistel, C. R., Allen, B. D., Frank, K. M., Gibson, J. M., & Brunner, D. (2009c). Acquisition of peak responding: what is learned?. *Behavioural Processes, 80*(1), 67-75. doi: 10.1016/j.beproc.2008.09.010
- Balci, F., Ludvig, E. A., Gibson, J. M., Allen, B. D., Frank, K. M., Kapustinski, B. J., Fedolak, T. E., & Brunner, D. (2008). Pharmacological manipulations of interval timing using the peak procedure in male C3H mice. *Psychopharmacology, 201*(1), 67-80. doi: 10.1007/s00213-008-1248-y
- Balci, F., Meck, W. H., Moore, H., & Brunner, D. (2009a). Timing deficits in aging and neuropathology. In *Animal Models of Human Cognitive Aging* (pp. 1-41). Humana Press. https://doi.org/10.1007/978-1-59745-422-3_8
- Balci, F., & Simen, P. (2016). A decision model of timing. *Current Opinion in Behavioral Sciences, 8*, 94-101.
- Balci, F., Simen, P., Niyogi, R., Saxe, A., Hughes, J. A., Holmes, P., & Cohen, J. D. (2011). Acquisition of decision making criteria: reward rate ultimately beats accuracy.

Attention, Perception, & Psychophysics, 73(2), 640-657. <https://doi.org/10.3758/s13414-010-0049-7>

Balcı, F., Wiener, M., Çavdaroğlu, B., & Coslett, H. B. (2013). Epistasis effects of dopamine genes on interval timing and reward magnitude in humans. *Neuropsychologia*, 51(2), 293-308.

Berkay, D., Eser, H. Y., Sack, A. T., Çakmak, Y. Ö., & Balcı, F. (2018). The modulatory role of pre-SMA in speed-accuracy tradeoff: a bi-directional TMS study. *Neuropsychologia* 31(109): 255-261.

Berry, A. S., Jagust, W. J., & Hsu, M. (2019). Age-related variability in decision-making: Insights from neurochemistry. *Cognitive, Affective, & Behavioral Neuroscience*, 19(3), 415-434.

Beste, C., Adelhöfer, N., Gohil, K., Passow, S., Roessner, V., & Li, S. C. (2018). Dopamine modulates the efficiency of sensory evidence accumulation during perceptual decision making. *International Journal of Neuropsychopharmacology*, 21(7), 649-655.

Bhatia, S. (2013). Associations and the accumulation of preference. *Psychological Review*, 120(3), 522-543.

Bogacz, R., Brown, E., Moehlis, J., Holmes, P., & Cohen, J. D. (2006). The physics of optimal decision making: a formal analysis of models of performance in two-alternative forced-choice tasks. *Psychological Review*, 113(4), 700-765.

Bogacz, R., Wagenmakers, E. J., Forstmann, B. U., & Nieuwenhuis, S. (2010). The neural basis of the speed–accuracy tradeoff. *Trends in Neurosciences*, 33(1), 10-16.

Bortz, D. M., & Grace, A. A. (2018a). Medial septum differentially regulates dopamine neuron activity in the rat ventral tegmental area and substantia nigra via distinct pathways. *Neuropsychopharmacology*, 43, 2093-2100. <https://doi.org/10.1038/s41386-018-0048-2>

Bossaerts, P., & Murawski, C. (2016). Decision neuroscience: why we become more cautious with age. *Current Biology*, 26(12), R495-R497.

- Brandt, M. D., Krüger-Gerlach, D., Hermann, A., Meyer, A. K., Kim, K. S., & Storch, A. (2017). Early postnatal but not late adult neurogenesis is impaired in the *pitx3*-mutant animal model of parkinson's disease. *Frontiers in Neuroscience, 11*, 471.
- Breton, Y. A., Seeland, K. D., & Redish, A. D. (2015). Aging impairs deliberation and behavioral flexibility in inter-temporal choice. *Frontiers in Aging Neuroscience, 7*, 41. doi: 10.3389/fnagi.2015.00041
- Bruin, K. J., & Wijers, A. A. (2002). Inhibition, response mode, and stimulus probability: a comparative event-related potential study. *Clinical Neurophysiology, 113*(7), 1172-1182. [https://doi.org/10.1016/S1388-2457\(02\)00141-4](https://doi.org/10.1016/S1388-2457(02)00141-4)
- Brunton, B. W., Botvinick, M. M., & Brody, C. D. (2013). Rats and humans can optimally accumulate evidence for decision-making. *Science, 340*(6128), 95-98. doi: 10.1126/science.1233912
- Burgess, C. P., Lak, A., Steinmetz, N. A., Zátka-Haas, P., Bai Reddy, C., Jacobs, E. A. K., Linden, J. F., Paton, J. J., Ranson, A., Schröder, S., Soares, S., Wells, M. J., Wool, L. E., Harris, K. D., Carandini, M. (2017) High-yield methods for accurate two-alternative visual psychophysics in head-fixed mice. *Cell Reports 20*(10), 2513–2524. <https://doi.org/10.1016/j.celrep.2017.08.047>
- Cheng, R. K., Dyke, A. G., McConnell, M. W., & Meck, W. H. (2011). Categorical scaling of duration as a function of temporal context in aged rats. *Brain Research, 1381*, 175-186.
- Cheng, K., & Westwood, R. (1993). Analysis of single trials in pigeons' timing performance. *Journal of Experimental Psychology: Animal Behavior Processes, 19*(1), 56-67.
- Chubykin, A. A., Roach, E. B., Bear, M. F., & Shuler, M. G. H. (2013). A cholinergic mechanism for reward timing within primary visual cortex. *Neuron, 77*(4), 723-735.
- Church, R. M., Meck, W. H., & Gibbon, J. (1994). Application of scalar timing theory to individual trials. *Journal of Experimental Psychology: Animal Behavior Processes, 20*(2), 135. <http://dx.doi.org/10.1037/0097-7403.20.2.135>

- Church, R. M., Miller, M. C., Freestone, D., Chiu, C., Osgood, D. P., Machan, J. T., Messier, A. A., Johanson, C. E., & Silverberg, G. D. (2014). Amyloid-beta accumulation, neurogenesis, behavior, and the age of rats. *Behavioral Neuroscience*, *128*(4), 523.
- Coull, J. T., Cheng, R.-K., & Meck, W. H. (2011). Neuroanatomical and Neurochemical Substrates of Timing. *Neuropsychopharmacology Reviews*, *36*, 3-25. <https://doi.org/10.1038/npp.2010.113>
- Coxon, J. P., Van Impe, A., Wenderoth, N., & Swinnen, S. P. (2012). Aging and inhibitory control of action: cortico-subthalamic connection strength predicts stopping performance. *Journal of Neuroscience*, *32*(24), 8401-8412. <https://doi.org/10.1523/JNEUROSCI.6360-11.2012>
- Çoşkun, F., Sayalı, Z. C., Gürbüz, E., & Balcı, F. (2015). Optimal time discrimination. *The Quarterly Journal of Experimental Psychology*, *68*(2), 381-401. <http://dx.doi.org/10.1080/17470218.2014.944921>
- Deary, I. J., Corley, J., Gow, A. J., Harris, S. E., Houlihan, L. M., Marioni, R. E., ... Starr, J. M. (2009). Age-associated cognitive decline. *British Medical Bulletin*, *92*(1), 135–152. <https://doi.org/10.1093/bmb/ldp033>
- De Corte, B. J., Wagner, L. M., Matell, M. S., & Narayanan, N. S. (2019). Striatal dopamine and the temporal control of behavior. *Behavioural Brain Research*, *356*, 375-379.
- de Lafuente, V., Jazayeri, M., & Shadlen, M. N. (2015). Representation of accumulating evidence for a decision in two parietal areas. *Journal of Neuroscience*, *35*(10), 4306-4318.
- Devan, B. D., Hong, N. S., & McDonald, R. J. (2011). Parallel associative processing in the dorsal striatum: segregation of stimulus–response and cognitive control subregions. *Neurobiology of Learning and Memory*, *96*(2), 95-120.
- Ding, L., & Gold, J. I. (2010). Caudate encodes multiple computations for perceptual decisions. *Journal of Neuroscience*, *30*(47), 15747-15759.

- Ding, L., & Gold, J. I. (2011). Neural correlates of perceptual decision making before, during, and after decision commitment in monkey frontal eye field. *Cerebral Cortex*, *22*(5), 1052-1067.
- Ebert, U., & Kirch, W. (1998). Scopolamine model of dementia: electroencephalogram findings and cognitive performance. *European Journal of Clinical Investigation*, *28*(11), 944-949. <https://doi.org/10.1046/j.1365-2362.1998.00393.x>
- Emmons, E. B., De Corte, B. J., Kim, Y., Parker, K. L., Matell, M. S., & Narayanan, N. S. (2017). Rodent medial frontal control of temporal processing in the dorsomedial striatum. *Journal of Neuroscience*, *37*(36), 8718-8733.
- Emmons, E. B., Kennedy, M., Kim, Y., & Narayanan, N. S. (2019). Corticostriatal stimulation compensates for medial frontal inactivation during interval timing. *Scientific Reports*, *9*, 14371 (2019) doi:10.1038/s41598-019-50975-7.
- Erhan, C., & Balci, F. (2017). Obsessive compulsive features predict cautious decision strategies. *Quarterly Journal of Experimental Psychology*, *70*(1), 179-190.
- Erhan, C., Bulut, G. Ç., Gökçe, S., Ozbas, D., Turkakin, E., Dursun, O. B., Yazgan, Y., & Balci, F. (2017). Disrupted latent decision processes in medication-free pediatric OCD patients. *Journal of Affective Disorders*, *207*, 32-37.
- Erlich, J. C., Brunton, B. W., Duan, C. A., Hanks, T. D., & Brody, C. D. (2015). Distinct effects of prefrontal and parietal cortex inactivations on an accumulation of evidence task in the rat. *Elife*, *4*, e05457. <https://doi.org/10.7554/eLife.05457>
- Forstmann, B. U., Anwander, A., Schäfer, A., Neumann, J., Brown, S., Wagenmakers, E. J., Bogacz, R., & Turner, R. (2010). Cortico-striatal connections predict control over speed and accuracy in perceptual decision making. *Proceedings of the National Academy of Sciences*, *107*(36), 15916-15920. <https://doi.org/10.1073/pnas.1004932107>
- Forstmann, B. U., Dutilh, G., Brown, S., Neumann, J., Von Cramon, D. Y., Ridderinkhof, K. R., & Wagenmakers, E. J. (2008). Striatum and pre-SMA facilitate decision-making under time pressure. *Proceedings of the National Academy of Sciences*, *105*(45), 17538-17542.

- Friedman, R. A. (2013, July 20). Fast Time and the Aging Mind. Retrieved from <https://www.nytimes.com/2013/07/21/opinion/sunday/fast-time-and-the-aging-mind.html>
- Garces, D., El Massioui, N., Lamirault, C., Riess, O., Nguyen, H. P., Brown, B. L., & Doyère, V. (2018). The alteration of emotion regulation precedes the deficits in interval timing in the BACHD rat model for Huntington disease. *Frontiers in Integrative Neuroscience, 12*, 14.
- Gibbon, J. (1977). Scalar expectancy theory and Weber's law in animal timing. *Psychological Review, 84*(3), 279-325.
- Gibbon, J., & Church, R. M. (1990). Representation of time. *Cognition, 37*(1-2), 23-54.
- Gibbon, J., & Church, R. M. (1992). Comparison of variance and covariance patterns in parallel and serial theories of timing. *Journal of the Experimental Analysis of Behavior, 57*(3), 393-406. <https://doi.org/10.1901/jeab.1992.57-393>
- Gibbon, J., Church, R. M., & Meck, W. H. (1984). Scalar timing in memory. *Annals of the New York Academy of Sciences, 423*(1), 52-77.
- Gold, J. I., & Shadlen, M. N. (2001). Neural computations that underlie decisions about sensory stimuli. *Trends in Cognitive Sciences, 5*(1), 10-16.
- Gold, J. I., & Shadlen, M. N. (2007). The neural basis of decision making. *Annual Review of Neuroscience, 30*(1), 535-574. <https://doi.org/10.1146/annurev.neuro.29.051605.113038>
- Goldberg, E. (1986). Varieties of perseveration: A comparison of two taxonomies. *Journal of Clinical and Experimental Neuropsychology, 8*(6), 710-726. <http://dx.doi.org/10.1080/01688638608405191>
- Gulcebi, M., Akman, O., Carcak, N., Karamahmutoglu, T., & Onat, F. (2017). Evaluation of GAD67 immunoreactivity in the region of substantia nigra pars reticulata in resistance to development of convulsive seizure in genetic absence epilepsy rats. *Northern Clinics of Istanbul, 3*(3): 161-167.

- Gür, E., Duyan, Y. A., & Balcı, F. (2018). Spontaneous integration of temporal information: implications for representational/computational capacity of animals. *Animal Cognition*, *21*(1), 3-19. <https://doi.org/10.1007/s10071-017-1137-z>
- Gür, E., Duyan, Y. A., & Balcı, F. (2019). Probabilistic Information Modulates the Timed Response Inhibition Deficit in Aging Mice. *Frontiers in Behavioral Neuroscience*, *13*, 196.
- Harada, C. N., Natelson Love, M. C., & Triebel, K. L. (2013). Normal Cognitive Aging. *Clinics in Geriatric Medicine*, *29*(4), 737-752. <https://doi.org/10.1016/j.cger.2013.07.002>
- Hasher, L., & Zacks, R. T. (1988). Working memory, comprehension, and aging: A review and a new view. In *Psychology of Learning and Motivation* (pp. 193-225). Academic Press.
- Head, D., Kennedy, K. M., Rodrigue, K. M., & Raz, N. (2009). Age differences in perseveration: cognitive and neuroanatomical mediators of performance on the Wisconsin Card Sorting Test. *Neuropsychologia*, *47*(4), 1200-1203.
- Hoebel, B. G., Avena, N. M., & Rada, P. (2007). Accumbens dopamine-acetylcholine balance in approach and avoidance. *Current Opinion in Pharmacology*, *7*(6), 617-627.
- Howard Jr, J. H., Howard, D. V., Dennis, N. A., & Kelly, A. J. (2008). Implicit learning of predictive relationships in three-element visual sequences by young and old adults. *Journal of Experimental Psychology: Learning, Memory, and Cognition*, *34*(5), 1139-1157. <http://dx.doi.org/10.1037/a0012797>
- JASP Team (2019). JASP (Version 0.9.0.1) [Computer software].
- Johnson, S. A., Turner, S. M., Santacrose, L. A., Carty, K. N., Shafiq, L., Bizon, J. L., Maurer, A. P., & Burke, S. N. (2017). Rodent age-related impairments in discriminating perceptually similar objects parallel those observed in humans. *Hippocampus*, *27*(7), 759-776.
- Kheifets, A., & Gallistel, C. R. (2012). Mice take calculated risks. *Proceedings of the National Academy of Sciences*, *109*(22), 8776-8779.

- Kramer, A. F., Humphrey, D. G., Larish, J. F., & Logan, G. D. (1994). Aging and inhibition: beyond a unitary view of inhibitory processing in attention. *Psychology and Aging, 9*(4), 491-512. <http://dx.doi.org/10.1037/0882-7974.9.4.491>
- Kroener, S., Chandler, L. J., Phillips, P. E., & Seamans, J. K. (2009). Dopamine modulates persistent synaptic activity and enhances the signal-to-noise ratio in the prefrontal cortex. *PloS one, 4*(8), e6507.
- LeBlanc, P., & Soffié, M.(1999). Effects of age on short-term memory for time in rats. *Experimental Aging Research, 25*(3), 267-284.
- LeBlanc, P., Weyers, M. H., & Soffié, M. (1996). Age-related differences for duration discrimination in rats. *Physiology & Behavior, 60*(2), 555-558.
- Lejeune, H., Ferrara, A., Sofie, M., Bronchart, M., & Wearden, J. H. (1998). Peak procedure performance in young adult and aged rats: acquisition and adaptation to a changing temporal criterion. *The Quarterly Journal of Experimental Psychology Section B, 51*(3b), 193-217.
- Liston, D. B., & Stone, L. S. (2013). Saccadic brightness decisions do not use a difference model. *Journal of Vision, 13*(8), 1. <https://doi.org/10.1167/13.8.1>
- Lo, C. C., & Wang, X. J. (2006). Cortico–basal ganglia circuit mechanism for a decision threshold in reaction time tasks. *Nature Neuroscience, 9*(7), 956-963.
- Lustig, C. (2003) Grandfather’s clock: Attention and interval timing in older adults. In *Functional and Neural Mechanisms of Internal Timing* (pp. 261-293). Boca Raton.
- MacDonald, C., Cheng, R. K., & Meck, W. H. (2012). Acquisition of “Start” and “Stop” response thresholds in peak-interval timing is differentially sensitive to protein synthesis inhibition in the dorsal and ventral striatum. *Frontiers in Integrative Neuroscience, 6*, 10. doi: 10.3389/fnint.2012.00010
- Maddox, W. T., & Bohil, C. J. (1998). Overestimation of base-rate differences in complex perceptual categories. *Perception & Psychophysics, 60*(4), 575-592.

- Malet-Karas, A., Noulhiane, M., & Doyère, V. (2019). Dynamics of Spatio-Temporal Binding in Rats. *Timing & Time Perception*, 7(1), 27-47. doi: 10.1163/22134468-20181124
- Marschner, A., Mell, T., Wartenburger, I., Villringer, A., Reischies, F. M., & Heekeren, H. R. (2005). Reward-based decision-making and aging. *Brain Research Bulletin*, 67(5), 382-390.
- Matell, M. S., & Portugal, G. S. (2007). Impulsive responding on the peak-interval procedure. *Behavioural Processes*, 74(2), 198-208.
- Meck, W. H. (1983). Selective adjustment of the speed of internal clock and memory processes. *Journal of Experimental Psychology: Animal Behavior Processes*, 9(2), 171-201.
- Meck, W. H. (2002). Choline uptake in the frontal cortex is proportional to the absolute error of a temporal memory translation constant in mature and aged rats. *Learning and Motivation*, 33(1), 88-104.
- Meck, W. H. (2006). Temporal memory in mature and aged rats is sensitive to choline acetyltransferase inhibition. *Brain Research*, 1108, 168-175.
- Meck, W. H., & Church, R. M. (1987). Cholinergic modulation of the content of temporal memory. *Behavioral Neuroscience*, 101(4), 457-464.
- Meck, W. H., Church, R. M., & Wenk, G. L. (1986). Arginine vasopressin inoculates against age-related increases in sodium-dependent high affinity choline uptake and discrepancies in the content of temporal memory. *European Journal of Pharmacology*, 130(3), 327-331.
- Mendez, I. A., Damborsky, J. C., Winzer-Serhan, U. H., Bizon, J. L., & Setlow, B. (2013). $\alpha 4\beta 2^*$ and $\alpha 7$ nicotinic acetylcholine receptor binding predicts choice preference in two cost benefit decision-making tasks. *Neuroscience*, 230, 121-131. doi: 10.1016/j.neuroscience.2012.10.067

- Moers-Hornikx, V. M., Sesia, T., Basar, K., Lim, L. W., Hoogland, G., Steinbusch, H. W., Gavilanes, D. A., Temel, Y., & Vles, J. S. (2009). Cerebellar nuclei are involved in impulsive behaviour. *Behavioural Brain Research*, *203*(2), 256-263.
- Morales-Vives, F., & Vigil-Colet, A. (2012). Are old people so gentle? Functional and dysfunctional impulsivity in the elderly. *International Psychogeriatrics*, *24*(3), 465-471.
- Mormann, M. M., Malmaud, J., Huth, A., Koch, C., & Rangel, A. (2010). The drift diffusion model can account for the accuracy and reaction time of value-based choices under high and low time pressure. *Judgment and Decision Making*, *5*(6), 437-449. <http://dx.doi.org/10.2139/ssrn.1901533>
- Muir, J. L. (1997). Acetylcholine, aging, and Alzheimer's disease. *Pharmacology Biochemistry and Behavior*, *56*(4), 687-696.
- Narayanan, N. S., Land, B. B., Solder, J. E., Deisseroth, K., & DiLeone, R. J. (2012). Prefrontal D1 dopamine signaling is required for temporal control. *Proceedings of the National Academy of Sciences*, *109*(50), 20726-20731.
- Odoemene, O., Pisupati, S., Nguyen, H., & Churchland, A. K. (2018). Visual evidence accumulation guides decision-making in unrestrained mice. *Journal of Neuroscience*, *38*(47), 10143-10155.
- Oprisan, S. A., & Buhusi, C. V. (2011). Modeling pharmacological clock and memory patterns of interval timing in a striatal beat-frequency model with realistic, noisy neurons. *Frontiers in Integrative Neuroscience*, *5*, 52.
- Onozuka, M., Watanabe, K., Fujita, M., Tomida, M., & Ozono, S. (2002). Changes in the septohippocampal cholinergic system following removal of molar teeth in the aged SAMP8 mouse. *Behavioural Brain Research*, *133*(2), 197-204.
- Packard, M. G., & McGaugh, J. L. (1996). Inactivation of hippocampus or caudate nucleus with lidocaine differentially affects expression of place and response learning. *Neurobiology of Learning and Memory*, *65*(1), 65-72.

- Paraskevoudi, N., Balci, F., & Vatakis, A. (2018). "Walking" through the sensory, cognitive, and temporal degradations of healthy aging. *Annals of the New York Academy of Sciences*, 1426(1), 72-92.
- Paxinos, G., & Franklin, K. B. (2012). *Paxinos and Franklin's the mouse brain in stereotaxic coordinates, 4th edition*. Academic press.
- Perbal, S., Droit-volet, S., Isingrini, M., & Pouthas, V. (2002). Relationships Between Age-Related Changes in Time Estimation and Age- Related Changes in Processing Speed , Attention , and Memory. *Aging Neuropsychology and Cognition*, 9(3), 201–216.
- Pioli, E. Y., Meissner, W., Sohr, R., Gross, C. E., Bezard, E., & Bioulac, B. H. (2008). Differential behavioral effects of partial bilateral lesions of ventral tegmental area or substantia nigra pars compacta in rats. *Neuroscience*, 153(4), 1213-1224.
- Potter, L. M., & Grealy, M. A. (2008). Aging and inhibition of a prepotent motor response during an ongoing action. *Aging, Neuropsychology, and Cognition*, 15(2), 232-255.
- Ratcliff, R. (2002). A diffusion model account of response time and accuracy in a brightness discrimination task: Fitting real data and failing to fit fake but plausible data. *Psychonomic Bulletin & Review*, 9(2), 278-291.
- Ratcliff, R., Cherian, A., & Segraves, M. (2003b). A comparison of macaque behavior and superior colliculus neuronal activity to predictions from models of two-choice decisions. *Journal of Neurophysiology*, 90(3), 1392-1407. <https://doi.org/10.1152/jn.01049.2002>
- Ratcliff, R., & Childers, R. (2015). Individual differences and fitting methods for the two-choice diffusion model of decision making. *Decision*, 2(4), 237-279.
- Ratcliff, R., & McKoon, G. (2008). The diffusion decision model: theory and data for two-choice decision tasks. *Neural Computation*, 20(4), 873-922.
- Ratcliff, R., & Rouder, J. N. (1998). Modeling response times for two-choice decisions. *Psychological Science*, 9(5), 347-356.
- Ratcliff, R., Thapar, A., Gomez, P., & McKoon, G. (2004a). A diffusion model analysis of the effects of aging in the lexical-decision task. *Psychology and Aging*, 19(2), 278-289.

- Ratcliff, R., Thapar, A., & McKoon, G. (2001). The effects of aging on reaction time in a signal detection task. *Psychology and Aging, 16*(2), 323–341.
- Ratcliff, R., Thapar, A., & Mckoon, G. (2003a). A diffusion model analysis of the effects of aging on brightness discrimination. *Perception & Psychophysics, 65*(4), 523-535.
- Ratcliff, R., Thapar, A., & McKoon, G. (2004b). A diffusion model analysis of the effects of aging on recognition memory. *Journal of Memory and Language, 50*(4), 408-424.
- Ratcliff, R., Thapar, A., & McKoon, G. (2006a). Aging and individual differences in rapid two-choice decisions. *Psychonomic Bulletin & Review, 13*(4), 626-635.
- Ratcliff, R., Thapar, A., & McKoon, G. (2006b). Aging, practice, and perceptual tasks: A diffusion model analysis. *Psychology and Aging, 21*(2), 353–371.
- Ratcliff, R., Thapar, A., & McKoon, G. (2007). Application of the diffusion model to two-choice tasks for adults 75-90 years old. *Psychology and Aging, 22*(1), 56–66.
- Ratcliff, R., & Tuerlinckx, F. (2002). Estimating parameters of the diffusion model: Approaches to dealing with contaminant reaction times and parameter variability. *Psychonomic Bulletin & Review, 9*(3), 438-481.
- Rey-Mermet, A., & Gade, M. (2018). Inhibition in aging: What is preserved? What declines? A meta-analysis. *Psychonomic Bulletin & Review, 25*(5), 1695-1716.
- Roberson, E. D., DeFazio, R. A., Barnes, C. A., Alexander, G. E., Bizon, J. L., Bowers, D., Foster, T. C., Glisky, E. L., Levin, B. E., Ryan, L., Wright, C. B., & Geldmacher, D. S. (2012). Challenges and opportunities for characterizing cognitive aging across species. *Frontiers in Aging Neuroscience, 4*, 1-6. <https://doi.org/10.3389/fnagi.2012.00006>
- Roberts, S. (1981). Isolation of an internal clock. *Journal of Experimental Psychology: Animal Behavior Processes, 7*(3), 242-268.
- Salthouse, T. A. (1996). The processing-speed theory of adult age differences in cognition. *Psychological Review, 103*(3), 403-428. doi: 10.1037/0033-295X.103.3.403.

- Samanez-Larkin, G. R., & Knutson, B. (2015). Decision making in the ageing brain: changes in affective and motivational circuits. *Nature Reviews Neuroscience*, *16*(5), 278-289.
- Sanabria, F., Thraillkill, E. A., & Killeen, P. R. (2009). Timing with opportunity cost: Concurrent schedules of reinforcement improve peak timing. *Learning & Behavior*, *37*(3), 217-229.
- Schliebs, R., & Arendt, T. (2011). The cholinergic system in aging and neuronal degeneration. *Behavioural Brain Research*, *221*(2), 555-563.
- Schulz, J. M., Redgrave, P., Mehring, C., Aertsen, A., Clements, K. M., Wickens, J. R., & Reynolds, J. N. (2009). Short-latency activation of striatal spiny neurons via subcortical visual pathways. *Journal of Neuroscience*, *29*(19), 6336-6347.
- Scott, B. B., Brody, C. D., & Tank, D. W. (2013). Cellular resolution functional imaging in behaving rats using voluntary head restraint. *Neuron*, *80*(2), 371-384.
- Scott, B. B., Constantinople, C. M., Erlich, J. C., Tank, D. W., & Brody, C. D. (2015). Sources of noise during accumulation of evidence in unrestrained and voluntarily head-restrained rats. *Elife*, *4*, e11308.
- Simen, P., Balci, F., deSouza, L., Cohen, J. D., & Holmes, P. (2011). A model of interval timing by neural integration. *Journal of Neuroscience*, *31*(25), 9238-9253.
- Simon, J. R., Howard Jr, J. H., & Howard, D. V. (2011). Age differences in implicit learning of probabilistic unstructured sequences. *Journals of Gerontology Series B: Psychological Sciences and Social Sciences*, *66*(1), 32-38. doi:10.1093/geronb/gbq066
- Simon, N. W., LaSarge, C. L., Montgomery, K. S., Williams, M. T., Mendez, I. A., Setlow, B., & Bizon, J. L. (2010). Good things come to those who wait: attenuated discounting of delayed rewards in aged Fischer 344 rats. *Neurobiology of Aging*, *31*(5), 853-862.
- Smith, P. L., & Ratcliff, R. (2004). Psychology and neurobiology of simple decisions. *Trends in Neurosciences*, *27*(3), 161-168.

- Spaniol, J., & Bayen, U. J. (2005). Aging and conditional probability judgments: a global matching approach. *Psychology and Aging, 20*(1), 165-181. doi: 10.1037/0882-7974.20.1.165
- Spiegelhalter, D. J., Best, N. G., Carlin, B. P., & Van Der Linde, A. (2002). Bayesian measures of model complexity and fit. *Journal of the Royal Statistical Society: Series B (Statistical Methodology), 64*(4), 583-639.
- Starns, J. J., & Ratcliff, R. (2010). The effects of aging on the speed–accuracy compromise: Boundary optimality in the diffusion model. *Psychology and Aging, 25*(2), 377. doi: 10.1037/a0018022
- Stocco, A. (2012). Acetylcholine-based entropy in response selection: a model of how striatal interneurons modulate exploration, exploitation, and response variability in decision-making. *Frontiers in Neuroscience, 6*, 18. doi: 10.3389/fnins.2012.00018
- Stone, W. S., Rudd, R. J., & Gold, P. E. (1992). Glucose attenuation of scopolamine- and age-induced deficits in spontaneous alternation behavior and regional brain [³H] 2-deoxyglucose uptake in mice. *Psychobiology, 20*(4), 270-279. <https://doi.org/10.3758/BF03332059>
- Suchy, Y., Lee, J. N., & Marchand, W. R. (2013). Aberrant cortico–subcortical functional connectivity among women with poor motor control: Toward uncovering the substrate of hyperkinetic perseveration. *Neuropsychologia, 51*(11), 2130-2141. doi: 10.1016/j.neuropsychologia.2013.07.004
- Thapar, A., Ratcliff, R., & McKoon, G. (2003). A diffusion model analysis of the effects of aging on letter discrimination. *Psychology and Aging, 18*(3), 415-429.
- Tosun, T., Berkay, D., Sack, A. T., Çakmak, Y. Ö., & Balçı, F. (2017). Inhibition of pre-supplementary motor area by continuous theta burst stimulation leads to more cautious decision-making and more efficient sensory evidence integration. *Journal of Cognitive Neuroscience, 29*(8), 1433-1444.
- Tosun, T., Gür, E., & Balçı, F. (2016). Mice plan decision strategies based on previously learned time intervals, locations, and probabilities. *Proceedings of the National Academy of Sciences, 113*(3), 787-792. <https://doi.org/10.1073/pnas.1518316113>

- Turgeon, M., Lustig, C., & Meck, W. H. (2016). Cognitive aging and time perception: roles of bayesian optimization and degeneracy. *Frontiers in Aging Neuroscience, 8*, 102.
- Turgeon, M., & Wing, A. M. (2012). Late onset of age-related difference in unpaced tapping with no age-related difference in phase-shift error detection and correction. *Psychology and Aging, 27*(4), 1152. doi: 10.1037/a0029925
- Van De Laar, M. C., Van Den Wildenberg, W. P., van Boxtel, G., & van der Molen, M. (2011). Lifespan changes in global and selective stopping and performance adjustments. *Frontiers in Psychology, 2*, 357. doi: 10.3389/fpsyg.2011.00357
- Vanneste, V., Pouthas, JH, Wearden, S. (2001). Temporal control of rhythmic performance: a comparison between young and old adults. *Experimental Aging Research, 27*(1), 83-102. <https://doi.org/10.1080/03610730125798>
- White, C. N., Ratcliff, R., Vasey, M. W., & McKoon, G. (2010). Using diffusion models to understand clinical disorders. *Journal of Mathematical Psychology, 54*(1), 39-52.
- Wiecki, T. V., Sofer, I., & Frank, M. J. (2013). HDDM: Hierarchical Bayesian estimation of the drift-diffusion model in Python. *Frontiers in Neuroinformatics, 7*, 14.
- Willig, F., Palacios, A., Monmaur, P., M'Harzi, M., Laurent, J., & Delacour, J. (1987). Short-term memory, exploration and locomotor activity in aged rats. *Neurobiology of Aging, 8*(5), 393-402. [https://doi.org/10.1016/0197-4580\(87\)90033-9](https://doi.org/10.1016/0197-4580(87)90033-9)
- Wittmann, M., & Lehnhoff, S. (2005). Age effects in perception of time. *Psychological Reports, 97*(3), 921-935.
- Wong, A. A., & Brown, R. E. (2007). Age-related changes in visual acuity, learning and memory in C57BL/6J and DBA/2J mice. *Neurobiology of Aging, 28*(10), 1577-1593.
- Xie, X., Arguello, A. A., Reittinger, A. M., Wells, A. M., & Fuchs, R. A. (2012). Role of nicotinic acetylcholine receptors in the effects of cocaine-paired contextual stimuli on impulsive decision making in rats. *Psychopharmacology, 223*(3), 271-279.
- Xu, R., & Church, R. M. (2017). Age-related changes in human and nonhuman timing. *Timing & Time Perception, 5*(3-4), 261-279. doi: 10.1163/22134468-00002092

Yartsev, M. M., Hanks, T. D., Yoon, A. M., & Brody, C. D. (2018). Causal contribution and dynamical encoding in the striatum during evidence accumulation. *Elife*, *7*, e34929.

Yoder, W. M., Gaynor, L. S., Burke, S. N., Setlow, B., Smith, D. W., & Bizon, J. L. (2017). Interaction between age and perceptual similarity in olfactory discrimination learning in F344 rats: relationships with spatial learning. *Neurobiology of Aging*, *53*, 122-137.

Zhang, Q., Jung, D., Larson, T., Kim, Y., & Narayanan, N. (2019). Scopolamine and medial frontal stimulus-processing during interval timing. *Neuroscience*, *414*, 219-227.



Appendix A

A.1 Operant Chambers

Experiments were conducted in operant chambers (21.6×17.8×12.7cm, ENV-307W; Med Associates) in sound-attenuating boxes. Three illuminable feeding hoppers (ENV-302RW) were mounted side by side on one of the end walls and a nose poke hole (ENV-313W) in the middle of the opposite wall. A houselight (ENV-315W) above the nose poke hole signaled the time intervals. There were two retractable levers (ENV-312-2W) on each side of the nose poke hole. The middle feeding hopper delivered 0.01 mL of diluted liquid food (Nestlé Nutrition Isosource, vanilla flavor) as the reward. MED-PC IV software was used to control operant chambers and record data (10 ms precision).

A.2 IHC Protocol & Histological Confirmation

One-to-four days after the completion of the behavioral phase of the experiment (2 days on average), mice were anesthetized with ketamine (90 mg/kg, i.p.) and xylazine (10 mg/kg), transcardially perfused with physiological saline and then with a fixative (10% solution of formaldehyde, Tekkim, Turkey) using a peristaltic perfusion pump (5 mL/min), and decapitated. Brains were collected and kept in the fixative solution overnight in falcon tubes. The next day, brains were transferred to 30% sucrose solution and stored at +4°C until they sank to the bottom. Finally, brains were snap-frozen in dry ice (2-isomethylbutane, Sigma-Aldrich) for 3 min at -20°C and were stored at -80°C until further use. The rest of the protocol was followed after all mice completed the behavioral phase.

The target regions of IHC staining for free-floating sections were substantia nigra pars compacta (SNc), ventral tegmental area (VTA), medial septal/diagonal band (MS/DB) complex, and striatum (STR; dorsolateral: DLS and dorsomedial: DMS). All coordinates were obtained from the stereotaxic atlas of Paxinos and Franklin (Paxinos and Franklin, 2012). Bregma was the reference point on the anteroposterior axis. The sections from the region between -2.7 mm and -3.8 mm were taken for the examination of SNc and VTA, and sections from the region between 1.7 mm and 0.2 mm were taken for the examination of MS/DB complex and STR.

After thawing, the whole brains were embedded in Tissue-Tek (Sakura-Finetek) and 40 μm sections were cut at -20°C using a cryostat. The free-floating sections were first immersed in PBS in well plates and then incubated with 3% H_2O_2 solution for 10 min using an orbital shaker. After being rinsed with TBS-Tween 20 (3x5 min), the sections were incubated with Ultra V Block solution (Thermo Scientific) for 30 min and then incubated with primary antibodies [Tyrosine Hydroxylase (1:500) & Choactase (1:100), Santa Cruz] in 0.5% TBS-Triton X-100 solution at $+4^{\circ}\text{C}$ overnight. On the following day, the sections were incubated for 20 min with secondary antibody (UltraVision Quanto Detection System, Thermo Scientific) and rinsed with TBS-Tween 20 (3x5 min). The sections were then incubated with horseradish peroxidase solution (Thermo Scientific) for 30 min and rinsed with TBS-Tween 20 (3x5 min). After staining with AEC Substrate System (Lab Vision Mount, Thermo Scientific), the sections were rinsed with TBS-Tween 20, mounted on positively charged slides and then coverslipped. During the staining protocol, brains were grouped in three such that there was one mouse from each age group.

Coronal sections containing the SNc, VTA, MS/DB complex, and STR were stained with thionin acetate (Sigma Aldrich) to confirm the localization and morphology of the targeted regions. Thionin staining protocol was as follows: xylene (2 min), 100%, 98%, 70%, 50% alcohol (each for 2 min), thionin acetate (1 min), 50%, 70%, 98%, 100% alcohol (each for 1-2 sec), xylene (1-2 sec).

A.3 Estimation of peak time & spread from the average response curves

Average response curves smoothed by three-second bins and normalized by the amplitude and the target intervals were used to calculate peak time and spread measures to examine the temporal accuracy (i.e. peak time) and precision (i.e. spread) of mice (Balcı et al., 2009c). In these normalized curves, the point at which the response rate was equal to 1, which is the time of maximum reward expectancy, was defined as the peak time. For the calculation of the spread, the difference between the first point that the normalized response rate exceeded .70 from the beginning of the trial and the first point that the normalized response rate fell below .70 following the peak time was used.

A.4 Estimation of start & stop times via single-trial analysis

In order to extract the start time and stop times from the steady-state data, a relative likelihood change point (CP) algorithm was run on the cumulative inter-response time (IRT) data from each PI trial of each subject to detect the breakpoints that correspond to the transition from low to high response state as the time of reinforcement availability approaches (i.e. start time) and the transition from high to low response state as the reinforcement availability time passes (i.e. stop time). The CP algorithm runs on the cumulative IRTs datum-by-datum and for each point, it compares the former part of the data with the rest of the data to decide whether these two fractions of the data come from the same or two different exponential distributions. For a given point, when the odds are in favor of a change relative to no change hypothesis according to a predefined (odds ratio) criterion, the algorithm decides that there has been a change in the rate at which the responses are emitted. We chose a conservative factor of 100 meaning that odds had to favor the change model over the no-change model by 100:1 for the CP algorithm to decide there has been a change. The algorithm first detects the start time and by truncating the data from this point onward it runs to detect the stop time (Balci et al., 2009c). In our analysis, after normalizing the detected start and stop times by the target intervals (to be able to compare the measures of two target intervals), the average of the normalized start and stop times and the absolute difference between the normalized start and stop times were defined as the middle time and spread, respectively.

A.5 Variability of Start and Stop Times

After pooling the normalized start and stop times for the short and long target intervals, coefficients of variation (CVs) were also calculated for the start and stop times. These measures were compared by 2 x 3 mixed-design ANOVA using age as the between-groups factor. Comparison of the CV of start and stop times by age groups showed that the CV of start times ($M = 0.92$, $SE = 0.03$) was significantly higher than the CV of stop times ($M = 0.35$, $SE = 0.01$), $F(1,34) = 453.85$, $p < 0.001$, $\eta_p^2 = 0.93$. Difference between the age groups was not statistically significant, $F(2,34) = 2.49$, $p = 0.098$. The interaction between the CV measures and age was statistically significant, $F(2,34) = 4.21$, $p = 0.02$, $\eta_p^2 = 0.20$. The CV of stop times were comparable between age groups (all $ps > 0.05$) while the CV of start times of the adult mice ($M = 0.82$, $SE = 0.05$) was significantly

lower than the CV of start times of young (MD = -0.15, SE = 0.07, $p = 0.03$) and old (MD = -0.15, SE = 0.06, $p = 0.02$) mice.

A.6 Examination of Acquisition of Stop Times

In order to do find the point (n^{th} trial) during the FI-PI phase at which the temporally controlled stop times emerged (i.e. acquisition of the stop time threshold) for each subject, the change point algorithm for binomial data was used. First, the stop times in each trial were defined as a success (1) or fail (0) trials and then the change point algorithm was run on the binomial data for each subject. The success trials were defined as the trials that had stop times shorter than 50 s and 100 s for short (25 s) and long (50 s) target intervals (i.e., 2xFI), respectively.

A.7 Start Times Throughout Session Blocks

For the short target interval, age differences were evident in the first three session blocks [1st block: $F(2,34) = 5.65$, $p = 0.01$, $\eta_p^2 = 0.25$; 2nd block: $F(2,34) = 11.99$, $p < 0.001$, $\eta_p^2 = 0.41$; 3rd block: $F(2,34) = 5.17$, $p = 0.01$, $\eta_p^2 = 0.23$]. Specifically, the average normalized start time of old mice was significantly later than the average normalized start time of young (MD = 0.09, SE = 0.03, $p = 0.01$) and adult (MD = 0.09, SE = 0.03, $p = 0.01$) mice but there was no significant difference between the young and adult mice (MD = -0.002, SE = 0.03, $p = 0.96$) in the first block. In the second block, similar to the first block, the average normalized start time of old mice was significantly later than the average normalized start time of young (MD = 0.14, SE = 0.03, $p < 0.001$) and adult (MD = 0.08, SE = 0.03, $p = 0.01$) mice but there was no significant difference between the young and adult mice (MD = -0.06, SE = 0.03, $p = 0.052$). In the third block, the difference between the normalized start times of adult and old mice disappeared (MD = -0.01, SE = 0.04, $p = 0.86$); however, the average normalized start time of young mice was significantly earlier than the average normalized start time of adult (MD = -0.11, SE = 0.04, $p = 0.01$) and old (MD = -0.12, SE = 0.04, $p = 0.01$) mice. In the following fourth and fifth blocks, age differences between the average normalized start time were not significant for the short target interval [4th block: $F(2,34) = 2.17$, $p = 0.13$; 5th block: $F(2,34) = 0.23$, $p = 0.80$]. Examination of the normalized start times between age groups for each block for the long target interval revealed that only in the first block age difference was significant [$F(2,34) = 6.14$, $p = 0.01$, $\eta_p^2 = 0.27$]. On average, the

normalized start time of young mice was significantly earlier than the normalized start time of adult (MD = -0.14, SE = 0.04, $p = 0.002$) and old (MD = -0.10, SE = 0.04, $p = 0.02$) mice; there was no significant difference between adult and old mice (MD = 0.04, SE = 0.04, $p = 0.31$). In the remaining four blocks, we did not find any significant differences between the normalized start times of three age groups [2nd block: $F(2,34) = 0.54$, $p = 0.59$; 3rd block: $F(2,34) = 0.41$, $p = 0.67$; 4th block: $F(2,34) = 0.95$, $p = 0.40$; 5th block: $F(2,34) = 0.80$, $p = 0.46$]. Overall, these results showed that any observed age differences in the normalized start times disappeared as sessions proceeded for both target intervals.

A.8 Stop Times Throughout Session Blocks

For the short target interval, we found that there were no age differences in the normalized stop times of the first [$F(2,34) = 0.84$, $p = 0.44$] and the second [$F(2,34) = 2.69$, $p = 0.08$] blocks. A significant age difference was apparent starting from the third block [$F(2,34) = 10.81$, $p < 0.001$, $\eta_p^2 = 0.39$]; old mice having significantly later normalized stop times compared to young (MD = 0.38, SE = 0.10, $p < 0.001$) and adult (MD = 0.41, SE = 0.10, $p < 0.001$) mice, while the young and adult mice had no such difference (MD = 0.03, SE = 0.10, $p = 0.79$). In the following blocks, significant effect of age was still evident for the short target interval [4th block: $F(2,34) = 14.89$, $p < 0.001$, $\eta_p^2 = 0.47$; 5th block: $F(2,34) = 19.22$, $p < 0.001$, $\eta_p^2 = 0.53$]. More specifically, in the fourth block, on average, the normalized stop time of old mice was later compared to the normalized stop time of young (MD = 0.46, SE = 0.11, $p < 0.001$) and adult (MD = 0.57, SE = 0.11, $p < 0.001$) mice with no difference between young and adult mice (MD = 0.11, SE = 0.11, $p = 0.36$). The same differences held for the normalized stop times in the fifth block of the short target interval, such that the normalized stop time of old mice was later compared to the normalized stop time of young (MD = 0.40, SE = 0.09, $p < 0.001$) and adult (MD = 0.52, SE = 0.09, $p < 0.001$) mice with no difference between young and adult mice (MD = 0.12, SE = 0.09, $p = 0.18$). For the long target interval, while there was no significant age differences between the normalized stop times in the first block [$F(2,34) = 2.15$, $p = 0.13$], age differences were significant in all the remaining blocks. In the second block, the normalized stop times were significantly different between the adult and old mice (MD = -0.53, SE = 0.15, $p = 0.001$), but not between the young and adult (MD = 0.28, SE = 0.15, $p = 0.07$) or young and old (MD = -0.25, SE = 0.15, $p = 0.11$) mice [$F(2,34) = 6.20$, $p =$

0.01, $\eta_p^2 = 0.27$]. In the third block [$F(2,34) = 9.78$, $p < 0.001$, $\eta_p^2 = 0.37$], the average normalized stop time of old mice was significantly later than the average normalized stop time of young (MD = 0.52, SE = 0.16, $p = 0.003$) and adult (MD = 0.68, SE = 0.16, $p < 0.001$) mice but young and adult mice did not differ (MD = 0.16, SE = 0.16, $p = 0.35$). In the fourth block [$F(2,34) = 10.51$, $p < 0.001$, $\eta_p^2 = 0.38$], the average normalized stop times were not different between young and adult mice (MD = 0.17, SE = 0.13, $p = 0.22$); however, the average normalized stop time of old mice was significantly later than young (MD = 0.41, SE = 0.13, $p = 0.003$) and adult (MD = 0.57, SE = 0.13, $p < 0.001$) mice. The significant age differences for the normalized stop times found in the third and fourth blocks also held in the fifth block [$F(2,34) = 8.77$, $p = 0.001$, $\eta_p^2 = 0.34$]. On average, the normalized stop time of old mice was later compared to young (MD = 0.23, SE = 0.10, $p = 0.02$) and adult (MD = 0.39, SE = 0.10, $p < 0.001$) mice, while there was no significant difference between young and adult mice (MD = 0.16, SE = 0.10, $p = 0.11$). Overall, these results showed that while initially the normalized stop times were comparable between the age groups, significant age differences emerged as sessions proceeded for both target intervals.

A.9 Dual Peak Task Illustration

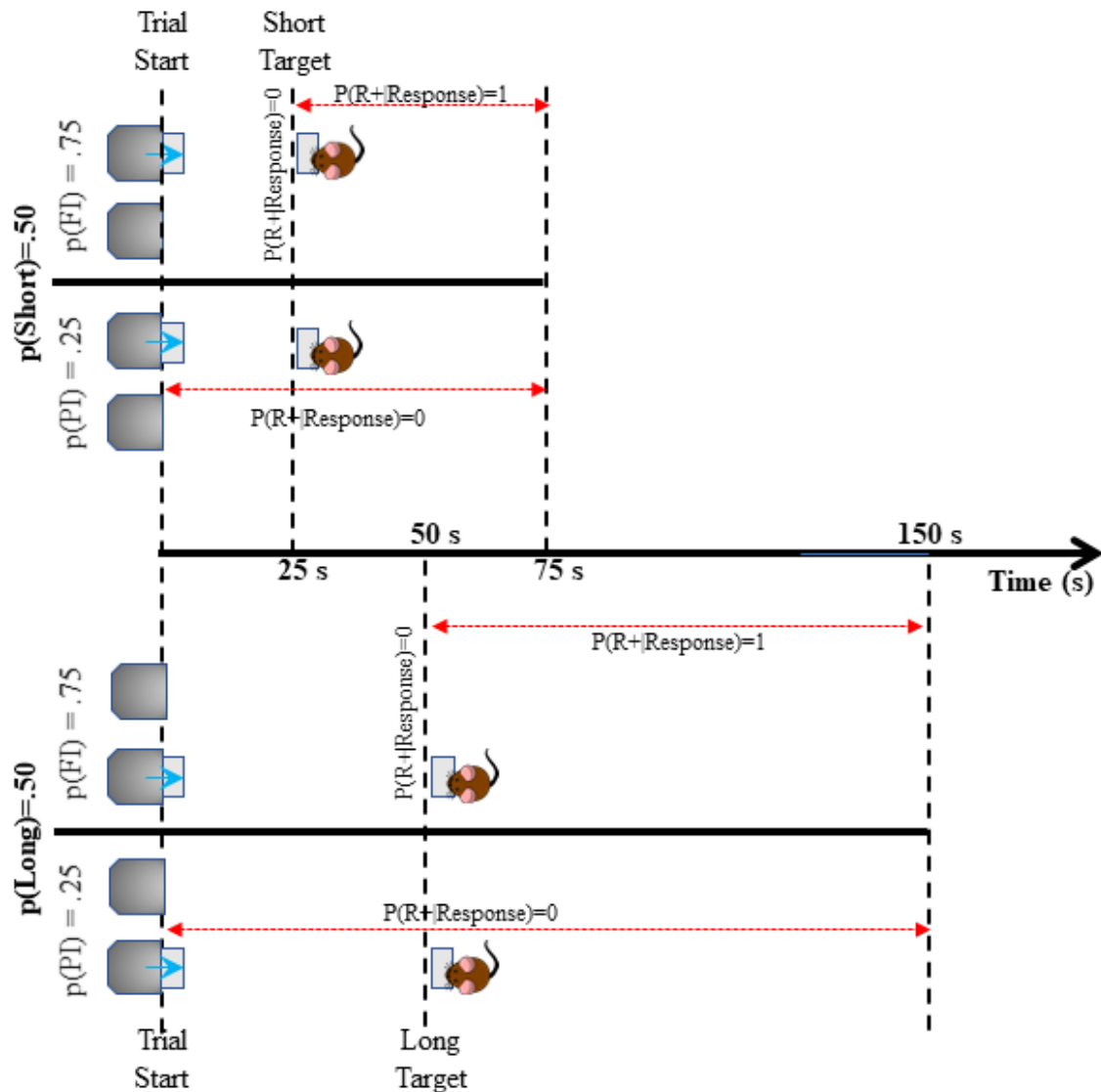


Figure A.1: A graphic representation of the dual peak procedure used in our experiment. There were two target intervals associated with two different levers (25 s and 50 s). The presentation probability of short and long target trials was equal. Within a session, there were fixed interval (FI) trials in which subjects learn the target interval associated with the presented lever and peak interval (PI) trials in which subjects were tested for the target interval associated with the presented lever. In FI trials, subjects received a reward for the first lever press after the target time. In PI trials, subjects did not receive any reward irrespective of their responding. PI trials were three times longer than the FI trials. The overall number of FI trials within a session was three times more than the number of PI trials (R+: reward).

A.10 Mean Neuron Counts

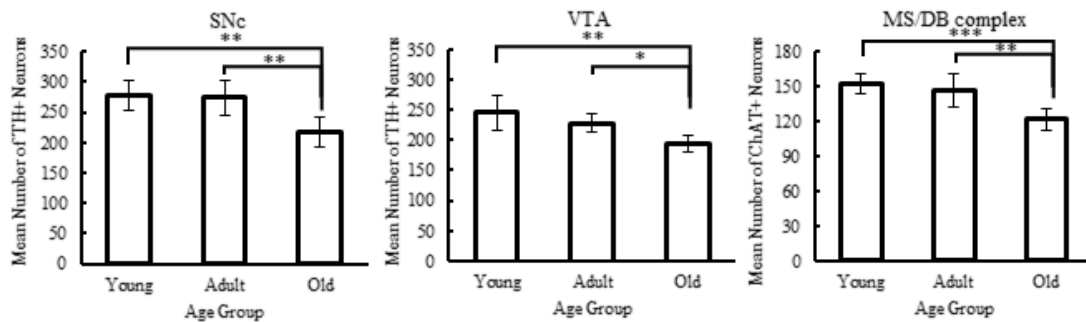


Figure A.2: Mean number of TH+ neurons in SNc and VTA and mean number of ChAT+ neurons in MS/DB complex for young, adult, old mice. Error bars show 95% confidence intervals. *: p < 0.05; **: p <= 0.01; ***: p <= 0.001

A.11 Mean Optic Density of Axon Terminals

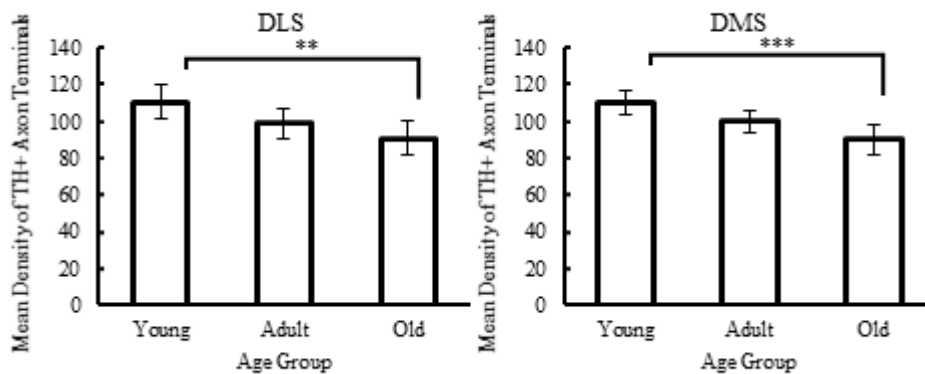


Figure A.3: The mean (optic) density of TH+ axon terminals. Error bars show 95% confidence intervals. **: p <= 0.01; ***: p <= 0.001.

A.12 Scatterplots

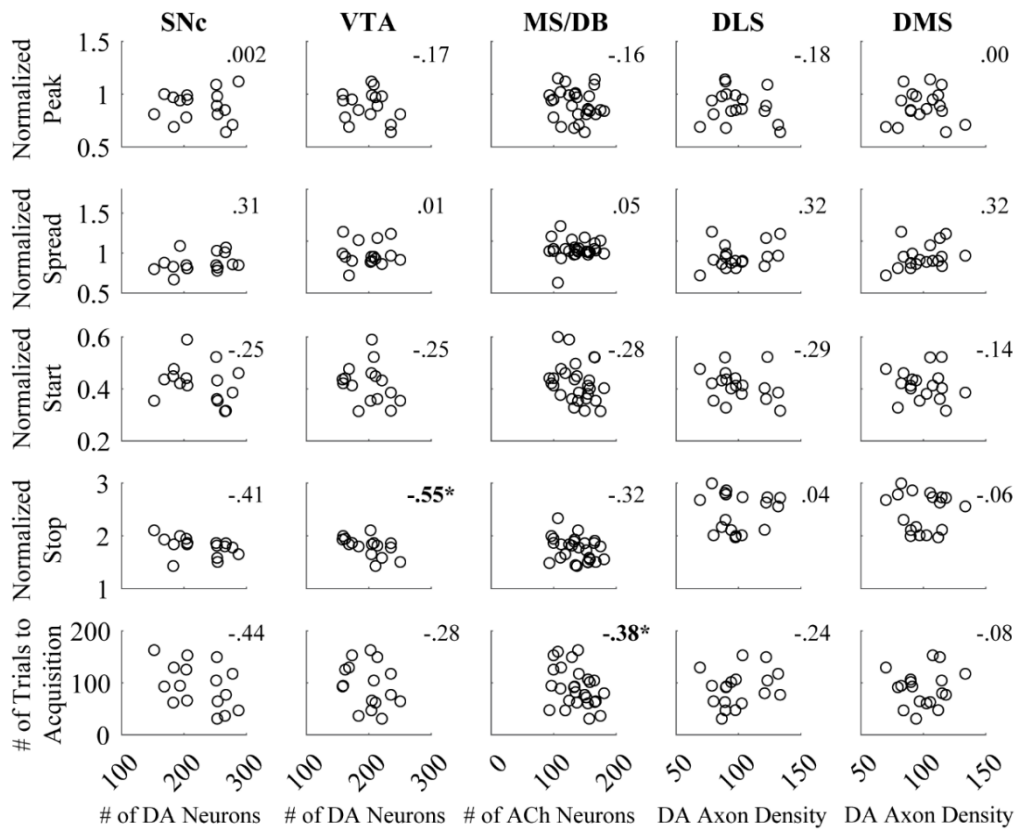


Figure A.4: Scatterplots displaying the relationships between the behavioral measures and the neurobiological parameters collected from the target regions. Correlation coefficients are shown on the top-right corner of each plot (*: $p < 0.05$).

Appendix B

B.1 Switch Rate and Switch Latencies (Times) in the First Hour of the Initial Test Session

Due to the insufficient number of observations, 3 mice from the young group and 4 mice from the old group were not included in the analysis of the first hour of the initial test session. With the remaining subjects, there were 13 mice in the young group, 11 mice in the old group. First, we conducted a mixed ANOVA to compare switch rates between phases (last the training session vs. the first hour of the first test session) and age (young vs. old) groups. Results showed that mice switch from the short location to the long location significantly more during the first hour of the first test session ($M = .72$, $SE = .04$) compared to last training session ($M = .22$, $SE = .05$), $F(1, 22) = 104.34$, $p < .001$, partial $\eta^2 = .83$. Main effect of age ($F(1,22) = .00$, $p = 1.00$) and age by phase interaction ($F(1,22) = .41$, $p = .53$) were not significant.

Comparison of switch times between age and probability groups revealed that there was a significant main effect of probability, $F(1,20) = 12.96$, $p = .002$, partial $\eta^2 = .39$. As expected, switch times were later in $p(\text{short}) = .75$ condition ($M = 5.42$, $SE = .17$) compared to $p(\text{short}) = .25$ condition ($M = 4.41$, $SE = .23$). Main effect of age ($F(1,20) = 2.43$, $p = .14$) and age by phase interaction ($F(1,20) = .22$, $p = .65$) were not significant.

Adjustment in switch times during the first hour of the test session was also examined by regressing the switch times on their order of occurrence for each mouse. Results revealed that there was no evidence for adjustment in majority of the cases. Slopes were significant in 8 out of 24 cases, and only in 4 of these cases we found moderate to strong evidence for a slope different from 0.

B.2 Results of Tosun et al. (2016) for Comparison to the Results of Current Study

Two experiments were run for this study. There were 15 mice in the first experiment and 12 in the second experiment. In the first experiment, short trials were presented by .25, .50, and .75 probability for three different groups. In the second experiment, presentation probability of short trial was determined as .50 and .75 for two groups. The analysis of the data from Tosun et al. (2016) based on parametric tests (as in the current study)

revealed results that are comparable to the results of the current study. We provide the results of these analyses below.

Experiment 1

Comparison of switch rates between the last training and first test sessions revealed that switch rates increased substantially from training to test phase all probability conditions ($p(\text{short}) = .25$: $t(4) = -17.95$, $p < .001$; $p(\text{short}) = .50$: $t(4) = -5.91$, $p < .01$; $p(\text{short}) = .75$: $t(4) = -5.27$, $p < .01$), consistent with the increase observed in the current experiment. Comparison of switch times between probability conditions revealed that probability manipulation significantly affected the switch times, $F(2,12) = 14.43$, $p < .001$. Comparison of probability conditions showed that average switch time of $p(\text{short}) = .75$ condition was significantly later than the average switch time of $p(\text{short}) = .25$ condition ($t(8) = -5.19$, $p < .01$). Differences observed between $p(\text{short}) = .25$ and $p(\text{short}) = .50$ ($t(8) = -2.86$, $p < .05$), and $p(\text{short}) = .50$ and $p(\text{short}) = .75$ ($t(8) = -2.68$, $p < .05$) did not hold after Holm-Bonferroni corrections.

Experiment 2

Switch rate comparison between the long trials of last training and first test sessions showed that switch rates were significantly higher during testing than training both in $p(\text{short}) = .50$ ($t(5) = -3.70$, $p < .05$) and $p(\text{short}) = .75$ ($t(5) = -7.53$, $p < .001$) conditions. Furthermore, in this experiment, there were probe trials for short and long trials without reinforcement. Provided that short probe trial duration was 9 second like the long trial durations, we also compared the switch rates from the last five training sessions to the switch rates from the long trials of the first test session (last five sessions were used to have enough trials for a meaningful comparison since probe trials constituted only 25% of presented trials for each option). Again, we found that switch rates were higher during testing than training in both probability conditions ($p(\text{short}) = .50$: $t(5) = -4.93$, $p < .01$; $p(\text{short}) = .75$: $t(5) = -7.15$, $p < .001$). This comparison showed that mice preferred to stick with the signaled short option during training phase even if there was time to explore the other option, which was not active. Switch times were comparable between $p(\text{short}) = .50$ and $p(\text{short}) = .75$ conditions, $t(10) = .07$, $p = .95$.

Note

Results of these experiments were published in Proceedings of the National Academy of Sciences (113: 787–792), entitled as Mice plan decision strategies based on previously learned time intervals, locations, and probabilities by Tosun, T., Gür, E., & Balci, F. (2016). In Tosun et al. (2016), we adopted a conservative approach and analyzed the data with non-parametric tests, the results of which are comparable to the results of the current study. Here the same data from Tosun et al. (2016) were reanalyzed with parametric tests, which provided nearly identical results to those reported in the original manuscript and are also comparable to the results of the current study. These observations point to the robustness of our original findings reported in Tosun et al. (2016).

B.3 Analysis of Complementary Measures***CV of the start time of short location responses***

We found the main effects of age ($F(1,27) = 6.94, p = .01, \text{partial } \eta^2 = .20$) and probability ($F(1,27) = 6.98, p = .01, \text{partial } \eta^2 = .20$) on the CV of the start time of short location responses. Mean CV of the start time of short location responses was lower for young mice ($M = .34, SE = .02$) compared to old mice ($M = .43, SE = .03$) independent of the probability conditions. Additionally, the CV of the start time of short location responses was lower for $p(\text{short}) = .75$ condition ($M = .33, SE = .02$) compared to $p(\text{short}) = .25$ condition ($M = .43, SE = .03$). The interaction effect of age and probability was not significant, $F(1,27) = .002, p = .96$.

CV of the stop time of short location responses

The effect of probability manipulation was also evident on mean CV of the stop time of short location responses, $F(1,27) = 37.91, p < .001, \text{partial } \eta^2 = .58$, with higher mean CV for mice in $p(\text{short}) = .25$ condition ($M = .35, SE = .02$) compared to $p(\text{short}) = .75$ condition ($M = .22, SE = .02$) independent of age. The effect of age ($F(1,27) = 1.08, p = .31$) or the interaction between age and probability ($F(1,27) = .67, p = .42$) were not statistically significant.

Middle time and spread of short location responses

Middle and spread values of short location responses derived from start and stop times were also compared between age and probability groups. There were no main effect of

age ($F(1,27) = 3.60, p = .07$), probability ($F(1,27) = 1.96, p = .17$), or interaction of age and probability ($F(1,27) = 3.38, p = .08$) on the middle times of short location responses (See the peak location of normalized response curves for short location responses in Figure 4 in the main text). Comparisons of spread values were done with separate independent t-tests after splitting data by probability or age due to assumption violations for running ANOVA. When we split data by the probability, we found that the spread of the short location responses of young mice ($M = 2.71, SE = .36$) was not different from the spread of the short location responses of old mice in $p(\text{short}) = .25$ condition [$M = 2.93, SE = .25$], $t(14) = -.51, p = .62$]. On the other hand, young mice ($M = 4.16, SE = .12$) had narrower spread compared to old mice ($M = 5.23, SE = .25$) in $p(\text{short}) = .75$ condition, $t(8.69) = -3.94, p = .004$. When comparisons were done for probability conditions after splitting data by age, the spread of the short location responses in $p(\text{short}) = .25$ condition was significantly narrower than the spread of the short location responses in $p(\text{short}) = .75$ condition both in the young ($t(8.46) = -3.83, p = .005$) and old mice ($t(13) = -6.47, p < .001$). However, note that significant differences observed between the groups for the spread value depend on the start and stop times as it is calculated as the difference between them.

Start times of the long location responses

Comparison of the start times of the long location responses between age and probability conditions revealed a main effect of probability, $F(1,27) = 19.09, p < .001$, partial $\eta^2 = .41$. The mean start time of the long location responses in the $p(\text{short}) = .25$ condition ($M = 5.80, SE = .19$) was significantly earlier than the mean start time of the long location responses in the $p(\text{short}) = .75$ condition ($M = 6.79, SE = .14$). The mean start time of the long location responses were not significantly different between young and old mice, $F(1,27) = .94, p = .34$. The interaction of age and probability was not significant, $F(1,27) = 3.01, p = .09$. CV of the start time of long location responses also differed between probability conditions, $F(1,27) = 29.00, p < .001$, partial $\eta^2 = .52$. The CV values was higher in the $p(\text{short}) = .25$ condition ($M = .28, SE = .02$) than in the $p(\text{short}) = .75$ condition ($M = .16, SE = .01$). There was no effect of age or the interaction of age and probability on CV of the start times of the long location responses (age: $F(1,27) = .50, p = .49$, age*probability: $F(1,27) = .06, p = .81$).

Appendix C

C.1 Model Fits

Table C.1: Models fit to the entire dataset categorized in 9 session blocks and associated Deviance Information Criteria (DIC).

Model	Included Parameters	Free Parameters	DIC	Δ DIC (from Null)
SP Null	a, v, t		169315.86	
SP1	a, v, t	a	165179.75	-4136.11
SP2	a, v, t	v	168395.48	-920.38
SP3	a, v, t	a, v	164365.90	-4949.96
SP4	a, v, t	a, v, t	163740.92	-5574.94

Table C.2: Models fit to the steady-state data and associated DIC values.

Model	Included Parameters	Free Parameters	DIC	Δ DIC (from Null)
SS0	a, v, t	a, v, t	10879.06	
SS1	a, v, t, z	a, v, t	10140.56	-738.5
SS2	a, v, t, z, dc	a, v, t	9994.69	-884.37
SS3	a, v, t, z, dc	a, v, t, z	9995.20	-883.86
SS4	a, v, t, z, dc	a, v, t, dc	9994.76	-884.3
SS5	a, v, t, z, dc	a, v, t, z, dc	9997.01	-882.05

C.2 Brightness Discrimination Task

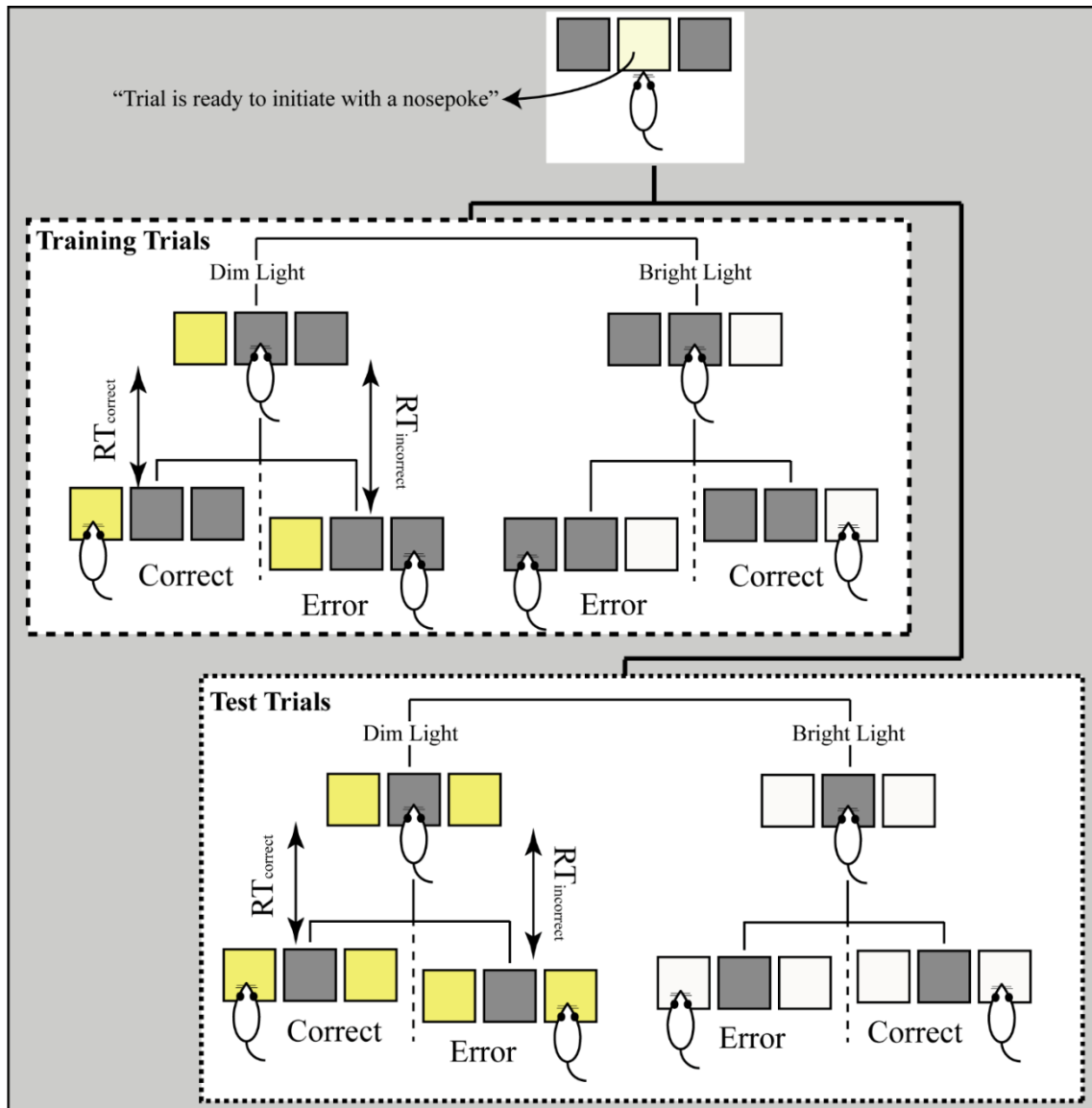


Figure C.1: An illustration of the task used in the experiment. Three nose-poke holes adjacent to each other were used in the experiment. The middle one was illuminated in a medium light density signaling that mice can initiate the trial by nose poking into it. During the training trials after a nose poke in the middle nose-poke hole, one of the other two holes was illuminated with either dim or bright light. The assignment of light intensity to the nose-poke holes was counterbalanced across subjects. Mice collected the reward when they respond in the illuminated nose-poke hole. In the test trials, trial initiation was the same as in the training trials. Once the trial was initiated, both nose-poke holes were illuminated with one of the light intensities (dim or bright) and mice collected the reward when they respond in the nose-poke hole associated with the presented light intensity during the training trials.

C.3 *Posterior Distributions*

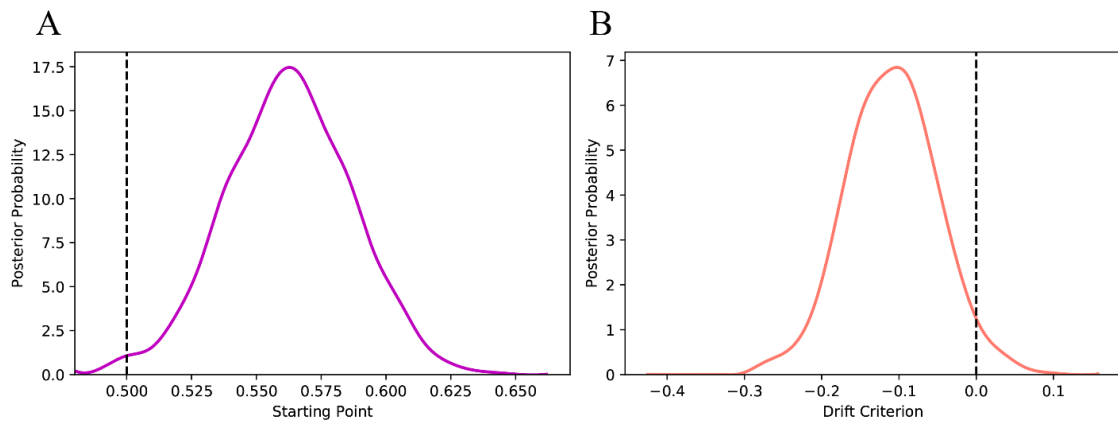


Figure C.2: The posterior distributions of starting point (A) and drift criterion (B) irrespective of age groups. Note that the best fit model included these two bias parameters as common parameters for all age groups.